TRANSPORT PROCESSES IN THE COMBUSTION OF CARBON

A THESIS

Presented to

The Faculty of the Division of Graduate

Studies and Research

by

Tomas Felipe Camacho

In Partial Fulfillment

of the Requirements for the Degree

Doctor of Philosophy in the School of Chemical Engineering

Georgia Institute of Technology

August, 1973

TRANSPORT PROCESSES IN THE

COMBUSTION OF CARBON

Approved:

Dr. C. W. Gorton, Chairman

Dr. G. T. Colwell

Dr. H. C. Ward

Date Approved by Chairman: August 15, 1973

ACKNOWLEDGMENTS

The author wishes to thank his thesis advisor, Dr. C. W. Gorton, for his guidance throughout the conduct of the present work. His advice and suggestions, based on a wealth of knowledge and experience, were always frank and timely, and proved to be invaluable to the completion of this work.

I am also indebted to Dr. G. T. Colwell and Dr. H. C. Ward for having served on the thesis reading committee. Their constructive comments have certainly improved the quality of this work.

Thanks are also due to Dr. G. L. Bridger for providing a teaching assistanship during the early part of the author's graduate work. Kaiser Chemical and Humble Oil fellowships were also received during the latter part of this study and are gratefully acknowledged.

Numerous people contributed to the conduct of this investigation, and the author is grateful to them. The staff of the Rich Electronic Computer Center provided frequent assistance. Mr. Robert C. Schucker was kind enough to discuss numerical techniques and methods of presentation with the author. Ms. Marie Laboon and the author's wife, Patty, worked cheerfully and very professionally in the typing and proofreading of this manuscript; their excellent work, in spite of the pressure, is sincerely appreciated.

The contributions that my wife Patty made to the completion of this work are too numerous to mention. Her constant encouragement, and her patience and understanding during the long days spent by the author

in the company of the computer, are sincerely appreciated. Both Patty and our daughter Kellie, each contributing in their own way, made this work possible.

TABLE OF CONTENTS

TABLE OF CONTENTS (Continued)

LIST OF TABLES

LIST OF TABLES (Continued)

LIST OF TABLES (Concluded)

LIST OF ILLUSTRATIONS

NOMENCLATURE

Symbol	Meaning	Units
A_{ij}	j^{th} constant in the heat capacity equation of species i	
B	defined by Equation (5.11)	none
C	defined by Equation (2.48)	none
C_1	constant in Equation (5.13)	none
C_2	constant in Equation (5.19)	none
C_p	mixture heat capacity, defined by Equation (3.15)	cal/g ·°K
C_{pi}	heat capacity of species i	cal/g ·°K
$\mathcal{D}_{ij}$	binary diffusion coefficient for the i-j species pair	cm^2/sec
D_i^T	thermal diffusion coefficient of species i	
$\tilde{D}_j$	effective elemental diffusion coefficient, defined by Equation (2.28)	cm^2/sec
e_{ij}	mass of element j per unit mass of species i	none
f	defined by Equation (2.35)	none
f'	velocity ratio, $u/U_e(x)$	none
g_i	external force per unit mass acting on species i	
G_n	denotes functional relationship, as in Equation (4.9)	
H	mixture enthalpy	cal/g
H_i	enthalpy of species i	cal/g

Symbol	Meaning	Units
J_i	mass flux of species i with respect to the mixture mass average velocity	g /cm^2·sec
$\tilde{J}_j$	mass flux of element j with respect to the mixture mass average velocity	g /cm^2·sec
k	mixture thermal conductivity	cal/cm·sec·°K
k_i	thermal conductivity of species i	cal/cm·sec·°K
K_i	equilibrium constant for the i^{th} chemical reaction	none
Le	Lewis number, defined by Equation (5.4)	none
M	mixture molecular weight, defined by Equation (2.9)	g /g · mole
M_i	molecular weight of species i	g /g. mole
m_i	mass flux of species i with respect to stationary coordinates	g /cm^2·sec
$\tilde{m}_j$	mass flux of element j with respect to stationary coordinates	g /cm^2·sec
m_w	mass transfer rate at the surface	g /cm^2·sec
N(x)	defined by Equation (2.43)	
P	static pressure	atm
Pr	Prandtl number, defined by Equation (2.52)	none
q	energy flux	cal/cm^2·sec
R	universal gas constant (82.0560)	atm·cm^3/g · mole°K
R_b	body radius	cm
Re	Reynolds number = $(2R_b U_e \rho_e)/\mu_e$	none
r_i	rate of production of species i by homogeneous chemical reactions	g /cm^3·sec

Symbol	Meaning	Units
Sc	Schmidt number, defined by Equation (5.3)	none
T	absolute temperature	°K
t	time	sec
U_e	approach velocity	cm/sec
$U_e(x)$	free stream velocity	cm/sec
u	velocity component in the x coordinate direction	cm/sec
v	velocity component in the y coordinate direction	cm/sec
$\underline{v}$	velocity vector	cm/sec
$\underline{v_i}$	velocity vector of species i with respect to stationary coordinates	cm/sec
$\underline{V_i}$	diffusion velocity vector of species i, $(\underline{v_i}-\underline{v})$	cm/sec
x_i	mole fraction of species i	none
x	coordinate (see Figure 1)	cm
y	coordinate (see Figure 1)	cm
α	acceleration parameter in Equation (4.9)	none
α_{jw}	mass fraction of element j in the solid	none
β	pressure gradient parameter, defined by Equation (2.49)	none
γ_i	equilibrium constant for the formation of species i from its constitutive elements in the standard state.	none
$\underline{\underline{\delta}}$	unit tensor	none
Δ	constant finite difference step size in the η plane	none

Symbol	Meaning	Units
ε_i	energy of interaction of species i	ergs/molecule
η	similarity transformed coordinate, defined by Equation (2.46)	none
θ	defined by Equation (2.57)	none
κ	Boltzmann's constant	ergs/molecule°K
λ	bulk viscosity coefficient	g /cm·sec
μ	mixture viscosity	g /cm·sec
μ_i	viscosity of species i	g /cm·sec
ξ	similarity transformed coordinate, defined by Equation (2.44)	
π	reduced profiles	none
ρ	mixture density	g /cm^3
σ_i	collision diameter of species i	Angstroms
$\underline{\underline{\tau}}$	shear stress tensor	g /cm·sec^2
ϕ	streamfunction, defined by Equation (2.31)	
Ψ_{ij}	viscosity and thermal conductivity mixture parameter, defined by Equation (3.4)	none
ω_i	mass fraction of species i	none
$\mathcal{\omega}_j$	mass fraction of element j	none
Ω_μ	collision integral for viscosity	none
$\Omega_\mathcal{D}$	collision integral for diffusivity	none

Superscripts

k	iteration index
'	differentiation
†	transpose of a vector

Subscripts

C	element carbon
e	at the boundary layer edge, or approach conditions
g	gas phase
i, j, k	refers to species and/or elements
O	element oxygen
N	element nitrogen
n	location in finite difference mesh
s	solid phase
w	at the wall

Overline

$\sim$	refers to elements

Underlines

$\underline{\quad}$	vector
$\underline{\underline{\quad}}$	tensor

SUMMARY

The quasi-steady state combustion of a carbon cylinder, in crossflow to an infinite stream of air, was studied by the application of the high Reynolds number laminar boundary layer equations to describe the multicomponent ideal gas flow. Solutions applicable to the forward stagnation streamline of the cylinder were obtained. Six chemical species were assumed present in the boundary layer (O_2, N_2, O, N, CO_2, and CO). The heterogeneous combustion reaction at the gas-solid interphase and the homogeneous reactions in the boundary layer were assumed to proceed, without kinetic hindrance, to a state of thermochemical equilibrium consistent with the prevailing temperature and gas composition; that is, the combustion process was assumed to be diffusion controlled. Upstream of the cylinder, the approaching air stream was considered to be at a constant temperature (T_e = 300°K) and pressure (P_e = 1.0 atm). The cylinder wall temperature was assumed constant (T_w = 1500°K). The approach gas velocity was sufficiently large to make free convection considerations negligible; the free stream flow, however, was in the low subsonic regime.

The transport and thermodynamic properties were calculated with their full pressure, temperature, and gas composition dependence. The diffusive fluxes for all the species were taken as truly multicomponent fluxes; however, to facilitate the integration of the elemental conservation equations, the effective elemental diffusivity concept was

employed. The resulting system of coupled, nonlinear, ordinary differential equations with split boundary conditions was numerically solved by the method of accelerated successive replacements.

The use of the effective elemental diffusivities provides a straightforward numerical technique for the solution of the elemental conservation equations. However, due to the sensitivity of the effective elemental diffusivities to the composition profiles from which they are calculated, an iterative numerical solution of the elemental conservation equations for the system studied would require a large amount of computation time and thus was not obtained in the present work. Instead, it was assumed that all binary diffusivities were equal to each other at each point in the flowfield. Two solutions were obtained, where the binary diffusivities were taken as $\mathcal{D}_{O_2\text{-}CO}$ and $\mathcal{D}_{N_2\text{-}CO_2}$. The solutions for the two binary diffusivity runs are very similar, and the slight differences existing can be explained by arguments involving the gas mixture Schmidt number.

Approximate equations for predicting combustion rates and subsurface heat transfer rates were obtained based on available solutions of the constant property boundary layer equations. The approximate equation predicted a combustion rate corresponding to the high diffusivity assumption that was ten percent low. Matching the approximate equation to the numerical solution for the high diffusivity assumption permitted the prediction of the combustion rate for the low diffusivity assumption to within two percent. The approximate equations developed should prove useful in predicting the results of carbon combustion taking place under conditions different from those in this investigation.

CHAPTER I

INTRODUCTION

The application of methods for the accurate prediction of momentum, energy and mass transfer rates is important in almost every phase of modern technological activity. The chemical engineering operations of heterogeneous combustion, drying, condensation, humidification, absorption and extraction are based on the transfer of mass across an interphase. Mass transfer also plays a critical role in the diffusional separation of gases and in the design of catalytic reaction systems. In many processes, momentum, heat and mass transfer are often so interdependent that an accurate analysis requires the treatment of all three phenomena, along with thermochemistry and chemical kinetic considerations. The transport processes are often complicated by heterogeneous chemical reactions taking place at an interphase, while homogeneous exothermic reactions (such as combustion) and endothermic reactions (such as dissociation of gaseous species) also take place in the gas phase. At sufficiently high temperatures many combustion reactions proceed so rapidly that the diffusion of the reactants to the reaction zone and of the products from the reaction zone become the rate controlling steps in the combustion process.

Description of the Flow System

In the present work, the quasi-steady combustion of a carbon

cylinder, in crossflow to an infinite stream of air, was studied. The high Reynolds number laminar boundary layer equations were used to describe the multicomponent gas flow over the cylinder. Solutions applicable to the forward stagnation streamline of the cylinder were obtained.

In this system, interfacial mass transfer results in the net addition of elemental carbon* into the boundary layer due to the heterogeneous chemical oxidation reaction taking place at the carbon surface. This heterogeneous reaction was assumed to be diffusion controlled; that is, at the surface, the solid and gas phases were assumed to be in thermochemical equilibrium. The six chemical species assumed present in the boundary layer were O_2, N_2, the combustion products CO and CO_2, and the dissociation products O and N; the gas mixture was considered to behave as an ideal gas mixture. Within the boundary layer itself, it was assumed that the chemical species were in thermochemical equilibrium, related to the local temperature and the prevailing elemental composition.

The partial differential equations describing the flow situation are presented in Chapter II. These equations take into account the variation of physical and transport properties with temperature and composition within the reacting boundary layer. Since the limiting case of local thermochemical equilibrium was considered, a knowledge of phenomenological chemical kinetics reaction rates was not necessary.

---

* Elemental carbon is added to the boundary layer at the interphase by the generation of CO and CO_2.

Previous Work

No treatments of multicomponent, variable property, low velocity, boundary layer combustion of carbon were found in the literature.

The oxidation of solid carbon by a flowing oxidizing stream can be characterized approximately by the prevailing temperature of the carbon surface. At low temperatures ($T_w < 1000°K$) the oxidation reactions are kinetically controlled and the reaction rate is influenced by the degree of crystallinity and the microstructure of the surface, in addition to the surface temperature and the composition of the oxidizing medium. Scala (1) has reviewed the voluminous literature of the low temperature oxidation of carbon and expressed the mass transfer rate at the surface by a kinetic equation of simple form, with the reaction velocity constant following a temperature dependence of the Arrhenius type. Since the rate of oxygen consumption at the surface in the kinetically controlled regime is very low, the mass fraction of elemental oxygen can be taken equal to that at the free stream and all flow considerations become unnecessary.

According to Scala (1), at higher surface temperatures ($1000 < T_w < 1200°K$), the combustion process is in a transition regime between kinetic control and diffusion control. At these temperatures, Scala (1) correlated the mass transfer rate data by the concept of resistances in series.

At sufficiently high surface temperatures, $T_w > 1200°K$, the combustion process becomes diffusion controlled; that is, surface reactions proceed extremely fast and the combustion rate is determined by

the diffusion of oxidizer to the vicinity of the surface. At temperatures in excess of approximately 2800°K, the sublimation of carbon from the surface proceeds at a significant rate as compared to the removal of carbon from the surface by diffusion controlled oxidation reactions, and therefore, the gaseous species $C_{(g)}$, $C_{3(g)}$ begin to appear in the gas phase (as well as CN if combustion takes place in air). In the wall temperature range $1200 < T_w < 7000°K$ the combustion of carbon is amenable to a diffusion controlled boundary layer analysis. (For $T_w > 7000°K$, the high Reynolds number laminar boundary layer equations no longer apply since a pressure gradient in the normal direction arises due to the high sublimation rate.)

Scala (1) and Scala and Gilbert (2) considered the multicomponent combustion of carbon in the diffusion controlled regime, including variation in the physical properties. Their studies, however, involved a hypersonic flight path in which the free stream gases were heated by the passage through a normal bow shock to a temperature of approximately 7000°K. They obtained numerical solutions of the laminar boundary layer equations for $0.17 \leq (T_w/T_e) \leq 0.6$ and approach velocities of 20,000 ft/sec in air at an altitude of 100,000 feet. (The equations solved by Scala (1) and Scala and Gilbert (2) are identical to those solved in this study, except that they neglected the variation of the (C_p/C_{pe}) term in the energy equation.)

Coffin and Brokaw (3) studied the burning of carbon spheres in an infinite oxidizing medium using a one dimensional diffusion-flame model with local thermochemical equilibrium prevailing in the gas

phase. These investigators simplified the diffusion equations by using the binary diffusivities of all species with respect to N_2; they also assumed a simplified variation of the thermal conductivity with composition and temperature in their energy equation. In spite of the differences in geometry, the analytical treatment of the problem and the lack of convective flow about the sphere, the results obtained in the present work agree qualitatively with those of Coffin and Brokaw.

The detailed analysis of multicomponent boundary layers in a general fashion applicable to various systems is precluded by the inherent mathematical difficulties of the problem. The literature, therefore, consists of solutions to the boundary layer equations for particular reacting systems, or for idealized general systems where the variation of physical properties has been neglected, wholly or in part. In all of the solutions discussed below, the diffusive fluxes of each component in the mixture are Fickian; that is, the assumption was made that at every point in the flowfield all of the binary diffusion coefficients are equal. When the assumption of equal binary diffusivities is made, it is convenient to write the energy equation in terms of the stagnation enthalpy; the effect of simplifying assumptions concerning the Lewis, Prandtl and Schmidt numbers becomes clearer. The particular similar solutions presented below are discussed by Dorrance (4). His energy equation, written in terms of the stagnation enthalpy, is identical to the energy equation in terms of the temperature that is solved in the present work, except for Dorrance's assumption of equal binary diffusivities. (If full variation of

physical and transport properties is to be permitted, it is more advantageous to write the energy equation with temperature as the independent variable, since the physical properties are functions of temperature and composition.)

Crocco (5) has shown that the boundary layer velocity profiles and the stagnation enthalpy profiles are similar for flow geometries without a pressure gradient if Pr = Le = 1. Similarly, Probstein (6) has shown that the species mass fraction profiles are similar to the stagnation enthalpy profile for frozen boundary layers with Pr = Le = 1; since this requires that Sc = 1, then the species mass fraction profiles are also similar to the velocity profile. Scala (7) has shown that stagnation streamline solutions for frozen boundary layers with Le = 1 are such that the species mass fraction profiles are again similar to the enthalpy profiles. Lees (8) has shown that if Le = 1 and either Pr = 1 or for a solution along the stagnation streamline, the elemental mass fraction profiles are similar to the stagnation enthalpy profiles. If in addition, Le = Pr = 1 and along the stagnation streamline, then the velocity and the elemental mass fraction profiles are similar.

The general solutions discussed above relate the stagnation enthalpy and the species or element mass fraction profiles with the velocity profile. However, a general solution of the momentum equation for arbitrary pressure gradients and mass transfer rates at the wall is not possible unless some assumptions are made concerning the variation of the density and viscosity across the boundary layer. Therefore, before compositions and enthalpy profiles can be established, it is

necessary to solve the momentum equation for the velocity profile.

Solutions to the boundary layer equations are available where all of the transport and thermodynamic properties are considered constant throughout the boundary layer. With no variation in physical properties, the similar boundary layer solutions for various pressure gradients, mass transfer rates at the wall and dimensionless ratios Le, Pr, and Sc, have been tabulated by Elzy and Sisson (9) over an extensive range of the above mentioned parameters. Prober (10) has presented constant property boundary layer solutions like those of Elzy and Sisson (Prober's results for unfavorable pressure gradient flows lend themselves better to the study of boundary later separation). The constant property solutions presented by Prober and Elzy and Sisson include the solutions previously obtained by many investigators such as: Blasius (11), Howarth (12), Pohlhausen (13), Emmons and Leigh (14), Falkner (15, 16), Hartree (17), Mangler (18), Goldstein (19), Eckert (20), and many others.

In the study of chemically reacting, multicomponent, laminar boundary layers the two limiting cases of frozen boundary layer and boundary layers in thermochemical equilibrium are often considered. Fay and Riddell (21), however, studied the problem of a stagnation streamline hypersonic boundary layer in which air species were assumed to dissociate (and recombine) subject to specific phenomenological chemical kinetics reaction rates. In their study, they allowed for the full variation of all physical properties but treated the diffusion coefficients between the atomic and molecular species as equal, thus

resulting in a Fickian diffusion flux expression rather than a full multicomponent flux expression. In addition, it should be noted that in their study there were no reactions at the body surface other than dissociation (or recombination) and, therefore, there was no net mass transfer rate at the surface.

CHAPTER II

THE MULTICOMPONENT HIGH REYNOLDS NUMBER LAMINAR BOUNDARY LAYER TRANSPORT EQUATIONS

The Equations of Change

The partial differential equations that describe the conservation of linear momentum, energy, and mass in the flow of a multicomponent ideal gas mixture are well known (22,23). These equations are presented below.

The continuity equation is:

$$\frac{\partial \rho}{\partial t} + (\nabla \cdot \rho \, \underline{v}) = 0 \tag{2.1}$$

The momentum equation is:

$$\rho\left(\frac{D\underline{v}}{Dt}\right) + \nabla P + (\nabla \cdot \underline{\underline{\tau}}) - \sum_i (\rho \, \omega_i \, \underline{g}_i) = 0 \tag{2.2}$$

The energy equation is:

$$\rho \, C_p\left(\frac{DT}{Dt}\right) + (\nabla \cdot \underline{q}) + (\underline{\underline{\tau}} : \nabla \underline{v}) - \frac{DP}{Dt} \tag{2.3}$$

$$- \sum_i H_i\left((\nabla \cdot \underline{J}_i) - r_i\right) - \sum_i (\underline{J}_i \cdot \underline{g}_i) = 0$$

The species conservation equations are:

$$\rho\left(\frac{D\,\omega_i}{Dt}\right) + (\nabla \cdot \underline{J}_i) - r_i = 0 \qquad (i = 1, \ldots, N) \qquad (2.4)$$

The above equations contain the momentum flux ($\underline{\underline{\tau}}$), the energy flux ($\underline{q}$), and the mass flux of species i ($\underline{J}_i$) with respect to the mixture mass average velocity. These fluxes may be expressed in terms of the transport coefficients and the gradients of velocity, temperature, and concentration. Onsager (24), in his study on the thermodynamics of irreversible processes, has shown that for a steady state process which is not far from equilibrium, the transport fluxes consist of a linear combination of thermodynamic and macroscopic gradients, with each gradient weighted by a transport coefficient. Further, he showed that based on entropy considerations, a coupling effect can arise between the various fluxes. This coupling gives rise to the Soret effect (mass transport due to a temperature gradient) and its counterpart, the Dufour effect (energy transport due to concentration gradients).

For the flow of Newtonian fluids, the momentum flux is given by Hirschfelder, Curtiss and Bird (25):

$$\underline{\underline{\tau}} = -\mu\left[(\nabla\,\underline{v}) + (\nabla\,\underline{v})^{\dagger}\right] + \frac{2}{3}(\mu - \lambda)(\nabla \cdot \underline{v})\,\underline{\underline{\delta}} \qquad (2.5)$$

The energy flux is made up of three additive contributions. The first contribution is the conductive term, which accounts for the energy flux that arises due to temperature gradients. The second term takes into account the energy flux that arises due to the diffusion of molecular species across the mixture mass average velocity interface, with each species carrying its own enthalpy. The last term is the contribution to

the energy flux associated with concentration gradients, the Dufour diffusion-thermo effect. The total energy flux is thus given by

$$\underline{q} = - k \nabla T + \sum_i H_i \underline{J}_i + RT \sum_i \sum_j \frac{x_j D_i^T}{M_i D_{ij}} (\underline{V}_i - \underline{V}_j) \tag{2.6}$$

The mass flux of species i with respect to the mixture mass average velocity consists of additive contributions due to concentration gradients, to pressure gradients, to the influence of external force fields, and to temperature gradients (Soret effect). For an ideal multicomponent gas, the mass flux vector $\underline{J}_i$ is given by

$$\begin{aligned} \underline{J}_i = {} & \frac{\rho}{M^2} \sum_j M_i M_j D_{ij} \nabla x_j \\ & + \frac{\rho}{M^2} \sum_j M_i M_j D_{ij} [\omega_j (1 - \omega_j)] \nabla (\ell n P) \\ & + \frac{\rho}{M^2 R T} \sum_j M_i M_j D_{ij} \left[x_j M_j \left(\underline{g}_j - \sum_k \omega_k \underline{g}_k \right) \right] \\ & - D_i^T \nabla (\ell n T) \qquad (i = 1, \ldots, N) \end{aligned} \tag{2.7}$$

In principle, then, the system of (N + 5) conservation equations is sufficient to calculate the (N + 5) independent variables ω_i, ρ, T, $\underline{v}$. In addition, the independent variables appearing in the equations are related by the ideal gas equation of state,

$$\rho R T = P M \tag{2.8}$$

where

$$M = \sum_i x_i M_i = \frac{M_i x_i}{\omega_i} \tag{2.9}$$

and the thermodynamic definition:

$$\left(\frac{\partial H_i}{\partial T}\right)_{P,\ \omega_i} = C_{pi} \tag{2.10}$$

Description of the Flow System and Assumptions

In the present work, the high Reynolds number laminar boundary layer equations were used as a model of the transport phenomena taking place in the flow of a multicomponent gas over a two-dimensional body with interfacial mass transfer. Specifically, the system studied was that of the quasi-steady state combustion of carbon in an infinite stream of oxidizer. Solutions applicable to the forward stagnation streamline of a carbon cylinder in crossflow were obtained.

Upstream from the object, the approach gas was considered to be at a constant temperature, pressure and composition. The laminar boundary layer was composed of N non-relaxing chemical species forming an ideal gas mixture and following Newtonian rheology with negligible bulk viscosity.

The contributions of the Dufour effect to the energy flux, and of the Soret effect to the mass fluxes, were considered negligible and were not included. The pressure gradient contribution to the mass fluxes was also neglected. No external body forces were acting on the system; specifically, gravitational forces were neglected.

In the boundary layer it was assumed that the chemical species were in a state of thermochemical equilibrium. At the carbon-gas interface, a diffusion controlled chemical reaction was assumed to take place and proceed, without kinetic hindrance, to a state of thermochemical equilibrium. This heterogeneous surface reaction results in the net addition of elemental carbon to the boundary layer. It was further assumed that the temperature and composition at the surface were time invariant. The six chemical species present in the boundary layer were assumed to be O_2, N_2, O, N, CO_2 and CO.

The body oriented orthogonal coordinate system shown in Figure 1 was used in the analysis of the equations. The forward stagnation point was taken as the origin of the system, with the x coordinate measured along the body surface and the y coordinate measured perpendicular to the body surface. The component of the velocity vector along the x coordinate was taken as u and the component along the y coordinate as v. Tollmien (26) has derived expressions for the complete continuity and momentum equations as they apply to the body oriented coordinate system. Schlichting (27) has shown that with the assumption of a boundary layer thickness which is small compared to the wall radius of curvature, and, provided that no large variations in curvature occur, the Tollmien equations reduce to those presented in the following section.

The Simplified Equations of Change

When the assumptions presented above are applied to the full equations of change, a significant simplification results. The simplified equations of change, written for a two-dimensional body, are:

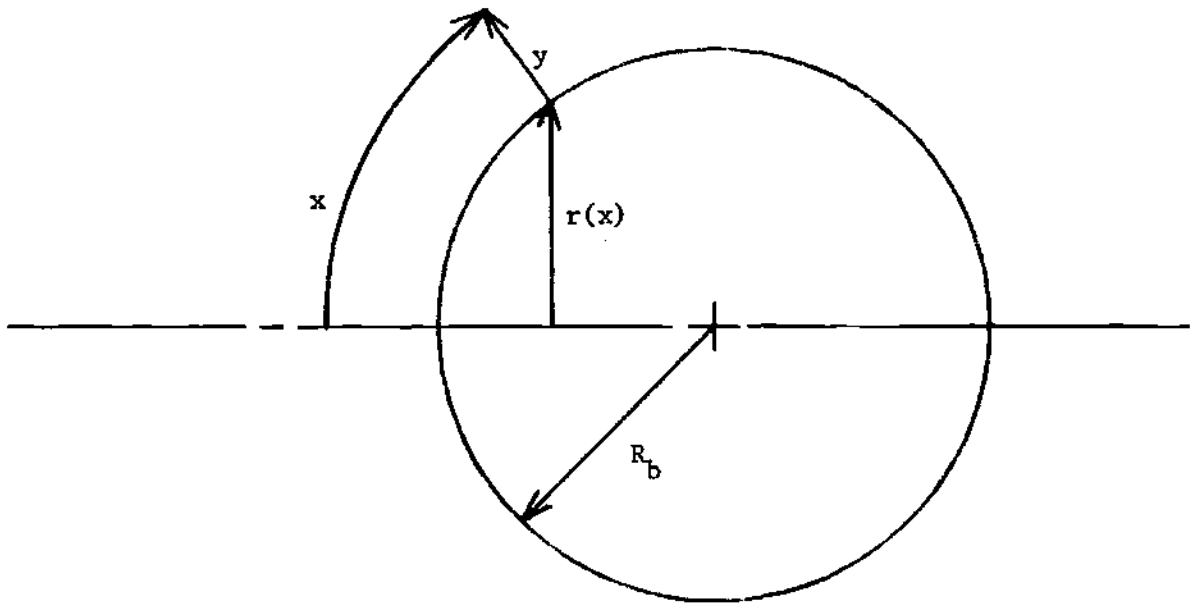

Figure 1. Body Oriented Orthogonal Coordinate System

Continuity Equation

$$\frac{\partial(\rho\, u)}{\partial\, x} + \frac{\partial(\rho\, v)}{\partial\, y} = 0 \tag{2.11}$$

x - Momentum Equation

$$\rho\left(u\,\frac{\partial\, u}{\partial\, x} + v\,\frac{\partial\, u}{\partial\, y}\right) + \frac{\partial\, P}{\partial\, x} - \frac{\partial}{\partial\, y}\left[\mu\left(\frac{\partial\, u}{\partial\, y} + \frac{\partial\, v}{\partial\, x}\right)\right] \tag{2.12}$$

$$- 2\,\frac{\partial}{\partial\, x}\left(\mu\,\frac{\partial\, u}{\partial\, x}\right) - \frac{2}{3}\,\frac{\partial}{\partial\, x}\left[\mu\left(\frac{\partial\, u}{\partial\, x} + \frac{\partial\, v}{\partial\, y}\right)\right] = 0$$

y - Momentum Equation

$$\rho\left(u\,\frac{\partial\, v}{\partial\, x} + v\,\frac{\partial\, v}{\partial\, y}\right) + \frac{\partial\, P}{\partial\, y} - \frac{\partial}{\partial\, x}\left[\mu\left(\frac{\partial\, u}{\partial\, y} + \frac{\partial\, v}{\partial\, x}\right)\right] \tag{2.13}$$

$$- 2\,\frac{\partial}{\partial\, y}\left(\mu\,\frac{\partial\, v}{\partial\, y}\right) - \frac{2}{3}\,\frac{\partial}{\partial\, y}\left[\mu\left(\frac{\partial\, u}{\partial\, x} + \frac{\partial\, v}{\partial\, y}\right)\right] = 0$$

Energy Equation

$$\rho\, C_p\left(u\,\frac{\partial\, T}{\partial\, x} + v\,\frac{\partial\, T}{\partial\, y}\right) - \frac{\partial}{\partial\, x}\left(k\,\frac{\partial\, T}{\partial\, x}\right) - \frac{\partial}{\partial\, y}\left(k\,\frac{\partial\, T}{\partial\, y}\right) \tag{2.14}$$

$$+ \sum_i H_i\, r_i + \sum_i J_{ix}\left(\frac{\partial\, H_i}{\partial\, x}\right) + \sum_i J_{iy}\left(\frac{\partial\, H_i}{\partial\, y}\right)$$

$$- \left(u\,\frac{\partial\, P}{\partial\, x} + v\,\frac{\partial\, P}{\partial\, y}\right) - 2\,\mu\left[\left(\frac{\partial\, u}{\partial\, x}\right)^2 + \left(\frac{\partial\, v}{\partial\, y}\right)^2\right]$$

$$- \mu\left(\frac{\partial\, v}{\partial\, x} + \frac{\partial\, u}{\partial\, y}\right)^2 + \frac{2}{3}\,\mu\left(\frac{\partial\, u}{\partial\, x} + \frac{\partial\, v}{\partial\, y}\right)^2 = 0$$

Species Conservation Equations

$$\rho u \frac{\partial \omega_i}{\partial x} + \rho v \frac{\partial \omega_i}{\partial y} + \frac{\partial J_{ix}}{\partial x} + \frac{\partial J_{iy}}{\partial y} - r_i = 0 \qquad (i = 1, \ldots, N) \quad (2.15)$$

The momentum flux ($\underline{\tau}$) and the energy flux ($\underline{q}$) have been introduced into the momentum and energy equations respectively. The mass flux of species i relative to the mixture mass average velocity is, after simplification,

$$\underline{J}_i = \rho_i \underline{V}_i = \rho_i (\underline{v}_i - \underline{v}) = \frac{\rho}{M^2} \sum_j M_i M_j D_{ij} \nabla x_j \qquad (i = 1, \ldots, N) \quad (2.16)$$

The High Reynolds Number Laminar Boundary Layer Equations

Equation (2.2) has been solved extensively for hypothetical inviscid fluids, but the treatment of viscous fluids is much more difficult and solutions are available for only a few simple flow geometries. Prandtl (28) in 1904 developed an asymptotic method of analysis for flows of viscous fluids about streamlined objects at high Reynolds numbers. Prandtl divided the flow field into two regions: a thin boundary layer near the surface, where large velocity gradients exist; and a potential flow regime outside the boundary layer, where velocity gradients are small. By solving the momentum equation separately for the two regimes and splicing the solutions at the edge of the boundary layer, the entire flow field can be accurately described (except in the vicinity of a vortex or separation region).

The high Reynolds number laminar boundary layer equations are obtained by performing an order of magnitude analysis on Eqns. (2.11 -

2.16). The procedure is straight forward and has been presented in considerable detail by previous authors (4, 27). The resulting boundary layer equations are:

Continuity Equation

$$\frac{\partial(\rho u)}{\partial x} + \frac{\partial(\rho v)}{\partial y} = 0 \tag{2.17}$$

x - Momentum Equation

$$\rho\left(u \frac{\partial u}{\partial x} + v \frac{\partial u}{\partial y}\right) + \frac{d P_e}{d x} - \frac{\partial}{\partial y}\left(\mu \frac{\partial u}{\partial y}\right) = 0 \tag{2.18}$$

y - Momentum Equation

$$\frac{d P}{d y} = 0 \quad ; \quad P = P_e (x) \text{ only} \tag{2.19}$$

Energy Equation

$$\rho C_p\left(u \frac{\partial T}{\partial x} + v \frac{\partial T}{\partial y}\right) - \frac{\partial}{\partial y}\left(k \frac{\partial T}{\partial y}\right) - u \frac{d P_e}{d x} \tag{2.20}$$

$$- \mu\left(\frac{\partial u}{\partial y}\right)^2 + \sum_i J_{iy} C_{pi} \left(\frac{\partial T}{\partial y}\right) + \sum_i H_i r_i = 0$$

Species Conservation Equations

$$\rho\left(u \frac{\partial \omega_i}{\partial x} + v \frac{\partial \omega_i}{\partial y}\right) + \frac{\partial J_{iy}}{\partial y} - r_i = 0 \qquad (i = 1, \ldots, N) \tag{2.21}$$

The Elemental Conservation Equations

The N species conservation equations can be replaced by K elemental

conservation equations, corresponding to the K chemical elements constituting the system, and (N - K) thermochemical equilibrium equations. This approach dispenses with the species generation terms (r_i) because chemical elements are always conserved, whereas chemical species are not necessarily conserved in a reacting system.

Defining e_{ij} to be the mass of element j per unit mass of species i, the mass fraction of element j in the mixture is given by

$$\tilde{\omega}_j = \sum_i e_{ij}\, \omega_i \qquad (j = 1, \ldots, K) \tag{2.22}$$

and the mass flux of element j with respect to the mixture mass average velocity is

$$\tilde{\underline{J}}_j = \sum_i e_{ij}\, \underline{J}_i \qquad (j = 1, \ldots, K) \tag{2.23}$$

Multiplying each of the i^{th} species conservation equations by e_{ij} and summing over all i, the result is:

$$\rho\left(u \frac{\partial \tilde{\omega}_j}{\partial x} + v \frac{\partial \tilde{\omega}_j}{\partial y}\right) + \frac{\partial}{\partial y}\left(\tilde{J}_{jy}\right) = 0 \qquad (j = 1, \ldots, K) \tag{2.24}$$

since

$$\tilde{r}_j \equiv \sum_i e_{ij}\, r_i = 0 \qquad (j = 1, \ldots, K) \tag{2.25}$$

where $\tilde{J}_{jy}$ is given by

$$\tilde{J}_{jy} = \frac{\rho}{M^2} \sum_i e_{ij} \left(\sum_k M_i\, M_k\, D_{ik} \frac{\partial x_k}{\partial y} \right) \qquad (j = 1, \ldots, K) \tag{2.26}$$

Equations (2.24) are the elemental conservation equations, with the elemental mass fluxes given by $\tilde{J}_{jy}$. Although Equation (2.26) is an exact multicomponent flux equation, it is in a form that does not readily yield to an iterative numerical solution since it contains the gradients of all the species in the gas mixture.

Effective Elemental Diffusivities

The coupling among the elemental conservation equations that arises through the gradients involved in the elemental mass fluxes, makes this system of equations very difficult to solve.

For an iterative numerical solution it is desirable to express each elemental mass flux explicitly in terms of that element concentration gradient. The effect of the concentration gradients of all the other elements can then be implicitly taken into an effective elemental diffusivity. Defining, after Tirskii (29, 30),

$$\tilde{J}_{jy} = - \rho \tilde{D}_j \left(\frac{\partial \tilde{\omega}_j}{\partial y} \right) \qquad (j = 1, \ldots, K) \tag{2.27}$$

and equating this to Equation (2.26), an expression for $\tilde{D}_j$ can be obtained which satisfies identically both Equations (2.26, 2.27)

$$\tilde{D}_j = - \frac{1}{M^2} \cdot \frac{\sum_i e_{ij} \left[\sum_k M_i M_k D_{ik} \left(\frac{\partial x_k}{\partial y} \right) \right]}{\left(\frac{\partial \tilde{\omega}_j}{\partial y} \right)} \qquad (j = 1, \ldots, K) \tag{2.28}$$

Substitution of Equations (2.27, 2.28) into (2.24) results in a form of the elemental conservation equation which is more suitable for

a numerical solution:

$$\rho\, u \frac{\partial \tilde{\omega}_j}{\partial x} + \rho\, v \frac{\partial \tilde{\omega}_j}{\partial y} - \frac{\partial}{\partial y}\left[\rho\, \tilde{D}_j \left(\frac{\partial \tilde{\omega}_j}{\partial y}\right)\right] \qquad (j = 1, \ldots, K) \qquad (2.29)$$

where $\tilde{D}_j$ is given by Equation (2.28).

In summary, the boundary layer equations to be solved are Equations (2.17 - 2.20, 2.29). In addition, (N - K) thermochemical equilibrium expressions applicable in the boundary layer will be required to relate the K elemental compositions with the N species compositions; these will be discussed later.

Similarity Transformation of the Boundary Layer Equations

The system of coupled, non-linear, partial differential equations in the boundary layer is extremely difficult to solve. These equations can be reduced to a simpler system of ordinary differential equations if a transformation can be found that maps the (x, y) plane into the (ξ, η) plane, as yet undefined, in such a manner that the derivatives of the dependent variables become separable. In the following pages the procedure outlined by Li and Nagamatsu (31) is followed. The similarity transformation presented is the Lees-Dorodnitsyn (32) transformation, which includes as special cases the transformations of Blasius (33), Mangler (19), and Illingworth-Levy (34, 35). The discussion of the similiarity transformation presented in this section is abstracted from that given by Dorrance (4).

Continuity Equation

Expanding Equation (2.17) and making use of Equations (2.8, 2.19),

$$P_e\left[\frac{\partial}{\partial x}\left(\frac{M u}{R T}\right) + \frac{\partial}{\partial y}\left(\frac{M v}{R T}\right)\right] + \frac{M u}{R T}\left(\frac{d P_e}{d x}\right) = 0 \qquad (2.30)$$

Introducing the stream function

$$\varphi(x, y) = \int_0^y \left(\frac{M u}{R T}\right) d y + \varphi(x, o) \qquad (2.31)$$

into Equation (2.30) gives

$$\frac{\partial}{\partial y}\left[\frac{\partial \varphi}{\partial x} + \frac{M v}{R T}\right] = -\frac{d}{d x}(\ell n\ P_e)\left(\frac{\partial \varphi}{\partial y}\right) \qquad (2.32)$$

and integrating Equation (2.32) with respect to y, gives

$$\frac{M v}{R T} = -\left[\frac{\partial \varphi}{\partial x} + \varphi \frac{d}{d x}(\ell n\ P_e)\right] \qquad (2.33)$$

x - Momentum Equation

Equation (2.18) can be expressed in terms of the stream function as:

$$\left(\frac{\partial \varphi}{\partial y}\right)\left(\frac{\partial u}{\partial x}\right) - \left[\frac{\partial \varphi}{\partial x} + \varphi \frac{d}{d x}(\ell n\ P_e)\right]\left(\frac{\partial u}{\partial y}\right) = \qquad (2.34)$$

$$-\frac{d}{d x}(\ell n\ P_e) + \frac{1}{P_e}\frac{\partial}{\partial y}\left(\mu \frac{\partial u}{\partial y}\right)$$

The objective is to seek solutions that would allow separation of the partial differential equations, such that

$$\varphi(x, \eta) = N(x) \cdot f(\eta) \qquad (2.35)$$

and $$u(x, \eta) = U_e(x) \cdot f'(\eta) \tag{2.36}$$

where η is a transformed independent variable as yet undefined, but, in general, $\eta = \eta(x, y)$.

Since $$\frac{\partial \varphi}{\partial y} = N(x)\ f'(\eta)\ \frac{\partial \eta}{\partial y} = \frac{M\ u}{R\ T} \tag{2.37}$$

and $$\frac{M\ u}{R\ T} = \frac{M}{R\ T}\ U_e(x) \cdot f'(\eta) \tag{2.38}$$

then, combining

$$\frac{\partial \eta}{\partial y} = \frac{M\ U_e(x)}{R\ T\ N(x)} = \left(\frac{\rho}{P_e}\right) \frac{U_e(x)}{N(x)} \tag{2.39}$$

and integrating with respect to y, and $\eta(x, o) = 0$

$$\eta = \frac{U_e(x)}{P_e\ N(x)} \int_o^y \rho\ d\ y \tag{2.40}$$

To determine N(x) the x-momentum equation is written in terms of the derivatives with respect to x and η, retained as independent variables. After considerable differentiation and rearrangement, it can be shown that

$$\frac{\rho_e\ \mu_e\ U_e(x)}{N(x)\ P_e\ \frac{d}{d\ x}\ (N(x)\ P_e)} \left(\frac{\rho\ \mu}{\rho_e\ \mu_e}\ f''\right)' + f\ f'' \tag{2.41}$$

$$+ \frac{\left[\left(\frac{\rho_e}{\rho}\right) - (f')^2\right]}{\frac{d}{d\ x}\ (\ell n\ N(x)\ P_e)} \cdot \frac{d}{d\ x}\ (\ell n\ U_e(x)) = 0$$

Letting the definition of N (x) be implied by

$$\frac{\rho_e \mu_e U_e(x)}{N(x) P_e \frac{d}{d x} (N(x) P_e)} = 1 \tag{2.42}$$

and integrating Equation (2.42) from x = 0 to x gives:

$$N(x) = \frac{\left[2 \int_o^x \rho_e \mu_e U_e(x) \, d x\right]^{\frac{1}{2}}}{P_e} \tag{2.43}$$

The other similarity independent variable can then be taken as

$$\xi(x) = \int_o^x \rho_e \mu_e U_e(x) \, d x \tag{2.44}$$

Substitution of Equations (2.43, 2.44) into Equation (2.35) then gives

$$\varphi = \frac{(2 \xi)^{\frac{1}{2}}}{P_e} f(\eta) \tag{2.45}$$

Substitution of Equations (2.43, 2.44) into Equation (2.40) yields

$$\eta = \frac{\rho_e U_e(x)}{(2 \xi)^{\frac{1}{2}}} \int_o^y \left(\frac{\rho}{\rho_e}\right) d y \tag{2.46}$$

Equations (2.44, 2.46) give the independent variables that permit a separation of the partial derivatives.

The final form of the x-momentum equation is obtained from Equation (2.41) upon substitution of Equations (2.43, 2.44) to yield

$$(C f'')' + f f'' + \beta \left[\frac{\rho_e}{\rho} - (f')^2\right] = 0 \tag{2.47}$$

where

$$C = \frac{\rho \mu}{\rho_e \mu_e} \tag{2.48}$$

and

$$\beta = 2 \frac{d\ (\ell n\ U_e)}{d\ (\ell n\ \xi)} \tag{2.49}$$

It should be noted that the introduction of the stream function and the posing of the equations in terms of the transformed coordinates identically satisfies the continuity equation, whereas the x-momentum equation is transformed from a second order non-linear partial differential equation to a third order non-linear ordinary differential equation in η.

The Mass Transfer Rate at the Solid Surface

Substituting Equations (2.35, 2.36, 2.42, 2.44 and 2.49) into Equation (2.33), and rearranging, an expression for the velocity component normal to the surface at the stagnation point is obtained

$$v = - \frac{1}{\rho} \left[\frac{\rho_e \mu_e}{\beta} \cdot \frac{d\ U_e(x)}{d\ x} \right]^{\frac{1}{2}} f \tag{2.50}$$

and for the mass transfer rate at the solid-gas interface, with $m_w = \rho_w v_w$

$$f_w = - m_w \left[\frac{\rho_e \mu_e}{\beta} \cdot \frac{d\ U_e(x)}{d\ x} \right]^{-\frac{1}{2}} \tag{2.51}$$

Mass Fluxes

The y-component of the mass transfer fluxes appearing in the energy equation is given by Equation (2.16). Noting from Equation (2.46) that

$$\frac{\partial \eta}{\partial y} = \frac{\rho U_e}{(2\xi)^{\frac{1}{2}}} = \rho\left[\frac{1}{\beta \rho_e \mu_e} \cdot \frac{d U_e(x)}{d x}\right]^{\frac{1}{2}} \tag{2.52}$$

the transformed species mass fluxes become

$$J_{i\eta} = \frac{\rho^2}{M^2}\left[\frac{1}{\beta \rho_e \mu_e} \cdot \frac{d U_e(x)}{d x}\right]^{\frac{1}{2}} \sum_j M_i M_j D_{ij} x_j' \qquad (i = 1, \ldots, N) \tag{2.53}$$

and, therefore, the similarity transformed elemental mass fluxes become

$$\tilde{J}_{j\eta} = \frac{\rho^2}{M^2}\left[\frac{1}{\beta \rho_e \mu_e} \cdot \frac{d U_e(x)}{d x}\right]^{\frac{1}{2}} \sum_i e_{ij}\left[\sum_k M_i M_k D_{ik} x_k'\right] \quad (j = 1, \ldots, K) \tag{2.54}$$

In terms of the effective elemental diffusivity, $\tilde{D}_j$, the fluxes are

$$\tilde{J}_{j\eta} = -\rho^2 \tilde{D}_j\left[\frac{1}{\beta \rho_e \mu_e} \cdot \frac{d U_e(x)}{d x}\right]^{\frac{1}{2}} \tilde{\omega}_j' \qquad (j = 1, \ldots, K) \tag{2.55}$$

and, equating Equations (2.54, 2.55), there results

$$\tilde{D}_j = -\frac{1}{M^2 \tilde{\omega}_j'} \sum_i e_{ij}\left[\sum_k M_i M_k D_{ik} x_k'\right] \qquad (j = 1, \ldots, K) \tag{2.56}$$

Energy Equation

The energy equation can be transformed by assuming the temperature profile to be given by

$$T = T_e(x) \cdot \theta(\eta) \tag{2.57}$$

and then rewriting Equation (2.20), while retaining η as the independent variable, to obtain

$$\left[\frac{C\,C_p}{Pr}\,T'\right]' + f\,C_p\,T' - \left[\frac{\beta}{\rho_e\,\mu_e} \cdot \frac{d\,U_e(x)}{d\,x}\right]^{\frac{1}{2}} \sum_i C_{pi}\,J_{i\eta}\,T' \tag{2.58}$$

$$+ U_e^{\,2}\left[C(f'')^2 + \beta\,f'\left(\frac{C_p\,T}{C_{pe}\,T_e} - \frac{\rho_e}{\rho}\right)\right] - \frac{\beta}{\rho\,\dfrac{d\,U_e(x)}{d\,x}} \sum_i H_i\,r_i = 0$$

where

$$Pr = \frac{C_p\,\mu}{k} \tag{2.59}$$

Species Conservation Equations

The species generation terms (r_i) appearing in Equation (2.58) may be obtained from the transformation of Equation (2.21) as

$$r_i = \frac{\rho}{\beta} - \frac{d\,U_e(x)}{d\,x}\left[-f\,\omega_i' + \left[\frac{\beta}{\rho_e\,\mu_e\,\dfrac{d\,U_e(x)}{d\,x}}\right]^{\frac{1}{2}} J_{i\eta}'\right] \quad (i = 1, \ldots, N) \tag{2.60}$$

Elemental Conservation Equations

The elemental conservation equations (2.29) can also be transformed to obtain:

$$f\,\rho_e\,\mu_e\,\tilde{\omega}_j' + \left(\rho^2\,\tilde{D}_j\,\tilde{\omega}_j'\right)' = 0 \qquad (j = 1, \ldots, K) \tag{2.61}$$

where the $\tilde{D}_j$ are now given by Equation (2.56).

Scala (1, 2) has presented the transformed momentum, energy and species continuity equations applicable to two dimensional stagnation streamline flow. The corresponding equations presented in this work, Equations (2.47, 2.58, 2.60), agree with those presented by Scala in all respects except that he appears to have set the (C_p/C_{pe}) ratio in the convective term of the energy equation equal to unity.

Pressure Gradient Parameter for a Cylinder in Crossflow at the Forward Stagnation Point

The potential flow solution to the inviscid flow of a fluid about a right circular cylinder in crossflow is given by Bird, Stewart and Lightfoot (22) (after conversion to the body oriented coordinate system) as:

$$U_e(x) = U_e\left[1 + \left(\frac{R_b}{y + R_b}\right)^2\right] \sin\left(\frac{x}{R_b}\right) \tag{2.62}$$

Since at any point in the boundary layer $y \approx 0$, then, this simplifies to

$$U_e(x) = 2\,U_e\,\sin\left(\frac{x}{R_b}\right) \tag{2.63}$$

To evaluate the pressure gradient parameter (β) along the stagnation streamline, note that from Equation (2.49)

$$\beta = \frac{2\,\xi}{U_e(x)} \cdot \frac{d\,U_e(x)}{d\,\xi} = \frac{2\,\xi}{U_e(x)} \cdot \frac{d\,U_e(x)}{d\,x} \cdot \frac{d\,x}{d\,\xi} \tag{2.64}$$

Substituting Equations (2.44, 2.63) into Equation(2.64), obtain an expression for β

$$\beta = \frac{-2\,\cos\left(\frac{x}{R_b}\right)\left[\cos\left(\frac{x}{R_b}\right) - 1\right]}{\sin^2\left(\frac{x}{R_b}\right)} \tag{2.65}$$

and using L'Hospital's rule to evaluate β at the forward stagnation point of the cylinder,

$$\beta\ (x = 0) = 1 \tag{2.66}$$

which is the well known result applicable to the forward stagnation point of a cylinder in crossflow.

Summary of the Boundary Layer Equations

For the purpose of convenience, the transformed boundary layer transport equations solved in this work are summarized below, as they apply to the forward stagnation streamline of a cylinder in crossflow.

Momentum Equation

$$(C\,f'')' + f\,f'' + \left[\frac{\rho_e}{\rho} - (f')^2\right] = 0 \tag{2.67}$$

Energy Equation

$$\left(\frac{C\,C_p}{Pr}\,T'\right)' + f\,C_p\,T' - \left[\frac{R_b}{2\,\rho_e\,\mu_e\,U_e}\right]^{\frac{1}{2}} \sum_i C_{pi}\,J_i\,T' + \tag{2.68}$$

$$+ U_e^2\left[C(f'')^2 + f'\left(\frac{C_p T}{C_{pe} T_e} - \frac{\rho_e}{\rho}\right)\right] - \frac{R_b}{2 \rho U_e}\sum_i H_i r_i = 0$$

Elemental Conservation Equations

$$f \rho_e \mu_e \tilde{\omega}_j' + (\rho^2 \tilde{D}_j \tilde{\omega}_j')' = 0 \qquad (j = 1, \ldots, K) \tag{2.69}$$

Species Generation Equations

$$r_i = \frac{2 \rho U_e}{R_b}\left[- f \omega_i' + \left(\frac{R_b}{2 \rho_e \mu_e U_e}\right)^{\frac{1}{2}} J_i'\right] \qquad (i = 1, \ldots, N) \tag{2.70}$$

Species Mass Fluxes

$$J_i = \frac{\rho^2}{M^2}\left[\frac{R_b}{\rho_e \mu_e U_e}\right]^{\frac{1}{2}} \sum_j M_i M_j D_{ij} x_j' \qquad (i = 1, \ldots, N) \tag{2.71}$$

Elemental Mass Fluxes

$$\tilde{J}_j = \frac{\rho^2}{M^2}\left[\frac{2 U_e}{\rho_e \mu_e R_b}\right]^{\frac{1}{2}} \sum_i e_{ij}\left[\sum_k M_i M_k D_{ik} x_k'\right] \qquad (j = 1, \ldots, K) \tag{2.72}$$

or

$$\tilde{J}_j = - \rho^2 \tilde{D}_j\left[\frac{2 U_e}{\rho_e \mu_e R_b}\right]^{\frac{1}{2}} \tilde{\omega}_j' \qquad (j = 1, \ldots, K) \tag{2.73}$$

where

$$\tilde{D}_j = - \frac{1}{M^2 \tilde{\omega}_j'} \sum_i e_{ij}\left[\sum_k M_i M_k D_{ik} x_k'\right] \qquad (j = 1, \ldots, K) \tag{2.74}$$

Mass Transfer Rate at the Surface

$$m_w = -f_w\left[\frac{2 \rho_e \mu_e U_e}{R_b}\right]^{\frac{1}{2}} \tag{2.75}$$

Boundary Conditions and Eigenvalues

The transformed boundary layer equations (2.67, 2.68, and 2.69) constitute a set of (K + 2) equations of order (2 K + 5) which, in principle, can be solved for the K elemental compositions, the velocity ratio f' and temperature T. In the following pages the boundary conditions are developed that, along with the transport equations, constitute the mathematical model of the reacting system under consideration in the present work.

Momentum Equation

Equation (2.67), the momentum equation, is a third order, nonlinear, ordinary differential equation and, therefore, requires three boundary conditions for its solution. Two of these boundary conditions are easily deduced from Equation (2.36); from the no slip condition at the surface

$$f'(\eta = 0) = f'_w = 0 \tag{2.76}$$

and from the matching of the boundary layer solution to the potential flow solution at the edge of the boundary layer

$$f'(\eta = \eta_e) = f'_e = 1 \tag{2.77}$$

The third momentum boundary condition, which in effect is an eigenvalue of the problem, is the expression for the mass transfer rate at the wall, given as:

$$f(\eta = 0) = f_w = -m_w\left[\frac{R_b}{2\,\rho_e\,\mu_e\,U_e}\right]^{\frac{1}{2}} \tag{2.78}$$

Energy Equation

Equation (2.68), the energy equation, is a second order, linear, ordinary differential equation, thus requiring two boundary conditions for its solution. These two boundary conditions are known a priori from the wall temperature, T_w, and the approach gas temperature, T_e, both of which are known constants. Therefore

$$T(\eta = 0) = T_w \tag{2.79}$$

$$T(\eta = \eta_e) = T_e \tag{2.80}$$

Elemental Conservation Equations

Equation (2.69), the elemental conservation equations, are a set of K second order, linear, ordinary differential equations. Each of these K equations requires two boundary conditions. From the approach gas composition, the elemental mass fractions at the edge of the boundary layer can be calculated; since these have been assumed constant, then for each of the K elemental conservation equations,

$$\tilde{\omega}_j(\eta = \eta_e) = \tilde{\omega}_{je} \qquad (j = 1, \ldots, K) \tag{2.81}$$

The boundary conditions at the wall ($\eta = 0$) can be deduced from the fact that the burning surface is assumed to be a pure condensed carbon phase. It thus follows that the mass fluxes of oxygen and nitrogen relative to stationary coordinates must individually go to zero at

the wall, while the mass flux of carbon relative to stationary coordinates at the wall must be equal to the net mass transfer rate at the wall. Since

$$\tilde{m}_j = \sum_i e_{ij}\, m_i = \sum_i e_{ij}(m\,\omega_i + J_i) \qquad (j = 1, \ldots, K) \tag{2.82}$$

then

$$\tilde{m}_j = m\,\tilde{\omega}_j + \tilde{J}_j \qquad (j = 1, \ldots, K) \tag{2.83}$$

Therefore, for elements oxygen and nitrogen

$$-m_w = \left(\frac{\tilde{J}_O}{\tilde{\omega}_O}\right)_w = \left(\frac{J_N}{\tilde{\omega}_N}\right)_w \tag{2.84}$$

while, from the compatibility constraint on carbon

$$-m_w = \left(\frac{\tilde{J}_C}{\tilde{\omega}_C - 1}\right)_w \tag{2.85}$$

Combining Equations (2.84, 2.85), two of the boundary conditions applicable at the wall are obtained:

$$\left(\frac{\tilde{J}_O}{\tilde{\omega}_O}\right)_w = \left(\frac{\tilde{J}_N}{\tilde{\omega}_N}\right)_w = \left(\frac{\tilde{J}_C}{\tilde{\omega}_C - 1}\right)_w \tag{2.86}$$

The third boundary condition at the wall can be obtained from the heterogeneous chemical equilibrium of the burning ideal gas reaction

$$C_{(s)} + \tfrac{1}{2}\, O_2 \rightleftharpoons CO \qquad K_s = x_{CO}\left(\frac{P}{x_{O_2}}\right)^{\frac{1}{2}} \tag{2.87}$$

The two boundary conditions given by Equation (2.86), the heterogeneous chemical equilibrium expression of Equation (2.87), and the three

homogenous equilibrium expressions presented in the next chapter, permit the calculation of the six equilibrium species compositions at the surface.

CHAPTER III

FLUID PROPERTIES

The Transport Coefficients

Molecular motion in non-uniform gases promotes uniformity of mass velocity, temperature and composition through the mechanisms of momentum, energy and mass transport. The resulting transport fluxes (Equations 2.5, 2.6, 2.7) involve the gradients of velocity, temperature and composition as well as the characteristic fluid transport coefficients.

Estimation of the transport coefficients is generally based on the Chapman-Enskog kinetic theory. The Maxwellian velocity distribution function of a gas in a uniform steady state satisfies the Boltzmann equations; for a gas in a non-equilibrium state, the distribution of molecular velocities can be obtained by inclusion of small perturbation terms in an infinite series beginning with the Maxwellian distribution. In the present work, the transport coefficients for the single species and species pairs are estimated using the Chapman-Enskog theory with the Lennard-Jones (6-12) potential energy of interaction, except for the estimation of the single species thermal conductivity.

Lennard-Jones (6-12) Potential

The empirical potential energy of interaction between a pair of molecules in the gas is given by the Lennard-Jones (6-12) potential as:

$$\Gamma(r) = 4\,\varepsilon\left[\left(\frac{\sigma}{r}\right)^{12} - \left(\frac{\sigma}{r}\right)^{6}\right] \qquad (3.1)$$

where σ is the characteristic diameter of the molecule (the collision diameter), ε is the characteristic energy of interaction between the molecules, and r is the distance between molecular centers.

The Lennard-Jones potential displays the typical features of molecular interactions and considerable research has shown it to be a good potential energy function. The values of the parameters σ and ε for the molecular species involved in this work are given in Table 1.

Viscosity

The single species viscosity coefficient for a pure monoatomic gas is given by Hirschfelder, Curtiss and Bird (25) as:

$$\mu_i = 2.6693 \times 10^{-5}\frac{(M_i\,T)^{\frac{1}{2}}}{\sigma_i^{\,2}\,\Omega_\mu} \quad \text{(g /cm sec)} \qquad (3.2)$$

for T in degrees Kelvin and σ_i in Å. Although this equation strictly applies only to a pure monoatomic gas, it has been found to be remarkably good for polyatomic gases as well.

The multicomponent gas mixture viscosity was estimated from the pure species viscosities and the mixture composition by the Wilke (25) mixture rule:

$$\mu = \sum_i \left[\frac{x_i\,\mu_i}{\sum_j x_j\,\psi_{ij}}\right] \qquad (3.3)$$

where

Table 1. Species and Molecular Parameters

Species	M_i (g / g . mole)	σ_i (Å)	$(\epsilon/\kappa)_i$ (1/°K)	$H_i(0°K)$ (cal/g .°K)
O_2	31.9988	3.433	113.0	-64.846
N_2	28.0134	3.681	91.5	-73.965
O	15.9994	7.990	113.0	3622.1
N	14.0067	7.940	91.5	7961.8
CO_2	44.0099	3.996	190.0	-2188.0
CO	28.0105	3.590	110.0	-1017.1

$$\psi_{ij} = \frac{1}{\sqrt{8}} \left(1 + \frac{M_i}{M_j}\right)^{-\frac{1}{2}} \left[1 + \left(\frac{\mu_i}{\mu_j}\right)^{\frac{1}{2}} \left(\frac{M_j}{M_i}\right)^{\frac{1}{4}}\right]^2 \tag{3.4}$$

The Wilke mixture rule formulation has been shown to reproduce measured values of viscosity of gas mixtures with an average deviation of about two percent.

Hirschfelder, Curtiss and Bird (25) give an exact expression for the mixture viscosity based on a rigorous first order kinetic theory; however, this formulation was not employed in an effort to conserve computation time.

Thermal Conductivity

The single species thermal conductivity was estimated by the semi-empirical Eucken correlation (25), which applies to monoatomic and polyatomic gases at low density:

$$k_i = \left(C_{pi} + 1.25 \frac{R}{M_i}\right) \mu_i \tag{3.5}$$

The inclusion of the species heat capacity in this equation accounts for the rotational and vibrational energy contributions of polyatomic gases.

The mixture thermal conductivity was obtained from the Wilke mixture rule in the form

$$k = \sum_i \left[\frac{x_i k_i}{\sum_j x_j \psi_{ij}}\right] \tag{3.6}$$

where ψ_{ij} is given by Equation (3.4).

Binary Diffusivities

In an N component mixture there are $(N^2 + N)/2$ binary diffusivities, of which N are the self-diffusion coefficients. The binary diffusivity of a pair of species is independent of composition, according to Hirschfelder, Curtiss and Bird (25), to a rigorous first order kinetic theory approximation, and is given by:

$$\mathcal{D}_{ij} = \mathcal{D}_{ji} = 1.8583 \times 10^{-3} \frac{\left[T^3\left(\frac{1}{M_i} + \frac{1}{M_j}\right)\right]^{\frac{1}{2}}}{P\,\sigma_{ij}^{\,2}\,\Omega_{\mathcal{D}}} \quad (cm^2/sec) \qquad (3.7)$$

where the collision diameter and energy of interaction for the pair of species are given respectively by:

$$\sigma_{ij} = (\sigma_i + \sigma_j)/2 \qquad (3.8)$$

$$\epsilon_{ij} = (\epsilon_i\,\epsilon_j)^{\frac{1}{2}} \qquad (3.9)$$

with T in degrees Kelvin, P in atmospheres, and σ_{ij} in Å.

The calculation of species fluxes in a multicomponent gas mixture from the Stefan-Maxwell equations (22) require the binary diffusivities for all species pairs in the mixture. The calculation of species mass fluxes with respect to the mass average velocity according to Equation (2.71) requires knowledge of the multicomponent diffusivities for all species pairs.

Multicomponent Diffusivities

The multicomponent diffusivities appearing in Equation (2.71) are a function of the gas mixture composition and all the species composi-

tions gradients. Hirschfelder, Curtiss and Bird (25) give the rigorous first order kinetic theory approximation to the multicomponent diffusivities as:

$$D_{ij} = - \frac{M}{M_j} \cdot \frac{[(-1)^{i+j+1}] \cdot |K^{ii}| + |K^{ji}|}{|K|} \qquad (3.10)$$

$$K_{ij} = \frac{x_i}{\mathcal{D}_{ij}} + \frac{M_j}{M_i} \sum_{k \neq i} \frac{x_k}{\mathcal{D}_{ik}} \qquad (i \neq j) \qquad (3.11)$$

$$K_{ii} = 0$$

In Equation (3.10), $|K|$ is the determinant of the matrix K having elements K_{ij} given by Equation (3.11), and $|K^{ji}|$ is the determinant of the matrix K after deletion of the j^{th} row and the i^{th} column.

The Collision Integrals

Equations (3.2, 3.7) require a knowledge of the single specie and the species pair collision integrals. The collision integrals Ω_μ $\Omega_\mathcal{D}$ depend upon the intermolecular forces between the gas molecules. Given a potential energy of interaction model it is possible to calculate the collision integrals; this has been done by Hirschfelder, Bird and Spotz (36), who give the collision integrals for the Lennard-Jones potential as tabulated functions of the reduced temperature ($\kappa T/\epsilon$), where κ is the Boltzmann's constant, over the range $0.30 \leq (\kappa T/\epsilon) \leq 100$.

To avoid the need for the computer storage and interpolation in order to obtain values for the collision integrals, it is desirable to express them as analytic functions of the reduced temperature. Luft and Kharbanda (37) fitted the tabular values of Ω_μ by the expression

$$(\Omega_\mu)^{-1} = 0.697 \left[1 + 0.323 \ln\left(\frac{\kappa T}{\epsilon}\right)\right] \qquad (3.12)$$

Similarly, in the present work, the collision integral Ω_D was fitted by least squares to an expression like that of Luft and Kharbanda over the range $1.45 \leq (\kappa T/\epsilon) \leq 30.0$ to obtain

$$(\Omega_D)^{-1} = 0.7549 \left[1 + 0.3476 \ln\left(\frac{\kappa T}{\epsilon}\right)\right] \qquad (3.13)$$

In the reduced temperature range of interest in this work (1.45 to 30.0) the Luft and Kharbanda equation has an average error of 1.7 percent; the fitted equation for Ω_D has an average error of 1.2 percent when compared to the tabulated values.

The Thermodynamic Properties

Thermodynamic data is widely available for many substances relative to their values at absolute zero. The heat capacity, heat of formation and free energy data for the species of interest in this work were obtained from the JANAF Tables (38), which combine the experimental results available with statistical thermodynamic calculations (based on the rigid rotator - harmonic oscillator model) to yield a reliable tabulation of thermochemical properties.

Ideal Gas Heat Capacity

The heat capacity data fits used in this work are all of the form

$$C_{pi} = A_{i1} + A_{i2}T + A_{i3}T^2 + A_{i4}T^3 + A_{i5}T^{-\frac{1}{2}} \qquad (3.14)$$

The constants for Equation (3.14), with T in degrees Kelvin, the range

Table 2. Ideal Gas Heat Capacity Equations

Species	Heat Capacity Equations	Range	Average Error
	C_{pi} (cal/g · °K) (T in °K)	(°K)	(%)
O_2	$(6.732 + 1.515\times10^{-3}T - 1.791\times10^{-7}T^2)/31.9988$	273-3800	1.20
N_2	$(6.529 + 1.488\times10^{-3}T - 2.271\times10^{-7}T^2)/28.0134$	273-3800	0.72
O	$(5.6916 - 1.5567\times10^{-3}T + 1.0398\times10^{-6}T^2 - 2.1550\times10^{-10}T^3)/15.9994$	273-2500	0.70
N	$(4.9545 + 5.7012\times10^{-5}T - 5.3510\times10^{-8}T^2 + 1.3738\times10^{-11}T^3)/14.0067$	273-3900	0.06
CO_2	$(18.036 - 4.474\times10^{-5}T - 158.08T^{-\frac{1}{2}})/44.0099$	273-3800	0.54
CO	$(6.480 + 1.566\times10^{-3}T - 2.387\times10^{-7}T^2)/28.0105$	273-3800	1.01

over which the equation was fitted by least squares multiple regression, and the average error from the tabulated JANAF values are presented in Table 2. The heat capacity data fits for O_2, N_2, CO_2 and CO are taken from Kobe (39); the third degree polynomial fits for O and N were obtained from a least squares multiple regression analysis. The mixture heat capacity is given by

$$C_p = \sum_i \omega_i \, C_{pi} \tag{3.15}$$

Ideal Gas Enthalpy

The species enthalpy can be obtained directly from the integration of the species heat capacity equations,

$$H_i(T) = H_i(T_o) + \int_{T_o}^{T} C_{pi} \, dT \tag{3.16}$$

Performing this integration with C_{pi} from Equation (3.14):

$$H_i(T) = H_i(T_o) + \left[A_{i1}T + \tfrac{1}{2}A_{i2}T^2 + \tfrac{1}{3}A_{i3}T^3 + \tfrac{1}{4}A_{i4}T^4 + 2A_{i5}T^{\frac{1}{2}}\right]_{T_o}^{T} \tag{3.17}$$

Letting $T_o = 0^oK$, the lower limit of integration vanishes and therefore

$$H_i(T) = H_i(0^oK) + A_{i1}T + \tfrac{1}{2}A_{i2}T^2 + \tfrac{1}{3}A_{i3}T^3 + \tfrac{1}{4}A_{i4}T^4 + 2A_{i5}T^{\frac{1}{2}} \tag{3.18}$$

The quantity $H_i(0^oK)$ is the enthalpy of the species at 0^oK, which can be determined by specifying a reference state at which the heats of formation of the species are known.

The reference state is established by defining the absolute enthalpy of the elements in their standard state equal to zero at 298.16°K. The enthalpy of an element at absolute zero (H_o) is then equal to the change in enthalpy from the reference temperature to absolute zero, i.e., $(H_{298.16} - H_o)_i$. For a compound the absolute enthalpy at the reference temperature is no longer equal to zero, but is equal to the heat of formation of the particular compound from the reference elements. Therefore, in order to determine the enthalpy of a compound at absolute zero, it is necessary to correct for the heat of formation

$$H_i(0^oK) = - (H_{298.16} - H_o)_i + (\Delta H_f)_{298.16,i} \qquad (3.19)$$

The values of $H_i(0^oK)$ for each of the species under consideration are also given in Table 1.

Thermochemical Equilibrium Constants

The possibility of either homogeneous reactions in the gas phase or of heterogeneous reactions at the solid-gas interphase is not precluded in the present work. Instead, it is assumed that the reactions taking place are not kinetically controlled but rather proceed, without kinetic hindrance, to attain thermochemical equilibrium.

Six species are contained in the gas phase (O_2, N_2, O, N, CO_2, CO) which are made up of three distinct elements (O, N, C). Since the number of independent equilibrium expressions relating the species compositions equals the number of species minus the number of elements, we thus have three independent equilibrium expressions, and are free to postulate any three reaction paths we desire (provided, of course, that

all six species present in the gas phase are represented in the three reactions).

The three homogeneous reactions postulated, along with their ideal gas equilibrium constants are:

$$CO_2 \rightleftarrows CO + \frac{1}{2} O_2 \qquad K_{CO} = \frac{x_{CO}}{x_{CO_2}} \left(P\, x_{O_2}\right)^{\frac{1}{2}} \tag{3.20}$$

$$\frac{1}{2} O_2 \rightleftarrows O \qquad K_O = x_O \left(\frac{P}{x_{O_2}}\right)^{\frac{1}{2}} \tag{3.21}$$

$$\frac{1}{2} N_2 \rightleftarrows N \qquad K_N = x_N \left(\frac{P}{x_{N_2}}\right)^{\frac{1}{2}} \tag{3.22}$$

The JANAF Tables (38) present data on $\log \gamma_i$ as a function of temperature, where γ_i is the equilibrium constant for the formation of the i^{th} species from its constitutive elements in the standard state. Therefore,

$$\log K_{CO} = \log \gamma_{CO} + \frac{1}{2} \log \gamma_{O_2} - \log \gamma_{CO_2} \tag{3.23}$$

$$\log K_O = \log \gamma_O - \frac{1}{2} \log \gamma_{O_2} \tag{3.24}$$

$$\log K_N = \log \gamma_N - \frac{1}{2} \log \gamma_{N_2} \tag{3.25}$$

The values of $\log K_{CO}$, $\log K_O$, and $\log K_N$ as functions of temperature were fitted by a least squares method to obtain

$$\log K_{CO} = 4.4864 - 14742.1/T \tag{3.26}$$

$$\log K_O = 3.3431 - 13037.8/T \tag{3.27}$$

$$\log K_N = 3.2222 - 24701.8/T \tag{3.28}$$

with T in degrees Kelvin. Over the temperature range of interest in this work, 100 $^oK \leq T \leq 2500\ ^oK$, the fitted equations for $\log K_{CO}$, $\log K_O$ and $\log K_N$ had average percent errors of 0.41, 0.80 and 0.54 percent respectively.

At the solid-gas interphase, in addition to the six gaseous species, solid carbon is also present. Therefore, four (7-3) equilibrium expressions are independent. Of these, three are the given homogeneous equilibrium expressions. The fourth, i.e., the heterogeneous equilibrium expression, can be obtained by postulating any reaction involving the solid carbon, such as

$$C_{(s)} + \frac{1}{2}\, O_2 \rightleftharpoons CO \qquad K_s = x_{CO}\left(\frac{P}{x_{O_2}}\right)^{\frac{1}{2}} \tag{3.29}$$

A least squares fit of

$$\log K_s = \log \gamma_{CO} - \frac{1}{2} \log \gamma_{O_2} \tag{3.30}$$

as a function of temperature, over the range of 100 $^oK \leq T \leq 2500\ ^oK$ resulted in the following equation, which has an average percent error of 0.39 percent:

$$\log K_s = 4.5855 + 5817.79/T \tag{3.31}$$

with T in degrees Kelvin.

Ideal Gas Equation of State

The ideal gas equation of state relates pressure, temperature and density by

$$P M = \rho R T \tag{3.32}$$

CHAPTER IV

NUMERICAL SOLUTION OF THE TRANSPORT EQUATIONS

In the previous chapters the transport equations were presented in forms suitable for numerical solution. In addition, models were presented for the estimation of the necessary transport and thermodynamic properties. This chapter contains a detailed description of the numerical implementation of the previously developed transport equations and physical property estimation models.

The method of presentation will be to first outline the overall numerical analysis with a general description of the logical process. Secondly, the technique employed in the integration of the transport equations will be discussed and its accuracy will be estimated by comparing the solution of the constant property momentum equation with the solutions available in the literature. Finally, each of the major operational subroutines involved in the numerical solution of the transport equations will be separately discussed in some detail.

The General Problem

A simplified flow diagram of the stagnation line analysis is given in Figure 2. Each element of this flow diagram represents an operational subroutine. The three logical subroutines (SPCLUP, MOMLUP, ENGLUP) are shown encompassing their respective operational subroutines; each of the logical subroutines corresponds to one of the three nested levels of iteration.

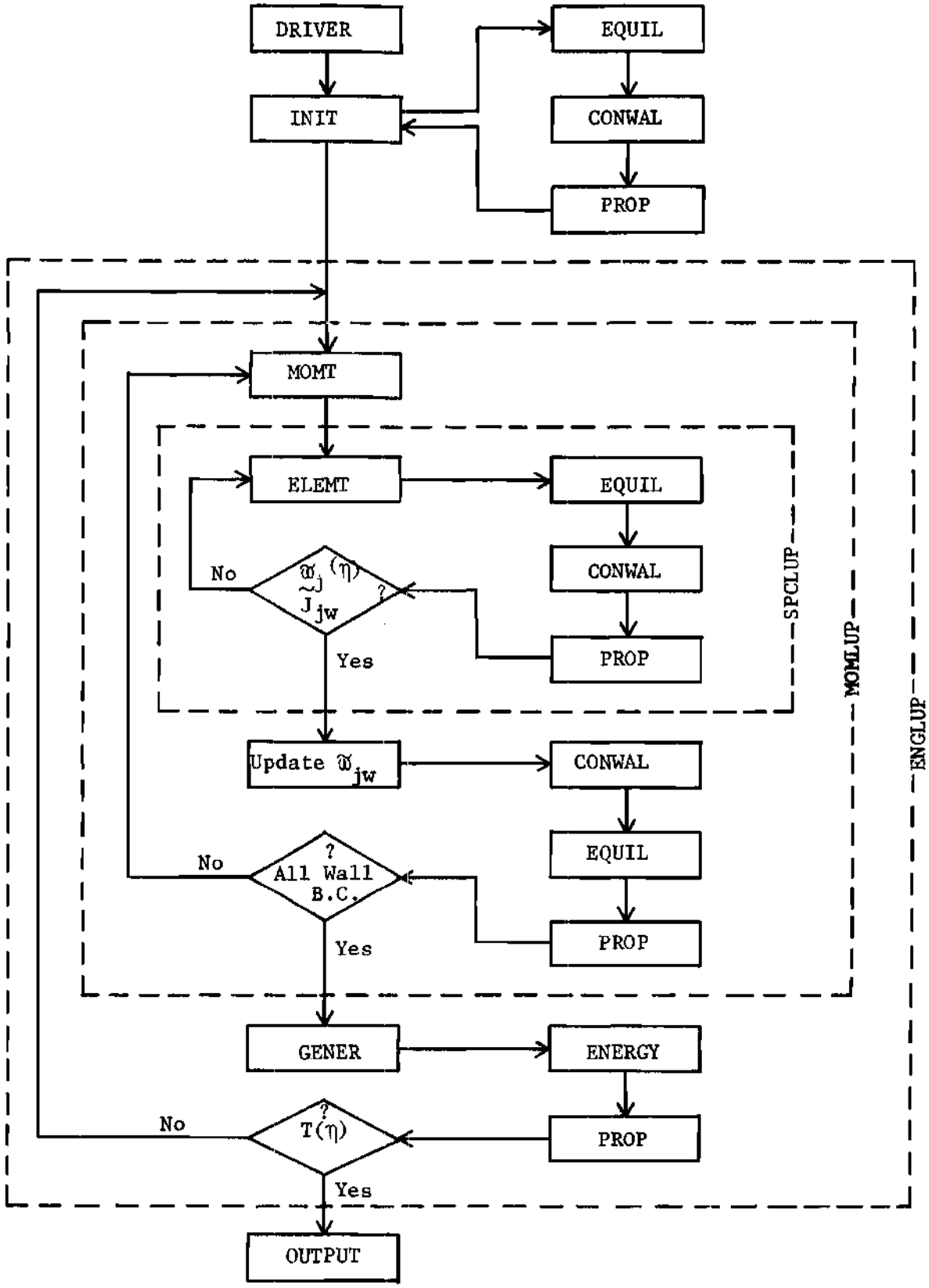

Figure 2. Simplified Flow Diagram of the Computer Program

The main program (DRIVER) reads in key parameters of the problem and serves to transfer control between the logical subroutines. The DRIVER program reads in the free stream velocity, temperature, pressure and composition; the body radius of curvature at the stagnation point and the surface temperature; and the finite difference step size along the η plane, as well as the number of finite difference stations to be considered. In addition, the DRIVER program reads in the maximum number of iterations and the convergence tolerance for each stage of the calculation.

The subroutine INIT initializes the numerical solution by loading in the data for the system under consideration (M_i, σ_i, ϵ_i, A_{ij}, B_{ij}, $H_i(0^oK)$, and e_{ij}). If desired, this subroutine will read in (from an input data deck) the elemental mass fraction, temperature and velocity profiles; otherwise, the subroutine loads into memory specified temperature and velocity profiles, and generates internally the elemental mass fraction profiles. Using the temperature profile, the values of the thermochemical equilibrium constants are computed throughout the flowfield and at the wall, which are used, along with the elemental mass fraction profiles, to calculate the species mole fractions in the flowfield (subroutine EQUIL) and at the wall (subroutine CONWAL). Finally, the subroutine INIT calls on the subroutine PROP to calculate all the transport and thermodynamic properties at each location (M, ρ, ω_i, C_{pi}, C_p, μ_i, μ, k_i, k, $\mathcal{D}_{ij}$, D_{ij}, H_i, H, $\widetilde{\omega}_j$, and K_i). The subroutine PROP also calculates species and elemental mass fluxes with respect to the mixture mass average velocity (diffusive fluxes), and with respect to stationary coordinates, as well as the effective elemental diffusivities, $\widetilde{D}_j$. Upon return of

control from PROP, the subroutine INIT makes an initial estimate of the wall mass transfer rate based on the fluxes computed previously.

Using the computed density and viscosity profiles, the subroutine MOMT solves the momentum equation to yield an update of the velocity distribution. In the solution of the momentum equation the most recent wall mass transfer rate is used as the unknown boundary condition on f_w.

The innermost iterative loop uses the most recent velocity profile and effective elemental diffusivities to solve the elemental conservation equations (subroutine ELEMT). The resulting elemental mass fraction profiles and the most recent temperature distribution are employed in the subroutines EQUIL and CONWAL to obtain new species mole fraction profiles. With the updated species mole fraction profiles the subroutine PROP is called to update the transport and thermodynamic properties and to calculate new values of $\tilde{\mathcal{D}}_j$ for the next pass through the subroutine ELEMT.

The sequence of subroutines ELEMT-EQUIL-CONWAL-PROP constitutes the innermost iterative loop and it is monitored by the logical subroutine SPCLUP. This subroutine iterates on the above sequence, for a given set of f_w and $\tilde{\omega}_{jw}$, until all three $\tilde{\omega}_j$ profiles and the boundary condition ratios $(\tilde{J}_0/\tilde{\omega}_0)_w$, $(\tilde{J}_N/\tilde{\omega}_N)_w$, and $(\tilde{J}_C/(\tilde{\omega}_C - 1))_w$ for the last two iterations differ by less than the desired convergence tolerance (TLSPCL). Convergence of the subroutine SPCLUP insures that the composition dependence of the coefficients in the elemental conservation equations is consistent with the compositions predicted from the solution of those equations.

In general, the wall boundary conditions will not be satisfied,

and it becomes necessary to search for new values of the pseudo-boundary conditions, $^{*}\ \widetilde{\omega}_{jw}$, with which to make another iterative pass through the subroutine SPCLUP. This is simply done by linearly extrapolating the ratio $(\widetilde{\omega}_0/\widetilde{\omega}_N)_w$ to the ratio $(\widetilde{J}_0/\widetilde{J}_N)_w$ from the last two iterative passes through the subroutine SPCLUP. If k and (k - 1) represent the last two passes, then

$$\frac{\left(\frac{\widetilde{\omega}_0}{\widetilde{\omega}_N}\right)_w^{k+1} - \left(\frac{\widetilde{\omega}_0}{\widetilde{\omega}_N}\right)_w^{k}}{\left(\frac{\widetilde{\omega}_0}{\widetilde{\omega}_N}\right)_w^{k} - \left(\frac{\widetilde{\omega}_0}{\widetilde{\omega}_N}\right)_w^{k-1}} = \frac{\left(\frac{\widetilde{\omega}_0}{\widetilde{\omega}_N}\right)_w^{k+1} - \left(\frac{\widetilde{J}_0}{\widetilde{J}_N}\right)_w^{k}}{\left(\frac{\widetilde{J}_0}{\widetilde{J}_N}\right)_w^{k} - \left(\frac{\widetilde{J}_0}{\widetilde{J}_N}\right)_w^{k-1}} \tag{4.1}$$

which can be solved for the desired value of $(\widetilde{\omega}_0/\widetilde{\omega}_N)_w^{k+1}$ to be used in the next iteration. The subroutine CONWAL is again accessed with the ratios $(\widetilde{\omega}_0/\widetilde{\omega}_N)_w$ and $((\widetilde{\omega}_C - 1)/\widetilde{\omega}_N)_w$, as well as the four thermochemical equilibrium relations at the wall. Converting the composition at the wall to elemental mass fractions, the new pseudo-boundary conditions at the wall are obtained. In order to avoid a sharp change in the $\widetilde{\omega}_j$ profiles near the wall due to the change in the $\widetilde{\omega}_{jw}$ pseudo-boundary conditions, the $\widetilde{\omega}_j$ profiles are smoothed by making them similar to the corresponding profiles from the last solution of the subroutine SPCLUP. With smoothed $\widetilde{\omega}_j$ profiles, the subroutine EQUIL is called to calculate the new equilibrium species mole fractions, and then the subroutine

---

* In the context of this discussion, the "pseudo-boundary conditions at the wall" refer to the value of the $\widetilde{\omega}_{jw}$ used in the current pass through the subroutine SPCLUP; these values are used in the iterative process, instead of the actual boundary conditions, (Equations 2.78, 2.86), until the actual boundary conditions are satisfied.

PROP is again called to estimate new physical properties and fluxes.

Using the fluxes calculated by the subroutine PROP, the boundary conditions at the wall are tested for convergence. The wall mass transfer rates calculated from Equations (2.78, 2.84, 2.85) are averaged to obtain the updated value of f_w:

$$f_w = \frac{1}{3}\left[f_O + f_N + f_C\right]_w \tag{4.2}$$

where,

$$\left(f_O\right)_w = \left[\frac{R_b}{2\ \rho_e\ \mu_e\ U_e}\right]^{\frac{1}{2}} \left(\frac{\mathcal{J}_O}{\tilde{\omega}_O}\right)_w \tag{4.3}$$

$$\left(f_N\right)_w = \left[\frac{R_b}{2\ \rho_e\ \mu_e\ U_e}\right]^{\frac{1}{2}} \left(\frac{\mathcal{J}_N}{\tilde{\omega}_N}\right)_w \tag{4.4}$$

$$\left(f_C\right)_w = \left[\frac{R_b}{2\ \rho_e\ \mu_e\ U_e}\right]^{\frac{1}{2}} \left(\frac{\mathcal{J}_C}{\tilde{\omega}_C - 1}\right)_w \tag{4.5}$$

The value calculated from Equation (4.2) is used as the new estimate of f_w in the next solution of the momentum equation; and the new pseudo-boundary conditions at the wall, $\tilde{\omega}_{jw}$, are then used in the next pass through the subroutine SPCLUP. The momentum and elemental conservation equation boundary conditions were adjusted as discussed above in the subroutine MOMLUP. The logical subroutine MOMLUP, which monitors the intermediate level of iterations in the numerical scheme, also serves to control access to the subroutines MOMT and SPCLUP.

The subroutine MOMLUP was considered convergent when the wall boundary conditions given by Equations (2.78, 2.86) were satisfied to

the desired level of accuracy. Once the subroutine MOMLUP has converged, all the previously unknown boundary conditions have been determined (for the temperature profile in use at the time). The results at this point would be the solution of the problem if the temperature profile used in the calculations were "correct."

The outermost level of iterations is accomplished by the subroutine ENGLUP. Following convergence of the subroutine MOMLUP, the species conservation equations are solved (subroutine GENER) to obtain the species generation terms, r_i. The energy equation is then solved (subroutine ENERGY) to obtain an updated temperature profile. If the resulting temperature profile differs from the old one by less than the desired convergence tolerance (TLENER), the entire numerical solution can be considered convergent; otherwise, the outermost energy loop (subroutine ENGLUP) is repeated until the last two temperature profiles have converged, along with all the boundary conditions at the wall.

Once the solution has been completed, Equation (2.52) is integrated to obtain the relationship between η and y that permits the transformation of the solution back to the real coordinate space. The above integration is performed by the subroutine OUTPUT, which also serves to print out the final results of the calculation.

Integration of the Transport Equations

Most analysis in boundary layer theory reduce to the solution of nonlinear ordinary differential equations with split boundary conditions. In the following pages, a few of the most frequently used techniques for the solution of ordinary differential equations are briefly discussed.

The numerical solutions of all the transport equations encountered in the present work were obtained by application of the method of successive replacements.

One technique that is suitable only to linear differential equations or to nonlinear differential equations that can be quasi-linearized employs matrix algebra. In this technique, the linear (or quasi-linearized nonlinear) differential equation is represented by a system of linear finite difference equations, one for each grid point in the mesh. The resulting system of linear finite difference equations can then be solved by matrix inversion. For example, the solution of a second order, linear, ordinary differential equation with split boundary conditions can always be reduced to the problem of inverting a tridiagonal matrix if the finite difference representation of the equation involves only first and second order central differences.

Sometimes it is necessary to solve a nonlinear differential equation without resorting to linearization; this is often done by one of the "shooting" methods. In these methods, the values of the function and its derivatives at one boundary are specified, thus converting the problem from a split boundary value problem to an initial value problem. The initial value problem can then be solved by one of the standard methods, such as fourth-order Runge-Kutta-Gill (40) or Adams-Moulton (41). However, once the solution of the initial value problem is obtained, it is necessary to iterate on the assumed boundary conditions at the first boundary until the specified boundary conditions at the second boundary are satisfied. For problems involving several high order differential equations with many split boundary conditions, it is often very diffi-

cult to obtain solutions by these methods due to the sensitivity of the solution to the assumed values at the first boundary (42).

The method of accelerated successive replacements (42, 43) is another numerical scheme which is often used to solve nonlinear differential equations with split boundary conditions. This method was employed in the numerical solution of the transport equations encountered in the present work. The main advantage of this method as compared to the "shooting" methods is that the boundary conditions at both boundaries are satisfied at every stage of the iteration. Furthermore, the method of accelerated successive replacements is applicable to nonlinear differential equations (such as the momentum equation) without requiring quasi-linearization.

To apply the method of accelerated successive replacements, the differential equation is represented by a system of finite difference equations which can then be solved by an iterative technique suitable for finding the roots of algebraic equations. The solution of the differential equation is begun by assuming some functional dependence of the dependent variable on the independent variable which satisfies all boundary conditions. The differential equation and the assumed profile are then represented in finite difference form; the iterative solution is then analogous to a mathematical relaxation of the assumed initial profile to the final solution. Since the conditions at both boundaries are fixed and satisfied at every iteration, the main disadvantage of the "shooting" methods is eliminated. The iterative solution of the nonlinear algebraic equations is generally achieved, as was done in the present work, by using the Newton-Raphson technique with an accelerating

factor and immediate replacement at each grid point.

As an example of the use of the method of accelerated successive replacements consider the following second order, nonlinear, ordinary differential equation (which is somewhat similar to the momentum equation):

$$y\,(y'' + 1) + (y')^2 = 0 \qquad \begin{matrix} y(1) = 1 \\ y(2) = 2 \end{matrix} \tag{4.6}$$

where y is the dependent variable and the primes denote differentiation with respect to the independent variable, x. Consider the interval $1 \le x \le 2$ to be divided into (s - 1) equal subintervals and let y_n be the value of the dependent variable at the point x_n, where the index n varies from n = 1, 2, ..., s, and the boundary conditions are known at the two points x_1 and x_s. The constant step size is given by $\Delta = (x_s - x_1)/(s - 1)$. The finite difference representation of Equation (4.6) that was used is:

$$y_n \left[\left(\frac{y_{n+1} - 2y_n + y_{n-1}}{\Delta^2}\right) - 1\right] + \left(\frac{y_{n+1} - y_{n-1}}{2\Delta}\right)^2 = 0 \quad (n=2,\ldots,s-1)$$

$$y_1 = 1 \tag{4.7}$$

$$y_s = 2$$

Assume initially a linear profile which satisfies both boundary conditions:

$$y_n = y_1 + \Delta\,(n - 1)\,(y_s - y_1) \qquad (n = 1,\ldots,s) \tag{4.8}$$

The system of algebraic Equations (4.7) is a system of (s - 2) non-linear equations for the (s - 2) unknowns of y_n.

The Newton-Raphson iterative technique (43) gives the value of y_n at the k^{th} iteration as:

$$y_n^k = y_n^{k-1} - \frac{\alpha\, G_n}{\left(\frac{\partial G_n}{\partial y_n}\right)} \qquad \begin{matrix}(n = 2,\ldots, s-1)\\ (k = 1,\ldots, k_{max})\end{matrix} \tag{4.9}$$

where G_n is the finite difference representation of Equation (4.7). The acceleration factor, α, is a real number such that $\alpha > 0$; generally, $\alpha = 1$ but, if desired, the rate of convergence can be accelerated ($\alpha > 1$) or decelerated ($0 < \alpha < 1$). Since, with successive replacements, new values of y_n are used in the iterative scheme as soon as they are obtained, then Equation (4.9) becomes:

$$y_n^k = y_n^{k-1} - \alpha \frac{\left[y_n^{k-1}\left(\frac{y_{n+1}^{k-1} - 2y_n^{k-1} + y_{n-1}^{k}}{\Delta^2} - 1\right) + \left(\frac{y_{n+1}^{k-1} - y_{n-1}^{k}}{2\Delta}\right)^2\right]}{\left[-\frac{2y_n^{k-1}}{\Delta^2} + \left(\frac{y_{n+1}^{k-1} - 2y_n^{k-1} + y_{n-1}^{k}}{\Delta^2} - 1\right)\right]} \tag{4.10}$$

$$(n = 2,\ldots, s-1)$$

$$(k = 1,\ldots, k_{max})$$

The Newton-Raphson iterative scheme is begun with k = 1 using the profile of Equation (4.8) as that of the zeroth iteration, and it is continued until a desired convergence tolerance has been satisfied (such as $\left|\left(y_n^k / y_n^{k-1}\right) - 1\right| \leq 10^{-4}$) at every location n, or until the specified maximum number of iterations, k_{max}, has been reached.

Accuracy of the Method of Accelerated Successive Replacements

A study of the accuracy of the method of accelerated successive replacements was conducted to estimate the accuracy of the numerical results obtained. For this study, the constant property momentum boundary layer equation for a cylinder in crossflow ($\beta = 1$) was solved and the results were compared to those available in the literature; the momentum equation was chosen since, due to its nonlinearity, it was expected to be more difficult to solve than the linear elemental conservation and energy equations.

The momentum equation solved was:

$$f''' + ff'' - (f')^2 + 1 = 0 \tag{4.11}$$

with the boundary conditions:

$$\begin{aligned} f\ (\eta = 0) &= f_w \\ f'\ (\eta = 0) &= 0 \\ f'\ (\eta = \eta_e) &= 1 \end{aligned} \tag{4.12}$$

The finite difference representation of Equation (4.11) was identical to that presented in the discussion of the variable property momentum equation which follows, except in that the coefficient $C = 1$ and $(\rho_e/\rho) = 1$. In the accuracy study the value of η_e was arbitrarily selected as 10; step sizes of 0.10, 0.05, and 0.025 were considered for each of two wall mass transfer rates, $f_w = 0$ and $f_w = -0.5$. In all cases a linear f' profile was initially assumed between $\eta = 0$ and $\eta_e = 10$. The iterative

scheme was considered to have converged when all of the following criteria were simultaneously met:

$$\left| \frac{(f'_n)^k}{(f'_n)^{k-1}} - 1 \right| \leq 10^{-6} \qquad (n = 2, \ldots, s-1) \qquad (4.13)$$

$$\left| \frac{(f''_w)^k}{(f''_w)^{k-1}} - 1 \right| \leq 10^{-6}$$

If the above convergence criteria was not met in less than 1000 iterations, the iterative process was stopped.

Elzy and Sisson (9) have calculated extensive similar solutions to the constant property boundary layer equations. For the two cases of interest here (the momentum equation with $\beta = 1$, $f_w = 0$; and with $\beta = 1$, $f_w = -0.5$) other investigators have published results. The Elzy and Sisson profiles of f, f', f'', and f''' agree with those of previous investigators to the accuracy estimated by the earlier workers. Moreover, by repeating the integration process with a smaller step size, Elzy and Sisson have verified their reported values of f''_w and the f' profiles to be accurate to at least eight significant figures. The method of solution employed by Elzy and Sisson was the multiple step predictor-corrector method of Milne (41). The results obtained in the integration of the constant property momentum equation by the method of accelerated successive replacements in the present work were thus compared to the results of Elzy and Sisson to estimate the accuracy of the numerical procedure.

The velocity profiles, $f'(\eta)$, calculated in the present work

(for $f_w = 0$, and for $f_w = -0.5$) agreed with those of Elzy and Sisson to approximately four significant figures* when $\Delta = 0.10$. As the step size was reduced to $\Delta = 0.05$, the velocity profiles became accurate to approximately five significant figures. A further reduction of the step size to $\Delta = 0.025$ was attempted, but the method failed to meet the required convergence criteria in less than 1000 iterations.

When solving finite difference equations it is generally more desirable to extrapolate the results to the "smallest" step size than to actually perform the calculations employing a very minute step size; as a rule, the extrapolation results in a considerable net savings in computational effort. One method of extrapolation to the "smallest" step size involves obtaining a solution using a step size half as large as the first; the extrapolated value of the solution variable $Z(\eta)$ is given by:

$$Z(\eta) = \frac{4\, Z(\eta, \Delta) - Z(\eta, \tfrac{1}{2}\Delta)}{3} \qquad (4.14)$$

When this method of extrapolation was applied to the solutions using $\Delta = 0.10$ and $\Delta = 0.05$ (for both $f_w = 0$ and $f_w = -0.5$) the velocity profiles were found to agree with those reported by Elzy and Sisson to approximately six significant figures.

---

*In the context of the present discussion, two profiles tabulated at discrete intervals agree to "approximately X significant figures" if, in fact, the profiles agree to X significant figures with the exception of a few values that agree to (X - 1) significant figures. These lower accuracy values generally occur in the vicinity of the wall and are due to the fact that multipoint central difference approximations can not be used at or near a boundary.

Table 3. Accuracy of the Method of Accelerated Successive Replacements in the Solution of the Constant Property Momentum Equation

f_w	Step Size	Iterations Required	$(f'')_w$
0	0.10	133	1.23312294
0	0.05	339	1.23269045
0	"smallest"	Eqn. (4.14)	1.23254629
0	Reference (9)		1.2325877*
-0.5	0.10	126	0.96954624
-0.5	0.05	350	0.96928412
-0.5	"smallest"	Eqn. (4.14)	0.96919675
-0.5	Reference (9)		0.96922955*

* Data from Elzy and Sisson (9)

Table 3 summarizes the results of the accuracy test with respect to the calculation of f''_w. Since f''_w was calculated from the $f'(\eta)$ profiles using a four point forward difference formula, the accuracy of the value of f''_w was expected to be about one significant figure less than that of the profile from which it was calculated. As shown in Table 3, the above was found to be the case for all four calculated solutions that met the desired convergence criteria; extrapolation of the computed results for $\Delta = 0.10$ and $\Delta = 0.05$ to the "smallest" step size improved the accuracy of the calculated values of f''_w by approximately one additional significant figure beyond that of $\Delta = 0.05$.

In summary, it was concluded that with a simple finite difference representation of the highly nonlinear momentum equation a solution was obtained, for $\Delta = 0.10$, in which the $f'(\eta)$ profiles were accurate to approximately four significant figures and the value f''_w was accurate to approximately three significant figures. It was shown that additional accuracy would be obtained by decreasing the step size (at the expense of computation time as indicated by the required number of iterations) and even further accuracy would be obtained by extrapolating to the "smallest" step size.

All the later calculations performed in the present work employed a step size of $\Delta = 0.10$. The results presented in the following chapter have been truncated to show only the figures that were considered accurate.

Finite Difference Representation of the Transport Equations

The high Reynolds number boundary layer transport equations solved

in the present work were presented in Chapter II. In the following sections these equations are presented in their finite difference forms. A complete listing of the computer programs, written in FORTRAN V for the UNIVAC 1108 computer is presented in the Appendix. The reader interested in further details on the numerical implementation of the equations should refer to the Appendix.

Momentum Equation

The momentum equation, written to take into account the variation in physical properties, is given by Equation (2.67). This equation can be considered as a third order equation for $f(\eta)$ or as a second order equation for the velocity ratio $f'(\eta)$, with $f(\eta)$ being the result of a simple integration:

$$f(\eta) = f_w + \int_o^{\eta} f'(\eta)\, d\,\eta \qquad (4.15)$$

For an initial $f'(\eta)$ profile and the given boundary conditions f_w, $f'(0) = 0$, $f'(\eta_e) = 1.0$, Equation (4.15) was integrated numerically using up to fourth order Newton-Cotes closed-end formulas (41). The $f(\eta)$ profile thus generated, along with the initial $f'(\eta)$ profile, were used in the first iteration of the method of successive replacement to generate a new $f'(\eta)$ profile; this new $f'(\eta)$ profile was again integrated by Equation (4.15), and the process was repeated until the solution attained the desired level of convergence. The criteria used to determine convergence was that

$$\left| \frac{(f'_n)^k}{(f'_n)^{k-1}} - 1 \right| \leq \text{TLMOMT} \qquad (n = 2,\ldots, s-1) \qquad (4.16)$$

$$\left| \frac{(f''_w)^k}{(f''_w)^{k-1}} - 1 \right| \leq \text{TLMOMT}$$

where TLMOMT is a predetermined input number (10^{-6} was used in this study).

The momentum equation, written in the form of Equation (4.9) becomes

$$(f'_n)^k = (f'_n)^{k-1} - \alpha \frac{G_n}{\left(\frac{\partial G_n}{\partial (f'_n)}\right)} \qquad \begin{matrix}(n = 2,\ldots, s-1) \\ (k = 1,\ldots, k_{max})\end{matrix} \qquad (4.17)$$

where

$$G_n = \frac{(f'_{n+1})^{k-1} - 2(f'_n)^{k-1} + (f'_{n-1})^k}{\Delta^2} \qquad (4.18)$$

$$+ \frac{(C_{n+1} - C_{n-1}) + (f_n)^{k-1}}{2\,\Delta\,C_n} \cdot \frac{(f'_{n+1})^{k-1} - (f'_{n-1})^k}{2\,\Delta}$$

$$+ \frac{\left(\frac{\rho_e}{\rho_n}\right) - \left((f'_n)^{k-1}\right)^2}{C_n} \qquad \begin{matrix}(n = 2,\ldots, s-1) \\ (k = 1,\ldots, k_{max})\end{matrix}$$

(The numerical solution of the momentum equation is implemented in the subroutine MOMT.)

Elemental Conservation Equations

The variable property elemental conservation equations are Equation (2.69) with boundary conditions given by Equations (2.78, 2.86). The elemental conservation equations were solved by assuming pseudo-boundary conditions, $\tilde{\omega}_{jw}$, and interating on those (in the subroutine MOMLUP) until Equations (2.78, 2.86) were satisfied.

The three elemental conservation equations are not independent; if all K elemental conservation equations are added, the result is the continuity equation, which is identically satisfied by the definition of the streamfunction. Therefore, only (K - 1) elemental conservation equations need to be solved; the K^{th} elemental mass fraction profile can be simply obtained by difference $\left(\sum_j \tilde{\omega}_j = 1 \right)$.

The iterative scheme for the solution of the elemental conservation equations, written in the form of Equation (4.9), is:

$$\tilde{\omega}_{jn}^{k} = \tilde{\omega}_{jn}^{k-1} - \alpha \frac{G_n}{\left[\frac{\partial G_n}{\partial \tilde{\omega}_{jn}}\right]} \qquad \begin{matrix} (j = 1, \ldots, K - 1) \\ (n = 2, \ldots, s - 1) \\ (k = 1, \ldots, k_{max}) \end{matrix} \qquad (4.19)$$

where G_n is, from Equation (2.69):

$$G_n = \left[\frac{(\rho^2 \tilde{D}_j)}{f \rho_e \mu_e + (\rho^2 \tilde{D}_j)'} \right]_n \cdot \frac{\tilde{\omega}_{j\ n+1}^{k-1} - 2\tilde{\omega}_{j\ n}^{k-1} + \tilde{\omega}_{j\ n-1}^{k}}{\Delta^2} \qquad (4.20)$$

(continued)

$$+ \frac{\tilde{\omega}_{j\ n+1}^{k-1} - \tilde{\omega}_{j\ n-1}^{k}}{2\Delta} \qquad \begin{matrix}(j = 1,\ldots, K-1)\\ (n = 2,\ldots, s-1)\\ (k = 1,\ldots, k_{max})\end{matrix}$$

The (K - 1) elemental conservation equations were solved by the iterative procedure of Equation (4.19) until the following conditions were met simultaneously:

$$\left| \frac{\tilde{\omega}_{j\ n}^{k}}{\tilde{\omega}_{j\ n}^{k-1}} - 1 \right| \leq \text{TLELEM} \qquad \begin{matrix}(j = 1,\ldots, K-1)\\ (n = 2,\ldots, s-1)\end{matrix} \qquad (4.21)$$

where the desired level of convergence was input as TLELEM (10^{-6} was used in this study). (The elemental conservation equations were solved in the subroutine ELEMT.)

Energy Equation

The energy equation (2.68) is a second order, linear, ordinary differential equation with boundary conditions given by Equations (2.79, 2.80). The iterative scheme for the solution of the energy equation by the method of accelerated successive replacements is:

$$T_n^{\,k} = T_n^{\,k-1} - \alpha \frac{G_n}{\left(\frac{\partial G_n}{\partial T_n}\right)} \qquad \begin{matrix}(n = 2,\ldots, s-1)\\ (k = 1,\ldots, k_{max})\end{matrix} \qquad (4.22)$$

where G_n is, from Equation (2.68):

$$G_n = \left(\frac{C\ C_p}{P_r}\right)_n \cdot \frac{T_{n+1}^{k-1} - 2\ T_n^{\,k-1} + T_{n-1}^{k}}{\Delta^2} + \frac{U_e^{\,2}\ f'_n\ C_{pn}\ T_n^{k-1}}{C_{pe}\ T_e} \qquad (4.23)$$

(continued)

$$+\left[\left(\frac{C\,C_p}{Pr}\right)' + C_p\,f - \left(\frac{R_b}{2\,\rho_e\,\mu_e\,U_e}\right)^{\frac{1}{2}}\left(\sum_i C_{pi}\,J_i\right)\right]_n \cdot \frac{T_{n+1}^{k-1} - T_n^k}{2\,\Delta}$$

$$+ U_e^2\left[C(f'')^2 - f'\left(\frac{\rho_e}{\rho}\right)\right]_n - \frac{R_b}{2\,U_e}\left(\frac{1}{\rho}\sum_i H_i\,r_i\right)_n \qquad (n = 2,\ldots,s-1)$$

$$(k = 1,\ldots,k_{max})$$

The iterative procedure of Equation (4.22) was repeated until the following conditions were met:

$$\left|\frac{T_n^k}{T_n^{k-1}} - 1\right| \leq \text{TLENER} \qquad (n = 2,\ldots,s-1) \qquad (4.24)$$

where the desired level of convergence (TLENER) was an input parameter of the problem (10^{-2} was used in this study). (The energy equation was solved in the subroutine ENERGY.)

Thermochemical Equilibrium

The gas phase was considered to be composed of N chemical species containing K chemical elements. The N species compositions were related therefore by (N - K) homogeneous equilibrium expressions, Equations (3.20-3.22). Using the K elemental mass fractions obtained from the solution of the elemental conservation equations, a system of N nonlinear algebraic equations were generated at each grid point in the boundary layer. These nonlinear algebraic equations were solved (in the subroutine EQUIL) by the Newton-Raphson iteration technique.

The gas-solid interphase was considered to be composed of N gaseous chemical species in addition to a solid carbon phase. The N gaseous

species were related by (N + 1 - K) equilibrium expressions; (N - K) of these are the homogeneous equilibrium expressions given by Equations (3.20, 3.22). The remaining equilibrium expression is given by Equation (3.29) which represents the heterogeneous reaction taking place at the surface of the body. Using the (K - 1) elemental mass fraction ratios (that were the pseudo-boundary conditions for the elemental conservation equations at the wall) a system of N nonlinear algebraic equations were generated and solved (in the subroutine CONWAL) by the Newton-Raphson iteration technique.

The iterative process for the calculation of the N species mole fractions (both at the wall and in the gas phase) was continued until the following conditions were met simultaneously at each grid point:

$$\left| \frac{x_{in}^{k}}{x_{in}^{k-1}} - 1 \right| \leq \text{TLCONC} \qquad (i = 1,\ldots, N) \qquad (n = 1,\ldots, s) \qquad (4.25)$$

where the desired level of convergence (TLCONC) was an input parameter of the problem (10^{-6} was used in this study).

Numerical Difficulties Encountered with the Fully Coupled Multicomponent Diffusion Equations

The numerical implementation of the method of solution of the transport equations previously discussed was applied to the fully coupled, multicomponent diffusion with variable physical properties system. The numerical difficulties encountered are discussed in this section.

As expected, the diffusive fluxes of each of the N chemical species in the gas mixture were found to be very sensitive functions of

the species mole fraction profiles; each specie flux is dependent upon (N - 1) species mole fraction gradients which, among themselves, are related by the extremely nonlinear thermochemical equilibrium relations. As a result, the elemental mass diffusion fluxes and the elemental effective diffusivities ($\widetilde{D}_j$) were also found to be heavily dependent upon composition profiles; this situation is particularly serious in the calculation of $\widetilde{D}_j$, since this quantity depends on all the species mole fraction gradients and the elemental mass fraction gradient of the element under consideration.

Each solution of the elemental conservation Equations (4.19, 4.20) involves a relaxation of the initial elemental mass fraction profiles to those obtained from the solution; if the coefficients

$$\left[\frac{(\rho^2 \widetilde{D}_j)}{f\ \rho_e\ \mu_e + (\rho^2 \widetilde{D}_j)'}\right]_n \qquad \begin{matrix}(j = 1,\ldots, K - 1)\\ (n = 2,\ldots, s - 1)\end{matrix} \qquad (4.26)$$

calculated from the final solution of the elemental mass fraction profiles were sufficiently close to those used to obtain such a solution, then the relaxation of the profiles to the solution would indeed be complete.

The coefficients of Equation (4.26) are extremely sensitive to the composition profiles used in their calculation; while the $\widetilde{D}_j$ dependence appears directly in the coefficients, this dependence is further magnified by the term $\frac{d}{d\eta}(\rho^2 \widetilde{D}_j)$ appearing in Equation (4.26). (Although it may be expected that this effect would be larger in the convection dominated region, where the diffusive fluxes and composition gradients begin

to loose significance, the convection term is of sufficient magnitude to insure an asymptotic approach to the free stream composition values as the edge of the boundary layer is approached.)

Ideally, each pass through the subroutine SPCLUP would produce a full and complete update of the composition profiles; convergence of the innermost loop would be insured when two consecutive composition profiles agreed to the desired level of convergence. In reality, however, the coefficients of Equation (4.26) are so sensitive to the composition profiles that a full update does not result in an asymptotic approach to the solution. Many techniques were used to overcome this difficulty, but all proved to be ineffective. It was found that if a "sufficiently good" profile was initially used, the technique was able to cause convergence of the composition profiles (in the innermost iterative loop).

The reduction of the multicomponent diffusion equations to pseudo-binary diffusion equations by means of the effective elemental diffusivity requires a very gradual update of the composition profiles at each pass through the innermost iterative loop (subroutine SPCLUP). An initial profile resulting from a binary diffusivity solution to the problem was used and updates of the composition profiles were made according to:

$$x_i(\text{updated}) = x_i(\text{old}) + 0.05\ [x_i(\text{new}) - x_i(\text{old})] \qquad (4.27)$$

This five percent partial update of the profiles was used on the species mole fractions (rather than the elemental mass fractions) to minimize as much as possible the effect of nonlinearities in the thermochemical equilibrium expressions. With this method of partial update, the depend-

ence of the J_i, $\mathcal{J}_j$ and $\tilde{D}_j$ on the profiles was smoothed out and successive compositions profiles were observed to be approaching a common value with very little cycling. After 30 iterations within the innermost iterative loop (approximately 25 minutes of Central Processing Unit time) the minimum convergence required had not been satisfied. It was estimated that the solution of the fully coupled multicomponent problem for the system under consideration would require about four to six hours of Central Processing Unit time on the UNIVAC 1108 computer, if a five percent update of composition profiles was used. (Other integration techniques were used in an attempt to reduce the overall computation time, such as the fourth-order Runge-Kutta-Gill method (40). With this method, a larger step size was made possible for the same level of accuracy, thus reducing the number of times that the transport and thermodynamics properties had to be evaluated. However, this technique required another level of iterations within the subroutine SPCLUP since it was necessary to iterate until the boundary conditions at the edge of the boundary layer were satisfied. The net result was an increase in the total computation time required.) It was estimated that approximately 85 percent of the computation time involved in the solution of the fully multicomponent system was used in the evaluation of the variable, multicomponent, transport and thermodynamic properties of the system. Since the solution of this problem was so sensitive to these properties, a slow and partial update was required. However, the availability of computer time made the solution of the fully multicomponent problem unattainable in the present work. The computer programs included in the Appendix are written, however, to solve fully multicomponent problems.

The numerical methods and programs presented above were used in the present work to obtain binary diffusion solutions to the problem under consideration. The diffusive fluxes were computed using the multicomponent formulations, but at each grid point, the binary diffusivities were all set to a common value. This, in effect, reduces the dependence of the J_i, $\tilde{J}_j$ and $\tilde{D}_j$ very greatly because the diffusive flux of species i now becomes only a function of x_i'(or ω_i') and all the $\tilde{D}_j$ at each grid point take on the value of the common binary diffusivity at that grid point. Two sets of calculations were run: in the first run, the binary diffusivities at each point were set to $\mathcal{D} = \mathcal{D}_{O_2\text{-}CO}$, which was the highest of all the binary diffusivities (excluding the self-diffusion coefficients, and the binary diffusion coefficients involving atomic species); in the second run, the binary diffusivities at each grid point were set to $\mathcal{D} = \mathcal{D}_{N_2\text{-}CO_2}$, which was the lowest of the binary diffusivities.

Complete binary solutions to the problem were obtained for each one of the assumed diffusivities. In addition, the multicomponent fluxes (using the full multicomponent flux equations with unequal $\mathcal{D}_{ij}$ at each grid point) were calculated from the resulting solutions to the binary problem by using the binary solution velocity, temperature and composition profiles. The results of these runs are presented in the following chapter.

CHAPTER V

NUMERICAL RESULTS

In the present work two solutions were obtained for the variable property reacting boundary layer equations with local thermochemical equilibrium prevailing at each point in the boundary layer. In both solutions all of the binary diffusivities were assumed to be equal at each point, $\mathcal{D} = \mathcal{D}_{ij}$, for all i, j; the first solution sets all $\mathcal{D}_{ij} = \mathcal{D}_{O_2\text{-}CO}$ which was the highest of all binary diffusivities (excluding the values of the self-diffusion coefficients, and the diffusion coefficients involving atomic species), and the second solution sets all $\mathcal{D}_{ij} = \mathcal{D}_{N_2\text{-}CO_2}$, which was the lowest of all binary diffusivities. In both cases the variation of $\mathcal{D}$ with temperature across the boundary layer was taken into account. In addition, the resulting velocity, temperature and composition profiles from each of the binary solutions were used to calculate the multicomponent fluxes without setting the binary diffusivities equal at each location.

The input parameters for each of the two binary runs were:

$$P_e = 1.0 \text{ atm}$$

$$T_e = 300.0°K$$

$$T_w = 1500.0°K$$

$$U_e = 1500.0 \text{ cm/sec}$$

$$R_b = 0.60 \text{ cm}$$

$$(x_{O_2})_e = 0.210$$

$$(x_{N_2})_e = 0.790$$

The results of the high diffusivity run, $\mathcal{D} = \mathcal{D}_{O_2\text{-}CO}$, are presented in Tables 4 through 12 (pages 79-87); for the low diffusivity run, $\mathcal{D} = \mathcal{D}_{N_2\text{-}CO_2}$, the results are presented in Tables 13 through 21 (pages 89-97). The fully multicomponent fluxes calculated from the high diffusivity profiles are presented in Tables 22 through 24 (pages 105-107); those same fluxes calculated from the low diffusivity profiles are presented in Tables 25 through 27 (pages 108-110). The discussion that follows will highlight the results obtained from the high diffusivity run. In general, the high and low diffusivity results are qualitatively very similar, but their significant differences will be discussed.

Results of the High Diffusivity Run

Table 4 (page 79) presents the functions $f(\eta)$, $f'(\eta)$ and $f''(\eta)$ obtained from the solution of the momentum equation. In the region very near the wall, the net mass flux (as indicated by f) takes place in the direction away from the wall, as the result of the removal of solid carbon from the wall by the heterogeneous chemical reaction.

The velocity profile (f') in the vicinity of the wall is almost linear and very steep. An interesting feature of the velocity profile is the velocity overshoot that takes place within the boundary layer; this phenomenon arises from the fact that $(\rho_e/\rho) > 1$ in this region, while under the influence of a favorable pressure gradient (β=1). For flows with a favorable pressure gradient and heated walls the velocity ratio increases, (and may exhibit a maximum, where possibly $f'_{max} > 1$ is reached), after which the velocity ratio begins to decrease in an asymptotic approach to $f' \to 1$. This phenomenon has been previously reported

by Cohen and Reshotko (44). It should be noted that if the reactions taking place in the boundary layer result in a significant decrease in the mixture molecular weight (such as in the case of dissociation of gaseous species), the effect would be to further increase the (ρ_e/ρ) ratio and to give a higher velocity overshoot. Lees (32) noted the effect of the (ρ_e/ρ) ratio in the momentum equation and argued that if the opposite case is being considered, $(T_w/T_e) \ll 1$, or $(\rho_e/\rho_w) \ll 1$, the influence of the pressure gradient term in the momentum equation is so small as to be negligible; in that case, a first approximation to the velocity profile could be obtained from existing flat plate solutions.

The temperature profile obtained from the high diffusivity solution of the energy equation is presented in Table 5 (page 80), along with the resulting mixture enthalpy profile. The peak in the temperature profile corresponds to the reaction of the CO generated at the wall with the oxygen-bearing CO_2 which is diffusing towards the reaction zone of the boundary layer from regions near the edge which are at much lower temperatures.

Table 6 (page 81) presents the elemental mass fraction profiles that satisfy the high diffusivity elemental conservation equations and in Table 7 (page 82) the corresponding six species mole fraction profiles are presented. Since the assumption was made that all $\mathcal{D}_{ij}$ are equal to each other $(\mathcal{D})$, the effective elemental diffusivities $\tilde{D}_j = \mathcal{D}$ and the three elemental conservation equations become identical. These equations, however, were solved as if the equal binary diffusivity assumption had not been made (in a truly multicomponent fashion). From the boundary conditions, it is easily shown that:

$$\frac{\tilde{\omega}_O}{\tilde{\omega}_{Oe}} = \frac{\tilde{\omega}_N}{\tilde{\omega}_{Ne}} = \frac{\tilde{\omega}_C^{-1}}{\tilde{\omega}_{Ce}^{-1}} \tag{5.1}$$

(as indeed it should be when all $\mathcal{D}_{ij}$ are equal).

The species mole fraction profiles of Table 7 (page 82) indicate the transport and thermochemical processes taking place in the boundary layer. At the wall, all available O and O_2 react with the solid carbon to form mostly CO and trace amounts of CO_2; increases in the wall temperature would exponentially increase the ratio $(x_{CO}/x_{CO_2})_w$. The mole fraction of CO decreases linearly in the region near the wall, as the CO diffuses outwardly (at an almost constant rate; Table 8, page 83) to meet and react with the incoming CO_2. As a result, the mole fraction of CO_2 reaches a maximum at a point where little CO remains and then falls gradually as the CO_2 diffuses outwardly towards the edge of the boundary layer. These same diffusional-reaction zone interactions are verified in Table 8 where the species diffusive mass fluxes are presented.

It should be noted that at a value of η=4.0 the diffusion fluxes are all essentially zero and the velocity ratio and temperature have already attained essentially their free stream values. It thus appears that for the mass transfer rates considered in this study, the value of η_e=4.0 would be entirely satisfactory; at higher mass transfer rates, it would be desirable to place the outward edge of the boundary layer further out to allow for the thickening of the boundary layer resulting from the addition of mass at the wall. In this connection, it is interesting to note that the ratio of the momentum to the energy boundary layer thickenesses is about $Pr^{-1/2}$, whereas the ratio of the

momentum to the composition boundary layer thickenesses is about $Sc^{-1/2}$ as can be predicted from the order of magnitude analysis used to derive the high Reynolds number laminar boundary layer equations.

The species mass fluxes with respect to stationary coordinates are presented in Table 9 (page 84) and the elemental diffusive fluxes and mass fluxes with respect to stationary coordinates are presented in Table 10 (page 85). Table 9 shows that the contributions of the dissociated species O and N are completely negligible in all respects at the temperatures encountered; these species were included, however, to extend the temperature range over which the computer programs would remain valid.

The variation in density, viscosity, thermal conductivity, heat capacity and diffusivity for the mixture is shown in Table 11 (page 86). The variation in Prandtl number,

$$Pr = \frac{C_p \mu}{k} \tag{5.2}$$

Schmidt number,

$$Sc = \frac{\mu}{\rho \mathcal{D}} \tag{5.3}$$

Lewis number,

$$Le = \frac{Pr}{Sc} = \frac{C_p \rho \mathcal{D}}{k} \tag{5.4}$$

and of the ratios $(\rho\mu/\rho_e u_e)$ and (ρ_e/ρ) is also shown in Table 12 (page 87). The assumption that $(\rho\mu)$ = (constant) is often made in order to simplify the momentum equation and thus was included in the table.

The (ρ_e/ρ) ratio is seen to increase from a wall value up to a maximum and then to decrease asymptotically to a boundary layer edge value of 1.0, exhibiting much the same behavior as the (T/T_e) ratio (as would be expected from the equation of state). This (ρ_e/ρ) ratio accounts for the boundary layer velocity overshoot discussed previously.

From the high diffusivity results, the assumption of constant Prandtl and Schmidt numbers appears to be quite good; however, since the temperature dependence of the Prandtl number is in the opposite direction to that of the Schmidt number, the Lewis number exhibits more variation (about 25 percent through the boundary layer), reaching its maximum value at about the point corresponding to the maximum in the temperature profile. The effect of the assumption of Pr = 1 (or constant), Sc = 1 (or constant), and Le = 1, taken individually or in combinations with themselves and several other assumptions, is that they often uncouple and simplify greatly the solution of the energy and species (or elemental) conservation equations; a discussion of these simplifying effects was presented in Chapter I.

Equation (2.52) was integrated numerically, using the resulting density profile, to obtain the relationship between the transformed coordinate η and the real space coordinate, y. This relationship, presented in Table 12 for the high diffusivity run, permits relating the results, presented throughout as functions of η, to the real space coordinate, y.

Table 4. Solution to the Momentum Equation.
High Diffusivity Run.

η	f	f'	f''
.00	-.1240	.0000	5.0442
.10	-.1007	.4657	4.2559
.20	-.0335	.8512	3.4312
.30	.0674	1.1520	2.5789
.40	.1940	1.3670	1.7225
.50	.3372	1.4965	.9027
.60	.4907	1.5475	.2092
.70	.6454	1.5383	-.2696
.80	.7972	1.4936	-.5256
.90	.9430	1.4332	-.6225
1.00	1.0837	1.3691	-.6270
1.10	1.2175	1.3078	-.5830
1.20	1.3454	1.2525	-.5175
1.30	1.4676	1.2043	-.4458
1.40	1.5866	1.1633	-.3760
1.50	1.7011	1.1291	-.3120
1.60	1.8126	1.1010	-.2553
1.70	1.9209	1.0781	-.2062
1.80	2.0283	1.0597	-.1646
1.90	2.1336	1.0451	-.1298
2.00	2.2375	1.0337	-.1011
2.10	2.3398	1.0249	-.0778
2.20	2.4425	1.0182	-.0591
2.30	2.5441	1.0131	-.0443
2.40	2.6452	1.0093	-.0328
2.50	2.7454	1.0066	-.0239
2.60	2.8465	1.0045	-.0173
2.70	2.9469	1.0031	-.0123
2.80	3.0472	1.0021	-.0086
2.90	3.1467	1.0014	-.0059
3.00	3.2475	1.0009	-.0041
3.50	3.7476	1.0001	-.0005
4.00	4.2476	1.0000	.0000
4.50	4.7470	1.0000	.0000
5.00	5.2476	1.0000	.0000
5.50	5.7476	1.0000	.0000
6.00	6.2476	1.0000	.0000

Table 5. Solution to the Energy Equation.
High Diffusivity Run.

η	T	$\frac{T - T_w}{T_e - T_w}$	H	$\frac{H - H_w}{H_e - H_w}$ *
.00	1500.	.0000	-1.	0.
.10	1630.	-.1081	-22.	349.
.20	1757.	-.2144	-43.	703.
.30	1882.	-.3186	-64.	1045.
.40	2000.	-.4164	-84.	1389.
.50	2034.	-.4449	-127.	2110.
.60	1870.	-.3080	-155.	2591.
.70	1553.	-.0441	-174.	2902.
.80	1241.	.2159	-194.	3249.
.90	997.	.4188	-201.	3354.
1.00	812.	.5731	-197.	3283.
1.10	674.	.6887	-186.	3100.
1.20	571.	.7742	-171.	2852.
1.30	495.	.8372	-154.	2573.
1.40	440.	.8832	-137.	2285.
1.50	400.	.9168	-120.	2003.
1.60	371.	.9412	-104.	1736.
1.70	350.	.9587	-90.	1489.
1.80	334.	.9714	-76.	1264.
1.90	324.	.9804	-64.	1064.
2.00	316.	.9868	-54.	887.
2.10	311.	.9912	-45.	734.
2.20	307.	.9943	-37.	602.
2.30	304.	.9963	-30.	489.
2.40	303.	.9977	-25.	394.
2.50	302.	.9986	-20.	315.
2.60	301.	.9992	-16.	251.
2.70	300.	.9996	-13.	197.
2.80	300.	.9998	-10.	154.
2.90	300.	.9999	-8.	119.
3.00	300.	1.0000	-7.	92.
3.50	300.	1.0001	-3.	23.
4.00	300.	1.0001	-2.	6.
4.50	300.	1.0000	-1.	2.
5.00	300.	1.0000	-1.	1.
5.50	300.	1.0000	-1.	1.
6.00	300.	1.0000	-1.	1.

*The quantity $(H_e - H_w)$ is non-zero; H_e and H_w, however, round off to -1.

Table 6. Solution to the Elemental Conservation Equations. High Diffusivity Run.

η	$\tilde{\omega}_O$	$\tilde{\omega}_N$	$\tilde{\omega}_C$
.00	.198259	.652043	.148798
.10	.201269	.662855	.135876
.20	.204299	.672836	.122865
.30	.207287	.682677	.110036
.40	.210191	.692241	.097568
.50	.212963	.701369	.085668
.60	.215550	.709888	.074562
.70	.217904	.717639	.064457
.80	.219999	.724539	.055462
.90	.221839	.730598	.047564
1.00	.223442	.735876	.040683
1.10	.224832	.740454	.034714
1.20	.226035	.744417	.029548
1.30	.227076	.747843	.025081
1.40	.227975	.750805	.021220
1.50	.228752	.753364	.017884
1.60	.229422	.755571	.015007
1.70	.229999	.757470	.012531
1.80	.230494	.759099	.010407
1.90	.230916	.760490	.008594
2.00	.231275	.761671	.007054
2.10	.231578	.762669	.005753
2.20	.231832	.763506	.004662
2.30	.232044	.764204	.003752
2.40	.232219	.764781	.003000
2.50	.232363	.765255	.002382
2.60	.232480	.765642	.001878
2.70	.232575	.765954	.001470
2.80	.232651	.766205	.001143
2.90	.232712	.766405	.000883
3.00	.232760	.766563	.000677
3.50	.232880	.766959	.000161
4.00	.232910	.767058	.000032
4.50	.232916	.767078	.000005
5.00	.232917	.767082	.000001
5.50	.232917	.767082	.000000
6.00	.232918	.767082	.000000

Table 7. Solution to the Thermochemical Equilibrium Equations. High Diffusivity Run.

η	x_{O_2}	x_{N_2}	x_O	x_N	x_{CO_2}	x_{CO}
.00	.000000	.652953	.000000	.000000	.000091	.346956
.10	.000000	.676550	.000000	.000000	.036232	.287218
.20	.000000	.701315	.000000	.000000	.074163	.224522
.30	.000000	.726783	.000000	.000000	.113172	.160044
.40	.000005	.752596	.000002	.000000	.152703	.094695
.50	.000146	.778164	.000011	.000000	.191723	.029956
.60	.016784	.789725	.000034	.000000	.192793	.000665
.70	.044511	.789996	.000002	.000000	.165482	.000009
.80	.068960	.790000	.000000	.000000	.141040	.000000
.90	.090048	.790000	.000000	.000000	.119952	.000000
1.00	.108137	.790000	.000000	.000000	.101862	.000000
1.10	.123619	.790000	.000000	.000000	.086381	.000000
1.20	.136864	.790000	.000000	.000000	.073135	.000000
1.30	.148206	.790000	.000000	.000000	.061794	.000000
1.40	.157926	.790000	.000000	.000000	.052074	.000000
1.50	.166261	.790000	.000000	.000000	.043739	.000000
1.60	.173405	.790000	.000000	.000000	.036595	.000000
1.70	.179520	.790000	.000000	.000000	.030481	.000000
1.80	.184739	.790000	.000000	.000000	.025261	.000000
1.90	.189178	.790000	.000000	.000000	.020822	.000000
2.00	.192937	.790000	.000000	.000000	.017063	.000000
2.10	.196101	.790000	.000000	.000000	.013899	.000000
2.20	.198750	.790000	.000000	.000000	.011250	.000000
2.30	.200953	.790000	.000000	.000000	.009047	.000000
2.40	.202773	.790000	.000000	.000000	.007227	.000000
2.50	.204266	.790000	.000000	.000000	.005735	.000000
2.60	.205481	.790000	.000000	.000000	.004519	.000000
2.70	.206463	.790000	.000000	.000000	.003537	.000000
2.80	.207251	.790000	.000000	.000000	.002749	.000000
2.90	.207878	.790000	.000000	.000000	.002122	.000000
3.00	.208374	.790000	.000000	.000000	.001627	.000000
3.50	.209613	.790000	.000000	.000000	.000387	.000000
4.00	.209923	.790000	.000000	.000000	.000077	.000000
4.50	.209987	.790000	.000000	.000000	.000013	.000000
5.00	.209997	.790000	.000000	.000000	.000003	.000000
5.50	.209999	.790000	.000000	.000000	.000001	.000000
6.00	.210000	.790000	.000000	.000000	.000000	.000000

Table 8. Species Mass Fluxes With Respect to the Mixture Mass Average Velocity. High Diffusivity Run.

η	J_{O_2}	J_{N_2}	J_O	J_N	J_{CO_2}	J_{CO}
.00	.000000	-.002629	.000000	.000000	-.014751	.017380
.10	.000000	-.002623	.000000	.000000	-.014722	.017345
.20	.000000	-.002660	.000000	.000000	-.014926	.017586
.30	-.000001	-.002656	.000000	.000000	-.014901	.017558
.40	-.000021	-.002615	-.000001	.000000	-.014612	.017249
.50	-.002504	-.002535	-.000002	.000000	-.007333	.012374
.60	-.006844	-.002422	.000001	.000000	.005233	.004031
.70	-.008574	-.002284	.000003	.000000	.010761	.000094
.80	-.008032	-.002127	.000000	.000000	.010157	.000001
.90	-.007389	-.001956	.000000	.000000	.009345	.000000
1.00	-.006732	-.001782	.000000	.000000	.008514	.000000
1.10	-.006082	-.001610	.000000	.000000	.007692	.000000
1.20	-.005454	-.001444	.000000	.000000	.006898	.000000
1.30	-.004858	-.001286	.000000	.000000	.006144	.000000
1.40	-.004298	-.001138	.000000	.000000	.005437	.000000
1.50	-.003779	-.001001	.000000	.000000	.004780	.000000
1.60	-.003301	-.000874	.000000	.000000	.004175	.000000
1.70	-.002864	-.000758	.000000	.000000	.003622	.000000
1.80	-.002468	-.000653	.000000	.000000	.003121	.000000
1.90	-.002111	-.000559	.000000	.000000	.002670	.000000
2.00	-.001794	-.000475	.000000	.000000	.002268	.000000
2.10	-.001512	-.000400	.000000	.000000	.001913	.000000
2.20	-.001266	-.000335	.000000	.000000	.001601	.000000
2.30	-.001052	-.000278	.000000	.000000	.001330	.000000
2.40	-.000867	-.000230	.000000	.000000	.001097	.000000
2.50	-.000709	-.000188	.000000	.000000	.000897	.000000
2.60	-.000576	-.000153	.000000	.000000	.000729	.000000
2.70	-.000464	-.000123	.000000	.000000	.000587	.000000
2.80	-.000371	-.000098	.000000	.000000	.000469	.000000
2.90	-.000295	-.000078	.000000	.000000	.000373	.000000
3.00	-.000232	-.000061	.000000	.000000	.000293	.000000
3.50	-.000063	-.000017	.000000	.000000	.000079	.000000
4.00	-.000014	-.000004	.000000	.000000	.000018	.000000
4.50	-.000002	-.000001	.000000	.000000	.000003	.000000
5.00	.000000	.000000	.000000	.000000	.000000	.000000
5.50	.000000	.000000	.000000	.000000	.000001	.000000
6.00	.000000	.000000	.000000	.000000	.000000	.000000

Table 9. Species Mass Fluxes With Respect to Stationary Coordinates. High Diffusivity Run.

η	m_{O_2}	m_{N_2}	m_O	m_N	m_{CO_2}	m_{CO}
.00	.000000	.000000	.000000	.000000	-.014750	.018776
.10	.000000	-.000456	.000000	.000000	-.014540	.018265
.20	.000000	-.001928	.000000	.000000	-.014804	.017820
.30	-.000001	-.004148	.000000	.000000	-.015266	.017229
.40	-.000022	-.006974	-.000001	.000000	-.016002	.016701
.50	-.002505	-.010213	-.000002	.000000	-.010305	.012078
.60	-.007118	-.013729	.000000	.000000	.000897	.004022
.70	-.009541	-.017318	.000003	.000000	.005813	.000094
.80	-.009901	-.020875	.000000	.000000	.004898	.000001
.90	-.010301	-.024319	.000000	.000000	.004011	.000000
1.00	-.010779	-.027669	.000000	.000000	.003270	.000000
1.10	-.011312	-.030874	.000000	.000000	.002665	.000000
1.20	-.011888	-.033956	.000000	.000000	.002170	.000000
1.30	-.012492	-.036914	.000000	.000000	.001766	.000000
1.40	-.013128	-.039806	.000000	.000000	.001432	.000000
1.50	-.013780	-.042602	.000000	.000000	.001161	.000000
1.60	-.014447	-.045330	.000000	.000000	.000939	.000000
1.70	-.015123	-.047989	.000000	.000000	.000759	.000000
1.80	-.015818	-.050634	.000000	.000000	.000610	.000000
1.90	-.016518	-.053229	.000000	.000000	.000489	.000000
2.00	-.017226	-.055796	.000000	.000000	.000391	.000000
2.10	-.017937	-.058326	.000000	.000000	.000312	.000000
2.20	-.018663	-.060872	.000000	.000000	.000247	.000000
2.30	-.019389	-.063389	.000000	.000000	.000195	.000000
2.40	-.020120	-.065898	.000000	.000000	.000153	.000000
2.50	-.020852	-.068385	.000000	.000000	.000120	.000000
2.60	-.021595	-.070899	.000000	.000000	.000093	.000000
2.70	-.022338	-.073394	.000000	.000000	.000072	.000000
2.80	-.023082	-.075887	.000000	.000000	.000055	.000000
2.90	-.023825	-.078363	.000000	.000000	.000042	.000000
3.00	-.024579	-.080869	.000000	.000000	.000032	.000000
3.50	-.028341	-.093319	.000000	.000000	.000007	.000000
4.00	-.032117	-.105768	.000000	.000000	.000002	.000000
4.50	-.035891	-.118202	.000000	.000000	.000000	.000000
5.00	-.039676	-.130668	.000000	.000000	.000000	.000000
5.50	-.043456	-.143118	.000000	.000000	.000001	.000000
6.00	-.047237	-.155568	.000000	.000000	.000000	.000000

Table 10. Elemental Mass Fluxes With Respect to the Mixture Mass Average Velocity and to Stationary Coordinates. High Diffusivity Run.

η	$\tilde{J}_O$	$\tilde{J}_N$	$\tilde{J}_C$	$\tilde{m}_O$	$\tilde{m}_N$	$\tilde{m}_C$
.00	-.000798	-.002629	.003427	.000000	.000000	.004026
.10	-.000797	-.002623	.003420	-.000139	-.000456	.003864
.20	-.000808	-.002660	.003467	-.000585	-.001928	.003601
.30	-.000806	-.002656	.003462	-.001260	-.004148	.003221
.40	-.000794	-.002615	.003409	-.002118	-.006974	.002794
.50	-.000770	-.002535	.003305	-.003101	-.010213	.002367
.60	-.000735	-.002422	.003157	-.004169	-.013729	.001969
.70	-.000693	-.002284	.002977	-.005258	-.017318	.001627
.80	-.000646	-.002127	.002773	-.006339	-.020875	.001337
.90	-.000594	-.001956	.002551	-.007384	-.024319	.001095
1.00	-.000541	-.001782	.002324	-.008401	-.027669	.000893
1.10	-.000489	-.001610	.002099	-.009375	-.030874	.000727
1.20	-.000439	-.001444	.001883	-.010311	-.033956	.000592
1.30	-.000391	-.001286	.001677	-.011209	-.036914	.000482
1.40	-.000346	-.001138	.001484	-.012087	-.039806	.000391
1.50	-.000304	-.001001	.001304	-.012936	-.042602	.000317
1.60	-.000265	-.000874	.001139	-.013764	-.045330	.000256
1.70	-.000230	-.000758	.000988	-.014572	-.047989	.000207
1.80	-.000198	-.000653	.000852	-.015375	-.050634	.000167
1.90	-.000170	-.000559	.000729	-.016163	-.053229	.000134
2.00	-.000144	-.000475	.000619	-.016942	-.055796	.000107
2.10	-.000122	-.000400	.000522	-.017710	-.058326	.000085
2.20	-.000102	-.000335	.000437	-.018483	-.060872	.000067
2.30	-.000085	-.000278	.000363	-.019248	-.063389	.000053
2.40	-.000070	-.000230	.000299	-.020009	-.065898	.000042
2.50	-.000057	-.000188	.000245	-.020765	-.068385	.000033
2.60	-.000046	-.000153	.000199	-.021528	-.070899	.000025
2.70	-.000037	-.000123	.000160	-.022286	-.073394	.000020
2.80	-.000030	-.000098	.000128	-.023042	-.075887	.000015
2.90	-.000024	-.000078	.000102	-.023794	-.078363	.000012
3.00	-.000019	-.000061	.000080	-.024555	-.080869	.000009
3.50	-.000005	-.000017	.000022	-.028335	-.093319	.000002
4.00	-.000001	-.000004	.000005	-.032115	-.105768	.000000
4.50	.000000	-.000001	.000001	-.035891	-.118202	.000000
5.00	.000000	.000000	.000000	-.039676	-.130668	.000000
5.50	.000001	.000000	.000000	-.043455	-.143118	.000000
6.00	-.000001	.000000	.000000	-.047237	-.155568	.000000

Table 11. Transport and Thermodynamic Properties.
High Diffusivity Run.

η	ρ	μ	k	c_p	$\mathcal{D}$
.00	.227599-03	.539140-03	.206873-03	.295035+00	3.2562
.10	.213811-03	.568357-03	.219886-03	.299761+00	3.7434
.20	.202500-03	.595943-03	.232217-03	.304127+00	4.2482
.30	.193085-03	.621978-03	.243858-03	.308108+00	4.7673
.40	.185608-03	.645470-03	.254325-03	.311603+00	5.2754
.50	.186237-03	.650677-03	.256434-03	.313197+00	5.4269
.60	.203141-03	.616423-03	.240740-03	.309279+00	4.7133
.70	.242009-03	.547662-03	.208719-03	.299801+00	3.4517
.80	.299978-03	.473170-03	.175425-03	.288703+00	2.3652
.90	.370118-03	.409554-03	.147976-03	.278491+00	1.6339
1.00	.451222-03	.356948-03	.126103-03	.269707+00	1.1521
1.10	.540719-03	.314449-03	.109047-03	.262511+00	.8366
1.20	.634582-03	.280792-03	.959548-04	.256845+00	.6297
1.30	.727970-03	.254589-03	.860271-04	.252528+00	.4930
1.40	.816140-03	.234493-03	.785759-04	.249335+00	.4016
1.50	.895334-03	.219280-03	.730334-04	.247034+00	.3399
1.60	.963177-03	.207914-03	.689511-04	.245419+00	.2978
1.70	.101872-02	.199550-03	.659813-04	.244316+00	.2688
1.80	.106257-02	.193458-03	.638393-04	.243581+00	.2487
1.90	.109615-02	.189063-03	.623065-04	.243104+00	.2348
2.00	.112092-02	.185957-03	.612320-04	.242807+00	.2251
2.10	.113866-02	.183799-03	.604907-04	.242632+00	.2185
2.20	.115101-02	.182323-03	.599881-04	.242537+00	.2140
2.30	.115931-02	.181344-03	.596577-04	.242494+00	.2110
2.40	.116474-02	.180705-03	.594444-04	.242481+00	.2090
2.50	.116836-02	.180280-03	.593046-04	.242485+00	.2076
2.60	.117066-02	.180009-03	.592168-04	.242497+00	.2067
2.70	.117192-02	.179857-03	.591695-04	.242515+00	.2062
2.80	.117228-02	.179810-03	.591576-04	.242538+00	.2059
2.90	.117246-02	.179784-03	.591518-04	.242558+00	.2058
3.00	.117265-02	.179758-03	.591457-04	.242573+00	.2057
3.50	.117250-02	.179764-03	.591550-04	.242618+00	.2055
4.00	.117237-02	.179775-03	.591607-04	.242631+00	.2055
4.50	.117204-02	.179813-03	.591741-04	.242637+00	.2056
5.00	.117200-02	.179817-03	.591756-04	.242638+00	.2056
5.50	.117198-02	.179819-03	.591763-04	.242638+00	.2056
6.00	.117198-02	.179820-03	.591765-04	.242638+00	.2056

Table 12. Dimensionless Ratios and Transverse Coordinate (y). High Diffusivity Run.

η	Pr	Sc	Le	$\left(\frac{\rho\,\mu}{\rho_e\,\mu_e}\right)$	$\left(\frac{\rho_e}{\rho}\right)$	y
.00	.769	.727	1.057	.582	5.15	.00000
.10	.775	.710	1.091	.577	5.48	.29445-02
.20	.780	.693	1.127	.573	5.79	.60681-02
.30	.786	.676	1.163	.570	6.07	.93533-02
.40	.791	.659	1.200	.568	6.31	.12786-01
.50	.795	.644	1.234	.575	6.29	.16301-01
.60	.793	.644	1.232	.594	5.77	.19665-01
.70	.787	.656	1.200	.629	4.84	.22613-01
.80	.779	.667	1.168	.674	3.91	.25025-01
.90	.771	.677	1.138	.719	3.17	.26986-01
1.00	.763	.687	1.112	.764	2.60	.28571-01
1.10	.757	.695	1.089	.807	2.17	.29881-01
1.20	.752	.703	1.070	.846	1.85	.30986-01
1.30	.747	.709	1.053	.879	1.61	.31950-01
1.40	.744	.715	1.040	.908	1.44	.32788-01
1.50	.742	.721	1.029	.932	1.31	.33542-01
1.60	.740	.725	1.021	.950	1.22	.34238-01
1.70	.739	.729	1.014	.965	1.15	.34903-01
1.80	.738	.732	1.008	.975	1.10	.35523-01
1.90	.738	.735	1.004	.983	1.07	.36120-01
2.00	.737	.737	1.001	.989	1.05	.36703-01
2.10	.737	.739	.998	.993	1.03	.37287-01
2.20	.737	.740	.996	.996	1.02	.37851-01
2.30	.737	.741	.994	.998	1.01	.38408-01
2.40	.737	.742	.993	.999	1.01	.38965-01
2.50	.737	.743	.992	.999	1.00	.39531-01
2.60	.737	.744	.991	1.000	1.00	.40083-01
2.70	.737	.744	.990	1.000	1.00	.40633-01
2.80	.737	.745	.990	1.000	1.00	.41184-01
2.90	.737	.745	.989	1.000	1.00	.41748-01
3.00	.737	.745	.989	1.000	1.00	.42298-01
3.50	.737	.746	.988	1.000	1.00	.45062-01
4.00	.737	.746	.988	1.000	1.00	.47829-01
4.50	.737	.746	.988	1.000	1.00	.50609-01
5.00	.737	.746	.988	1.000	1.00	.53375-01
5.50	.737	.746	.988	1.000	1.00	.56140-01
6.00	.737	.746	.988	1.000	1.00	.58908-01

Results of the Low Diffusivity Run and Comparison of High and Low Diffusivity Runs

The results obtained from the low diffusivity run are presented in Tables 13 through 21 (pages 89-97). Since these results closely resemble those obtained from the high diffusivity run, only the significant differences between the two runs will be discussed. Figures 3 through 7 (pages 98-102) highlight these differences.

As expected, with the lower diffusivity, the mass transfer rate at the wall, f_w, is lower than that of the high diffusivity run. In addition, the amount of overshoot in f' is reduced by approximately six percent, and the maximum point in the velocity profile is further removed from the wall. The velocity profiles for the high and low diffusivity run are presented in Figure 3 (page 98) for comparison.

Figure 4 (page 99) shows the temperature profile for the low diffusivity run (the data is presented in Table 14, page 90). Although the profiles are similar, the low diffusivity temperature profile has a maximum that is about nine percent lower than the high diffusivity temperature maximum. Although the low diffusivity maximum temperature point is shifted slightly closer to the wall, the corresponding temperature gradient at the wall is about two thirds of the temperature gradient at the wall obtained from the high diffusivity run.

The low diffusivity elemental mass fraction profiles are presented in Table 15 (page 91), and the corresponding species mole fraction profiles appear in Table 16 (page 92). Since with the low diffusivity the temperature is always lower than at the same η with the high diffusivity, the mole fraction of CO is everywhere lower than the corresponding x_{CO}

Table 13. Solution to the Momentum Equation.
Low Diffusivity Run.

η	f	f'	f''
.00	-.1039	.0000	4.8461
.10	-.0818	.4431	4.0163
.20	-.0181	.8053	3.1872
.30	.0768	1.0805	2.3702
.40	.1954	1.2773	1.5766
.50	.3290	1.3959	.8435
.60	.4722	1.4460	.2508
.70	.6172	1.4460	-.1461
.80	.7605	1.4168	-.3651
.90	.8994	1.3730	-.4645
1.00	1.0349	1.3239	-.4896
1.10	1.1648	1.2751	-.4718
1.20	1.2900	1.2295	-.4315
1.30	1.4102	1.1887	-.3815
1.40	1.5279	1.1532	-.3291
1.50	1.6417	1.1229	-.2787
1.60	1.7527	1.0975	-.2323
1.70	1.8607	1.0765	-.1909
1.80	1.9681	1.0593	-.1549
1.90	2.0734	1.0455	-.1240
2.00	2.1773	1.0345	-.0981
2.10	2.2797	1.0259	-.0766
2.20	2.3826	1.0192	-.0591
2.30	2.4842	1.0141	-.0450
2.40	2.5854	1.0102	-.0338
2.50	2.6856	1.0073	-.0251
2.60	2.7869	1.0052	-.0184
2.70	2.8873	1.0036	-.0133
2.80	2.9876	1.0025	-.0095
2.90	3.0872	1.0017	-.0067
3.00	3.1880	1.0012	-.0047
3.50	3.6882	1.0001	-.0006
4.00	4.1883	1.0000	-.0001
4.50	4.6876	1.0000	.0000
5.00	5.1883	1.0000	.0000
5.50	5.6883	1.0000	.0000
6.00	6.1883	1.0000	.0000

Table 14. Solution to the Energy Equation.
Low Diffusivity Run.

η	T	$\frac{T - T_w}{T_e - T_w}$	H	$\frac{H - H_w}{H_e - H_w}$ *
.00	1500.	.0000	-1.	0.
.10	1589.	-.0742	-40.	1080.
.20	1678.	-.1481	-79.	2145.
.30	1769.	-.2238	-115.	3132.
.40	1860.	-.2999	-147.	4035.
.50	1844.	-.2864	-207.	5690.
.60	1627.	-.1058	-188.	5155.
.70	1336.	.1363	-192.	5261.
.80	1097.	.3359	-187.	5132.
.90	907.	.4945	-176.	4817.
1.00	758.	.6185	-160.	4390.
1.10	643.	.7142	-143.	3909.
1.20	555.	.7872	-125.	3416.
1.30	489.	.8425	-108.	2937.
1.40	439.	.8843	-91.	2491.
1.50	401.	.9156	-77.	2087.
1.60	373.	.9389	-64.	1729.
1.70	352.	.9563	-53.	1417.
1.80	337.	.9690	-43.	1149.
1.90	326.	.9783	-35.	922.
2.00	318.	.9850	-28.	732.
2.10	312.	.9898	-22.	576.
2.20	308.	.9932	-17.	448.
2.30	305.	.9955	-14.	345.
2.40	303.	.9971	-11.	263.
2.50	302.	.9982	-8.	199.
2.60	301.	.9989	-7.	149.
2.70	301.	.9994	-5.	110.
2.80	300.	.9996	-4.	81.
2.90	300.	.9998	-3.	59.
3.00	300.	.9999	-3.	42.
3.50	300.	1.0000	-1.	8.
4.00	300.	1.0000	-1.	2.
4.50	300.	1.0000	-1.	1.
5.00	300.	1.0000	-1.	1.
5.50	300.	1.0000	-1.	1.
6.00	300.	1.0000	-1.	1.

* The quantity $(H_e - H_w)$ is non-zero; H_e and H_w, however, round off to -1.

Table 15. Solution to the Elemental Conservation Equations. Low Diffusivity Run.

η	$\tilde{\omega}_O$	$\tilde{\omega}_N$	$\tilde{\omega}_C$
.00	.198273	.652918	.148809
.10	.201596	.663865	.134539
.20	.204905	.674769	.120325
.30	.208129	.685393	.106478
.40	.211224	.695590	.093186
.50	.214143	.705208	.080649
.60	.216840	.714094	.069067
.70	.219275	.722117	.058608
.80	.221430	.729220	.049349
.90	.223310	.735416	.041274
1.00	.224932	.740757	.034311
1.10	.226317	.745321	.028362
1.20	.227492	.749194	.023314
1.30	.228483	.752461	.019056
1.40	.229315	.755202	.015483
1.50	.230009	.757490	.012501
1.60	.230585	.759390	.010025
1.70	.231061	.760958	.007982
1.80	.231451	.762243	.006307
1.90	.231768	.763288	.004944
2.00	.232024	.764132	.003844
2.10	.232229	.764808	.002963
2.20	.232391	.765345	.002264
2.30	.232519	.765769	.001715
2.40	.232618	.766094	.001287
2.50	.232695	.766348	.000957
2.60	.232754	.766541	.000705
2.70	.232798	.766687	.000515
2.80	.232831	.766796	.000373
2.90	.232855	.766878	.000267
3.00	.232873	.766937	.000190
3.50	.232910	.767059	.000031
4.00	.232916	.767079	.000005
4.50	.232916	.767082	.000002
5.00	.232917	.767082	.000001
5.50	.232917	.767082	.000001
6.00	.232918	.767082	.000000

Table 16. Solution to the Thermochemical Equilibrium Equations. Low Diffusivity Run.

η	x_{O_2}	x_{N_2}	x_O	x_N	x_{CO_2}	x_{CO}
.00	.000000	.652929	.000000	.000000	.000091	.346981
.10	.000000	.679041	.000000	.000000	.040086	.280873
.20	.000000	.706267	.000000	.000000	.081783	.211951
.30	.000000	.734037	.000000	.000000	.124314	.141649
.40	.000001	.761932	.000000	.000000	.167037	.071030
.50	.000538	.789006	.000004	.000000	.207968	.002482
.60	.031815	.789990	.000003	.000000	.178178	.000023
.70	.060469	.789992	.000000	.000000	.149539	.000000
.80	.085318	.789993	.000000	.000000	.124689	.000000
.90	.106599	.789994	.000000	.000000	.103407	.000000
1.00	.124663	.789995	.000000	.000000	.085343	.000000
1.10	.139892	.789995	.000000	.000000	.070113	.000000
1.20	.152668	.789996	.000000	.000000	.057337	.000000
1.30	.163342	.789996	.000000	.000000	.046662	.000000
1.40	.172228	.789997	.000000	.000000	.037775	.000000
1.50	.179597	.789997	.000000	.000000	.030406	.000000
1.60	.185680	.789997	.000000	.000000	.024323	.000000
1.70	.190676	.789996	.000000	.000000	.019326	.000000
1.80	.194757	.789998	.000000	.000000	.015245	.000000
1.90	.198067	.789998	.000000	.000000	.011934	.000000
2.00	.200733	.789999	.000000	.000000	.009269	.000000
2.10	.202863	.789999	.000000	.000000	.007139	.000000
2.20	.204550	.789999	.000000	.000000	.005451	.000000
2.30	.205875	.789999	.000000	.000000	.004126	.000000
2.40	.206905	.789999	.000000	.000000	.003096	.000000
2.50	.207699	.789999	.000000	.000000	.002301	.000000
2.60	.208305	.790000	.000000	.000000	.001695	.000000
2.70	.208763	.790000	.000000	.000000	.001238	.000000
2.80	.209105	.790000	.000000	.000000	.000895	.000000
2.90	.209358	.790000	.000000	.000000	.000642	.000000
3.00	.209544	.790000	.000000	.000000	.000456	.000000
3.50	.209926	.790000	.000000	.000000	.000073	.000000
4.00	.209988	.790000	.000000	.000000	.000012	.000000
4.50	.209995	.790001	.000000	.000000	.000005	.000000
5.00	.209997	.790000	.000000	.000000	.000003	.000000
5.50	.209998	.790000	.000000	.000000	.000002	.000000
6.00	.210000	.790000	.000000	.000000	.000000	.000000

Table 17. Species Mass Fluxes With Respect to the Mixture Mass Average Velocity. Low Diffusivity Run.

η	J_{O_2}	J_{N_2}	J_O	J_N	J_{CO_2}	J_{CO}
.00	.000000	-.002204	.000000	.000000	-.012370	.014574
.10	.000000	-.002211	.000000	.000000	-.012407	.014619
.20	.000000	-.002241	.000000	.000000	-.012576	.014818
.30	.000000	-.002231	.000000	.000000	-.012518	.014750
.40	-.000062	-.002185	.000000	.000000	-.012087	.014333
.50	-.003750	-.002102	.000000	.000000	-.001478	.007330
.60	-.007354	-.001987	.000000	.000000	.009078	.000263
.70	-.006982	-.001849	.000000	.000000	.008829	.000003
.80	-.006392	-.001693	.000000	.000000	.008085	.000000
.90	-.005768	-.001528	.000000	.000000	.007296	.000000
1.00	-.005140	-.001361	.000000	.000000	.006501	.000000
1.10	-.004527	-.001199	.000000	.000000	.005725	.000000
1.20	-.003945	-.001045	.000000	.000000	.004989	.000000
1.30	-.003403	-.000901	.000000	.000000	.004304	.000000
1.40	-.002908	-.000770	.000000	.000000	.003678	.000000
1.50	-.002461	-.000652	.000000	.000000	.003113	.000000
1.60	-.002064	-.000547	.000000	.000000	.002610	.000000
1.70	-.001714	-.000454	.000000	.000000	.002169	.000000
1.80	-.001411	-.000374	.000000	.000000	.001785	.000000
1.90	-.001150	-.000305	.000000	.000000	.001454	.000000
2.00	-.000928	-.000246	.000000	.000000	.001174	.000000
2.10	-.000742	-.000197	.000000	.000000	.000939	.000000
2.20	-.000587	-.000156	.000000	.000000	.000743	.000000
2.30	-.000460	-.000122	.000000	.000000	.000582	.000000
2.40	-.000357	-.000095	.000000	.000000	.000452	.000000
2.50	-.000274	-.000073	.000000	.000000	.000347	.000000
2.60	-.000208	-.000055	.000000	.000000	.000264	.000000
2.70	-.000157	-.000042	.000000	.000000	.000198	.000000
2.80	-.000117	-.000031	.000000	.000000	.000148	.000000
2.90	-.000086	-.000023	.000000	.000000	.000109	.000000
3.00	-.000063	-.000017	.000000	.000000	.000080	.000000
3.50	-.000011	-.000003	.000000	.000000	.000014	.000000
4.00	-.000001	.000000	.000000	.000000	.000002	.000000
4.50	.000000	.000000	.000000	.000000	.000000	.000000
5.00	.000000	.000000	.000000	.000000	.000000	.000000
5.50	.000000	.000000	.000000	.000000	.000000	.000000
6.00	.000000	.000000	.000000	.000000	.000000	.000000

Table 18. Species Mass Fluxes With Respect to Stationary Coordinates. Low Diffusivity Run.

η	m_{O_2}	m_{N_2}	m_O	m_N	m_{CO_2}	m_{CO}
.00	.000000	-.000002	.000000	.000000	-.012370	.015745
.10	.000000	-.000449	.000000	.000000	-.012244	.015347
.20	.000000	-.001846	.000000	.000000	-.012504	.014936
.30	.000000	-.003940	.000000	.000000	-.012973	.014420
.40	-.000062	-.006596	.000000	.000000	-.013606	.013922
.50	-.003756	-.009633	.000000	.000000	-.004597	.007306
.60	-.007858	-.012934	.000000	.000000	.005199	.000263
.70	-.008247	-.016317	.000000	.000000	.004527	.000003
.80	-.008613	-.019694	.000000	.000000	.003621	.000000
.90	-.009078	-.022998	.000000	.000000	.002881	.000000
1.00	-.009625	-.026246	.000000	.000000	.002277	.000000
1.10	-.010227	-.029381	.000000	.000000	.001796	.000000
1.20	-.010870	-.032417	.000000	.000000	.001412	.000000
1.30	-.011538	-.035347	.000000	.000000	.001108	.000000
1.40	-.012236	-.038227	.000000	.000000	.000864	.000000
1.50	-.012944	-.041020	.000000	.000000	.000672	.000000
1.60	-.013663	-.043752	.000000	.000000	.000521	.000000
1.70	-.014386	-.046417	.000000	.000000	.000402	.000000
1.80	-.015124	-.049071	.000000	.000000	.000308	.000000
1.90	-.015862	-.051676	.000000	.000000	.000235	.000000
2.00	-.016603	-.054253	.000000	.000000	.000179	.000000
2.10	-.017343	-.056793	.000000	.000000	.000135	.000000
2.20	-.018094	-.059347	.000000	.000000	.000101	.000000
2.30	-.018842	-.061874	.000000	.000000	.000075	.000000
2.40	-.019592	-.064389	.000000	.000000	.000056	.000000
2.50	-.020338	-.066882	.000000	.000000	.000041	.000000
2.60	-.021095	-.069401	.000000	.000000	.000030	.000000
2.70	-.021848	-.071900	.000000	.000000	.000022	.000000
2.80	-.022601	-.074396	.000000	.000000	.000015	.000000
2.90	-.023350	-.076874	.000000	.000000	.000011	.000000
3.00	-.024109	-.079383	.000000	.000000	.000008	.000000
3.50	-.027886	-.091839	.000000	.000000	.000001	.000000
4.00	-.031666	-.104289	.000000	.000000	-.000001	.000000
4.50	-.035441	-.116723	.000000	.000000	-.000001	.000000
5.00	-.039227	-.129189	.000000	.000000	-.000001	.000000
5.50	-.043008	-.141640	.000000	.000000	.000000	.000000
6.00	-.046788	-.154090	.000000	.000000	.000000	.000000

Table 19. Elemental Mass Fluxes With Respect to the Mixture Mass Average Velocity and to Stationary Coordinates. Low Diffusivity Run.

η	$\tilde{J}_O$	$\tilde{J}_N$	$\tilde{J}_C$	$\tilde{m}_O$	$\tilde{m}_N$	$\tilde{m}_C$
.00	-.000669	-.002205	.002874	.000000	-.000002	.003376
.10	-.000671	-.002211	.002882	-.000136	-.000449	.003239
.20	-.000680	-.002241	.002922	-.000560	-.001846	.002992
.30	-.000677	-.002231	.002908	-.001196	-.003940	.002643
.40	-.000663	-.002185	.002848	-.002002	-.006596	.002257
.50	-.000638	-.002102	.002740	-.002925	-.009633	.001878
.60	-.000603	-.001987	.002591	-.003927	-.012934	.001532
.70	-.000561	-.001849	.002411	-.004954	-.016317	.001237
.80	-.000514	-.001693	.002207	-.005980	-.019694	.000988
.90	-.000464	-.001528	.001991	-.006983	-.022998	.000786
1.00	-.000413	-.001361	.001774	-.007969	-.026246	.000621
1.10	-.000364	-.001199	.001563	-.008921	-.029381	.000490
1.20	-.000317	-.001045	.001362	-.009843	-.032417	.000385
1.30	-.000273	-.000901	.001175	-.010733	-.035347	.000302
1.40	-.000234	-.000770	.001004	-.011607	-.038227	.000236
1.50	-.000198	-.000652	.000850	-.012455	-.041020	.000183
1.60	-.000166	-.000547	.000712	-.013285	-.043752	.000142
1.70	-.000138	-.000454	.000592	-.014094	-.046417	.000110
1.80	-.000113	-.000374	.000487	-.014900	-.049071	.000084
1.90	-.000092	-.000305	.000397	-.015691	-.051676	.000064
2.00	-.000075	-.000246	.000320	-.016474	-.054253	.000049
2.10	-.000060	-.000197	.000256	-.017245	-.056793	.000037
2.20	-.000047	-.000156	.000203	-.018020	-.059347	.000028
2.30	-.000037	-.000122	.000159	-.018787	-.061874	.000021
2.40	-.000029	-.000095	.000123	-.019551	-.064389	.000015
2.50	-.000022	-.000073	.000095	-.020308	-.066882	.000011
2.60	-.000017	-.000055	.000072	-.021073	-.069401	.000008
2.70	-.000013	-.000042	.000054	-.021832	-.071900	.000006
2.80	-.000009	-.000031	.000040	-.022590	-.074396	.000004
2.90	-.000007	-.000023	.000030	-.023342	-.076874	.000003
3.00	-.000005	-.000017	.000022	-.024104	-.079383	.000002
3.50	-.000001	-.000003	.000004	-.027886	-.091839	.000000
4.00	.000000	.000000	.000001	-.031666	-.104289	.000000
4.50	.000000	.000000	.000000	-.035442	-.116723	.000000
5.00	.000000	.000000	.000000	-.039227	-.129189	.000000
5.50	.000000	.000000	.000000	-.043008	-.141640	.000000
6.00	.000000	.000000	.000000	-.046788	-.154090	.000000

Table 20. Transport and Thermodynamic Properties.
Low Diffusivity Run.

η	ρ	μ	k	C_p	$\mathcal{D}$
.00	.227599-03	.539141-03	.206873-03	.295035+00	2.4675
.10	.219757-03	.558640-03	.215474-03	.298757+00	2.7196
.20	.212991-03	.577403-03	.223760-03	.302310+00	2.9802
.30	.206730-03	.596092-03	.232017-03	.305727+00	3.2572
.40	.201064-03	.614302-03	.240051-03	.308936+00	3.5448
.50	.207170-03	.608662-03	.237245-03	.309522+00	3.4932
.60	.232139-03	.563502-03	.216103-03	.302527+00	2.8299
.70	.279451-03	.496657-03	.185820-03	.292371+00	2.0301
.80	.337149-03	.436661-03	.159470-03	.282618+00	1.4522
.90	.404530-03	.384972-03	.137543-03	.273902+00	1.0493
1.00	.480461-03	.341457-03	.119713-03	.266488+00	.7720
1.10	.562758-03	.305531-03	.105458-03	.260426+00	.5820
1.20	.648254-03	.276383-03	.942157-04	.255634+00	.4517
1.30	.733048-03	.253148-03	.854662-04	.251961+00	.3622
1.40	.813689-03	.234838-03	.787070-04	.249208+00	.3001
1.50	.887173-03	.220593-03	.735321-04	.247188+00	.2566
1.60	.951429-03	.209649-03	.696080-04	.245735+00	.2260
1.70	.100548-02	.201351-03	.666630-04	.244708+00	.2044
1.80	.104935-02	.195141-03	.644771-04	.243994+00	.1890
1.90	.108380-02	.190556-03	.628743-04	.243505+00	.1781
2.00	.111005-02	.187221-03	.617147-04	.243176+00	.1704
2.10	.112950-02	.184831-03	.608876-04	.242959+00	.1650
2.20	.114354-02	.183146-03	.603071-04	.242819+00	.1612
2.30	.115343-02	.181979-03	.599064-04	.242731+00	.1586
2.40	.116022-02	.181186-03	.596353-04	.242678+00	.1569
2.50	.116477-02	.180658-03	.594556-04	.242647+00	.1557
2.60	.116774-02	.180315-03	.593393-04	.242631+00	.1549
2.70	.116962-02	.180097-03	.592661-04	.242624+00	.1545
2.80	.117077-02	.179964-03	.592217-04	.242622+00	.1541
2.90	.117144-02	.179886-03	.591961-04	.242622+00	.1540
3.00	.117180-02	.179843-03	.591822-04	.242624+00	.1539
3.50	.117203-02	.179814-03	.591741-04	.242635+00	.1538
4.00	.117192-02	.179826-03	.591786-04	.242639+00	.1538
4.50	.117190-02	.179828-03	.591793-04	.242639+00	.1538
5.00	.117194-02	.179824-03	.591780-04	.242639+00	.1538
5.50	.117195-02	.179823-03	.591777-04	.242639+00	.1538
6.00	.117198-02	.179820-03	.591765-04	.242638+00	.1538

Table 21. Dimensionless Ratios and Transverse Coordinate (y). Low Diffusivity Run.

η	Pr	Sc	Le	$\left(\frac{\rho\ \mu}{\rho_e\ \mu_e}\right)$	$\left(\frac{\rho_e}{\rho}\right)$	y
.00	.769	.960	.801	.582	5.15	.00000
.10	.775	.935	.829	.583	5.33	.29034-02
.20	.780	.910	.858	.584	5.50	.59059-02
.30	.785	.885	.887	.585	5.67	.90000-02
.40	.791	.862	.917	.586	5.83	.12186-01
.50	.794	.841	.944	.598	5.66	.15400-01
.60	.789	.858	.920	.621	5.05	.18370-01
.70	.781	.875	.893	.659	4.19	.20941-01
.80	.774	.892	.868	.699	3.48	.23042-01
.90	.767	.907	.845	.739	2.90	.24829-01
1.00	.760	.921	.826	.778	2.44	.26274-01
1.10	.754	.933	.809	.816	2.08	.27539-01
1.20	.750	.944	.795	.850	1.81	.28596-01
1.30	.746	.953	.783	.881	1.60	.29565-01
1.40	.744	.962	.773	.907	1.44	.30377-01
1.50	.742	.969	.765	.929	1.32	.31157-01
1.60	.740	.975	.759	.946	1.23	.31846-01
1.70	.739	.980	.754	.961	1.17	.32537-01
1.80	.738	.984	.751	.972	1.12	.33141-01
1.90	.738	.987	.748	.980	1.08	.33766-01
2.00	.738	.990	.745	.986	1.06	.34341-01
2.10	.738	.992	.744	.991	1.04	.34948-01
2.20	.737	.993	.742	.994	1.02	.35491-01
2.30	.737	.994	.741	.996	1.02	.36073-01
2.40	.737	.995	.741	.997	1.01	.36617-01
2.50	.737	.996	.740	.998	1.01	.37204-01
2.60	.737	.997	.740	.999	1.00	.37732-01
2.70	.737	.997	.740	1.000	1.00	.38305-01
2.80	.737	.997	.739	1.000	1.00	.38843-01
2.90	.737	.997	.739	1.000	1.00	.39425-01
3.00	.737	.998	.739	1.000	1.00	.39951-01
3.50	.737	.998	.739	1.000	1.00	.42737-01
4.00	.737	.998	.739	1.000	1.00	.45491-01
4.50	.737	.998	.739	1.000	1.00	.48288-01
5.00	.737	.998	.739	1.000	1.00	.51030-01
5.50	.737	.998	.739	1.000	1.00	.53817-01
6.00	.737	.998	.739	1.000	1.00	.56570-01

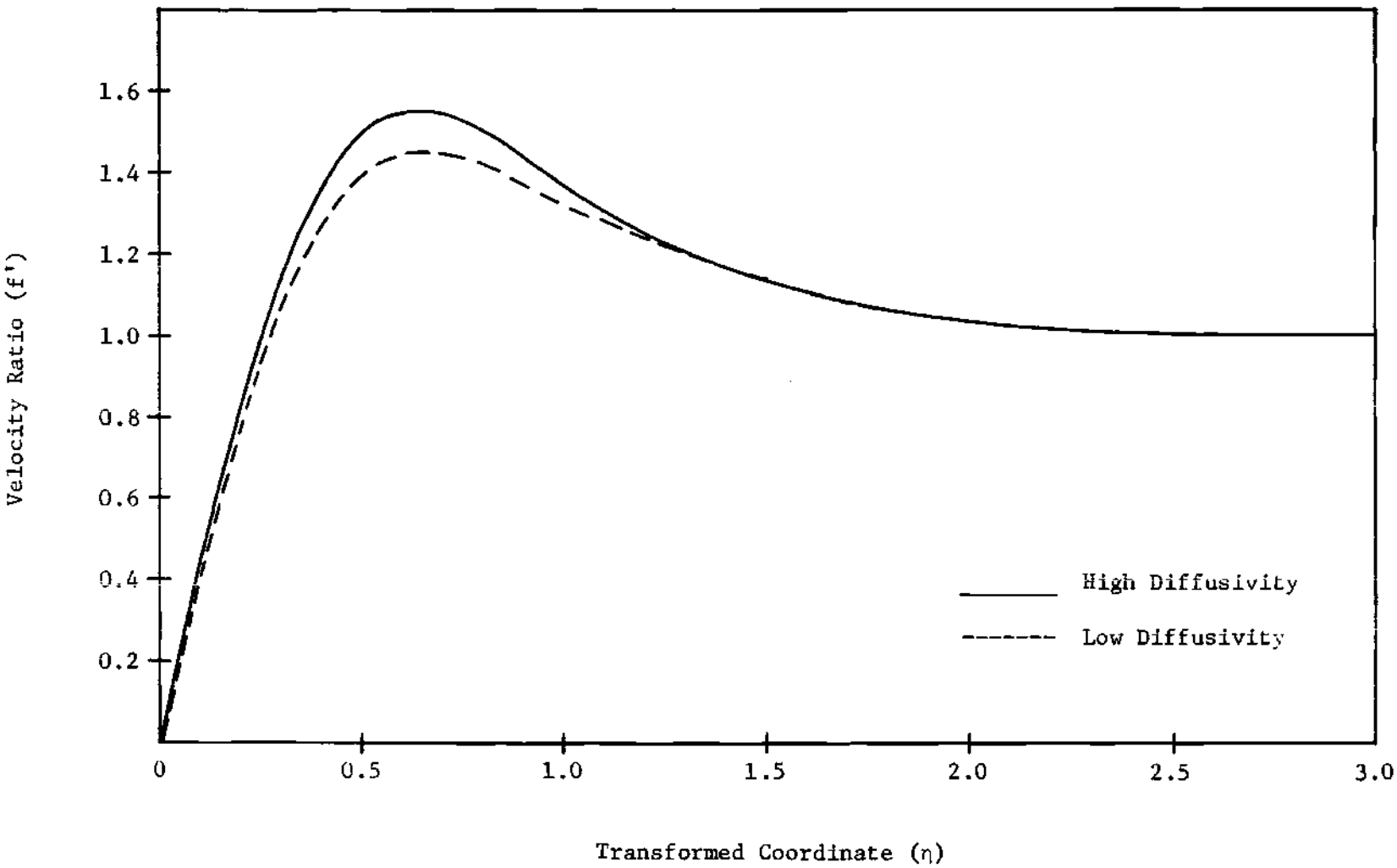

Figure 3. Velocity Profiles

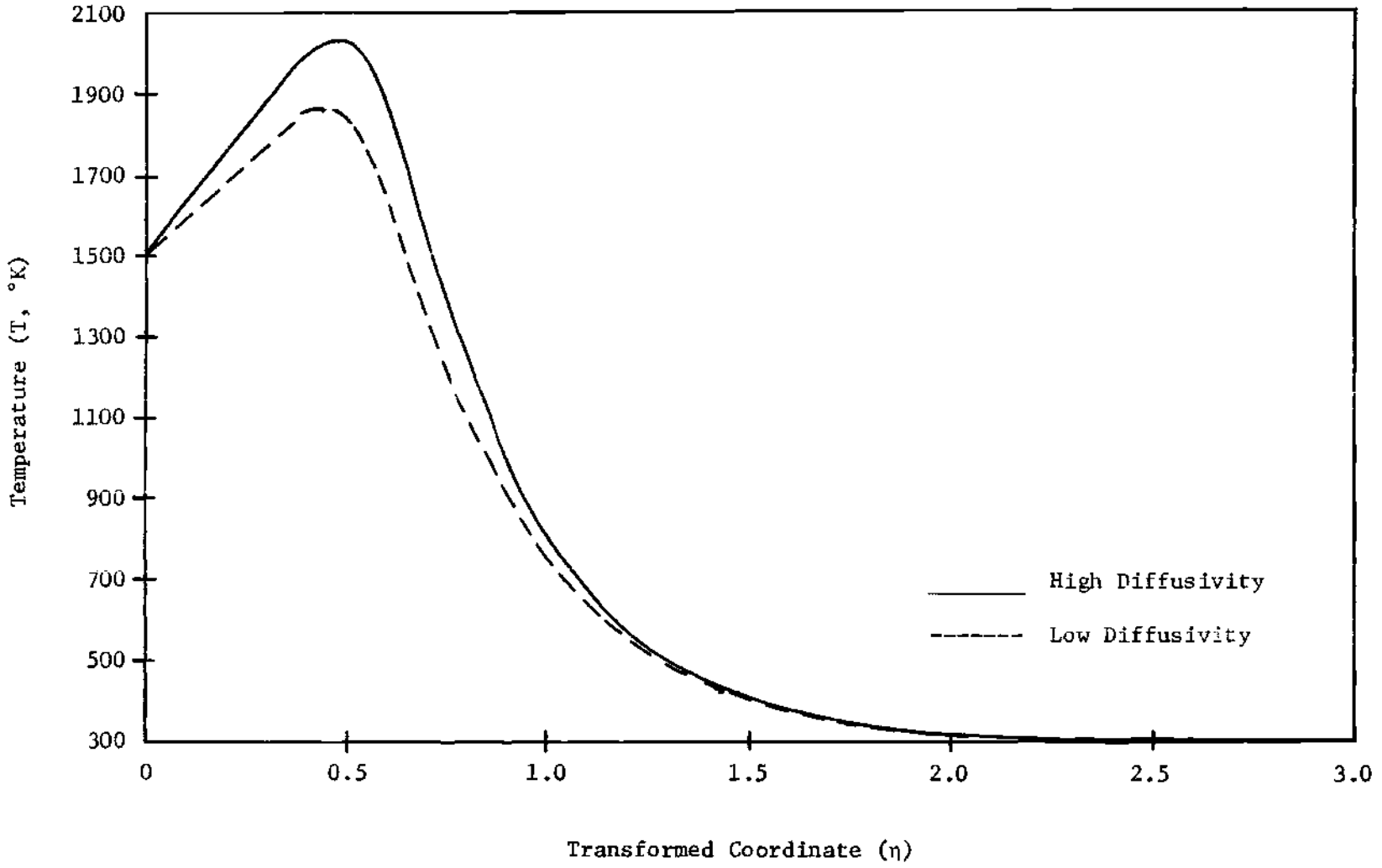

Figure 4. Temperature Profiles

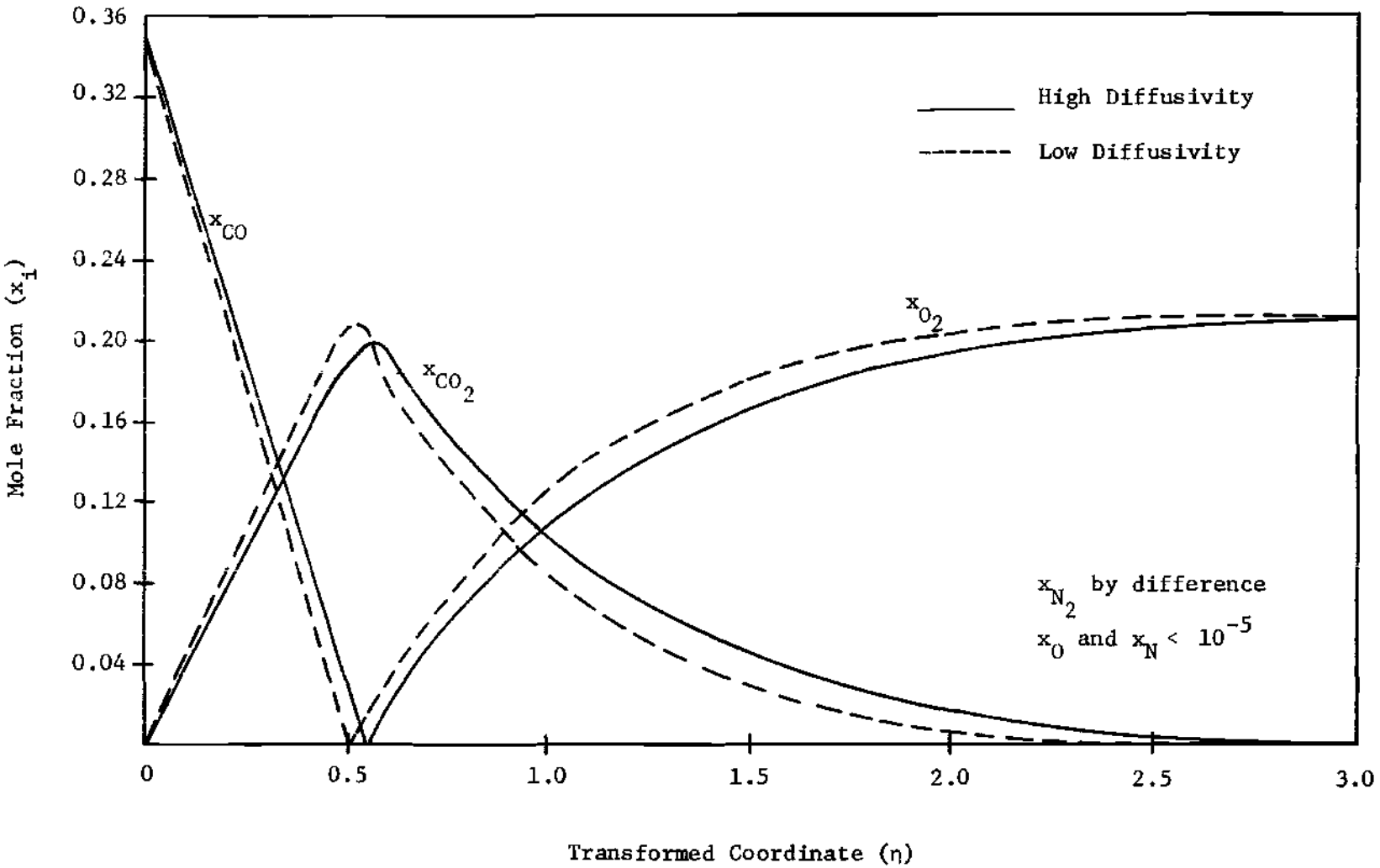

Figure 5. Species Mole Fraction Profiles

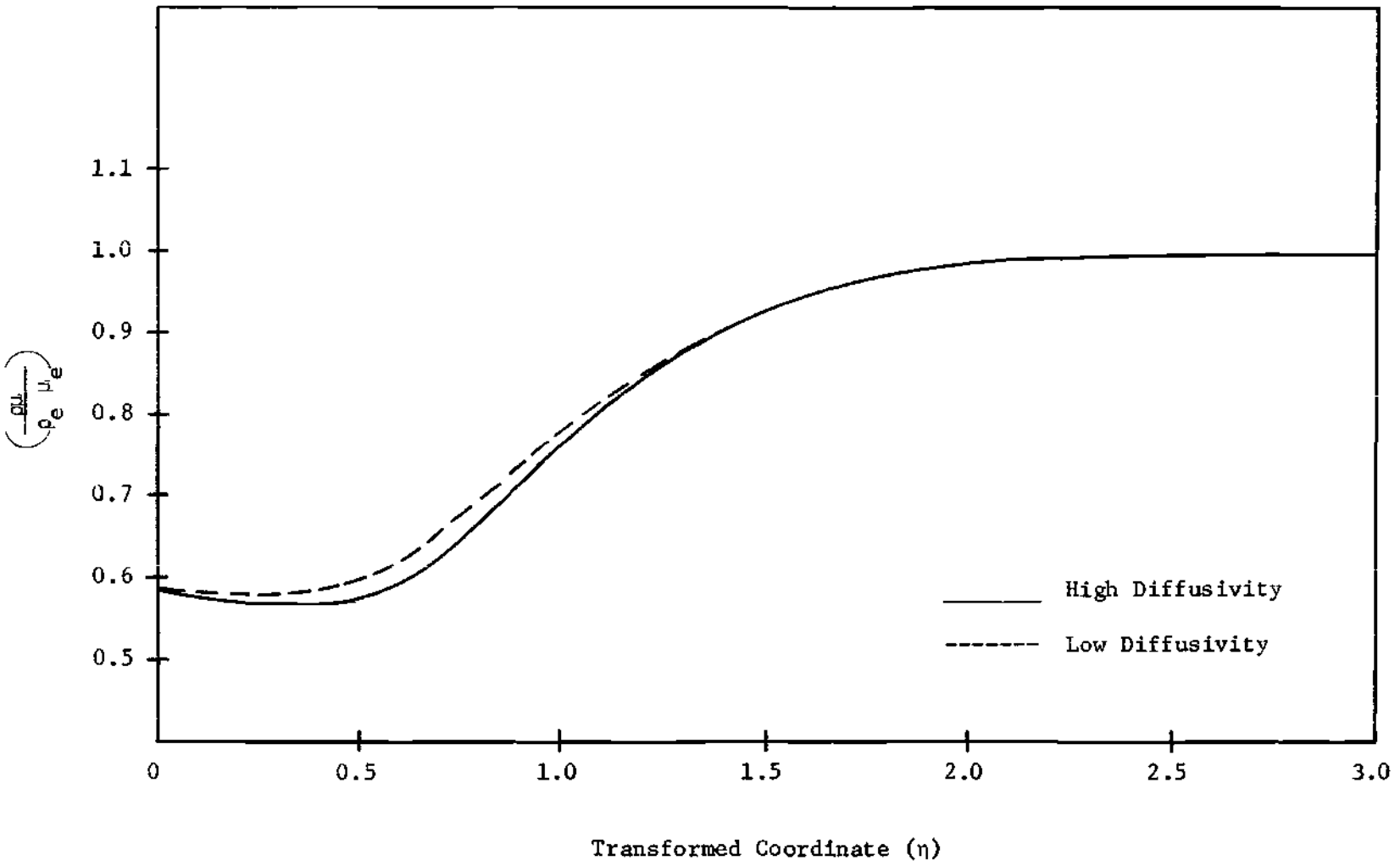

Figure 6. Density-Viscosity Product Variation

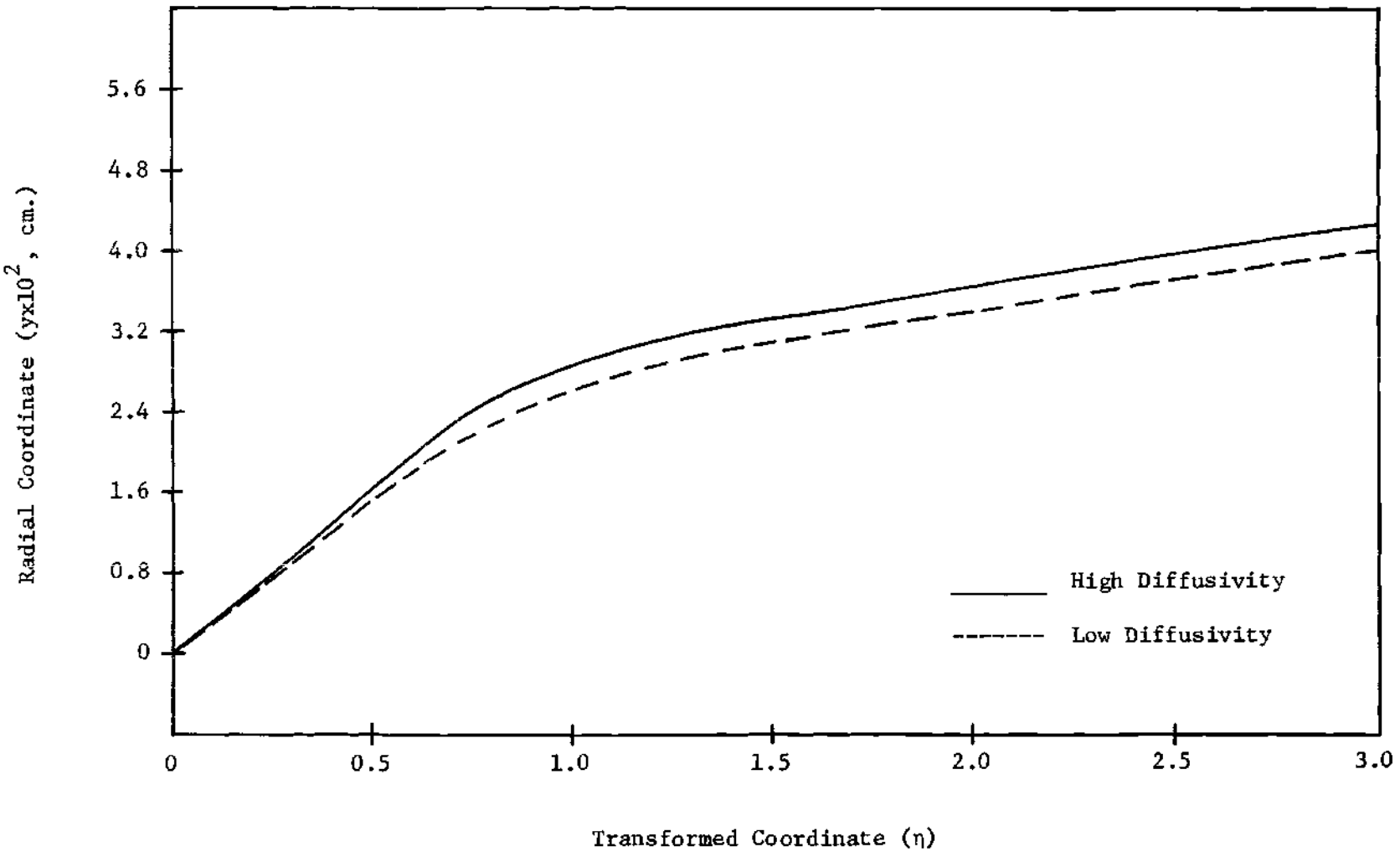

Figure 7. Radial Coordinate as a Function of η

for the high diffusivity run. The reaction zone is located in the region $0.5 < \eta < 1.0$ and, as observed before, this is the region where the greatest changes in the species diffusive fluxes take place (see Tables 17 through 19, pages 93-95). The species mole fraction profiles for each of the two runs are presented in Figure 5 (page 100) for comparison. The $(\rho\mu/\rho_e\mu_e)$ ratios for both runs are compared in Figure 6 (page 101).

The Prandtl and the Schmidt numbers remained essentially constant for the low diffusivity run (Table 21, page 97), but they are not approximately equal. The Lewis number varied 27 percent across the boundary layer.

Integration of the density profile results in the relationship between η and y, presented in Figure 7 (page 102) (for both runs); this relationship permits the transformation of the previous results from the transformed coordinate plane to the real coordinate plane.

Multicomponent Fluxes from the Results of the Equal Diffusivity Solutions

The velocity, temperature and composition profiles obtained from the solutions in which the binary diffusivities were assumed equal were used to calculate the multicomponent fluxes without setting all of the binary diffusivities equal. The multicomponent fluxes (Equations 2.71, 2.72, and 2.82) calculated from the profiles obtained from the high diffusivity run are presented in Tables 22 through 24 (pages 105-107); these same fluxes, calculated from the low diffusivity run profiles are presented in Tables 25 through 27 (pages 108-110).

A comparison of the multicomponent diffusive fluxes with the corresponding binary diffusive fluxes shows that, in the vicinity of the wall, the multicomponent flux of N_2, J_{N_2}, is high. The dependence of the multicomponent fluxes on the species mole fraction gradients (further complicated by nonlinearities in the thermochemical equilibrium expressions) has been discussed previously. In the region near the wall, where the mole fraction profiles of CO and CO_2 are very steep, a small change in the elemental mass fraction profile of O has a strong influence on the mole fraction profiles of CO and CO_2 and, consequently, on all the diffusive fluxes. The diffusive fluxes of CO and CO_2 are opposite in direction and in a ratio consistent with an O_2 deficient zone in the boundary layer; since CO and CO_2 are the only oxygen containing species in this region, the elemental diffusive flux of O, $\tilde{J}_O$, is then calculated by difference from two fluxes that themselves are extremely sensitive to the composition profiles. Thus, it becomes necessary to calculate elemental mass fraction profiles, especially in the region near the wall, that are consistent with the multicomponent diffusive fluxes; this, however, is a time consuming effort due to the high sensitivity of the effective elemental diffusivities to the composition profiles from which they were calculated (this has been discussed previously in Chapter IV).

Although the wall boundary conditions are not satisfied by the calculated multicomponent fluxes, computational experience with this system supports the belief that the elemental mass fraction profile and the elemental flux for carbon are "close" to those predicted by the binary diffusivity solutions. (Note that there is little difference between the values of the multicomponent $\tilde{m}_{Cw}$ calculated from the high and

Table 22. Species Mass Fluxes With Respect to the Mixture Mass Average Velocity. Multicomponent Fluxes Based on the High Diffusivity Profiles.

η	J_{O_2}	J_{N_2}	J_O	J_N	J_{CO_2}	J_{CO}
.00	.000000	-.004738	.000000	.000000	-.011203	.015941
.10	.000000	-.004748	.000000	.000000	-.011188	.015936
.20	.000000	-.004836	.000000	.000000	-.011350	.016186
.30	-.000001	-.004851	.000000	.000000	-.011337	.016189
.40	-.000017	-.004791	.000000	.000000	-.011131	.015939
.50	-.002343	-.003553	-.000001	.000000	-.005582	.011478
.60	-.006394	-.001375	.000000	.000000	.004023	.003746
.70	-.007983	-.000320	.000001	.000000	.008224	.000079
.80	-.007465	-.000269	.000000	.000000	.007733	.000001
.90	-.006861	-.000238	.000000	.000000	.007099	.000000
1.00	-.006246	-.000207	.000000	.000000	.006453	.000000
1.10	-.005639	-.000179	.000000	.000000	.005818	.000000
1.20	-.005054	-.000153	.000000	.000000	.005207	.000000
1.30	-.004499	-.000130	.000000	.000000	.004629	.000000
1.40	-.003979	-.000110	.000000	.000000	.004089	.000000
1.50	-.003497	-.000093	.000000	.000000	.003590	.000000
1.60	-.003053	-.000079	.000000	.000000	.003132	.000000
1.70	-.002648	-.000067	.000000	.000000	.002715	.000000
1.80	-.002281	-.000056	.000000	.000000	.002338	.000000
1.90	-.001952	-.000047	.000000	.000000	.001999	.000000
2.00	-.001658	-.000040	.000000	.000000	.001697	.000000
2.10	-.001398	-.000033	.000000	.000000	.001431	.000000
2.20	-.001170	-.000028	.000000	.000000	.001197	.000000
2.30	-.000972	-.000023	.000000	.000000	.000995	.000000
2.40	-.000801	-.000019	.000000	.000000	.000820	.000000
2.50	-.000655	-.000015	.000000	.000000	.000671	.000000
2.60	-.000532	-.000013	.000000	.000000	.000545	.000000
2.70	-.000429	-.000010	.000000	.000000	.000439	.000000
2.80	-.000343	-.000008	.000000	.000000	.000351	.000000
2.90	-.000272	-.000006	.000000	.000000	.000278	.000000
3.00	-.000214	-.000005	.000000	.000000	.000219	.000000
3.50	-.000058	-.000001	.000000	.000000	.000059	.000000
4.00	-.000013	.000000	.000000	.000000	.000013	.000000
4.50	-.000002	.000000	.000000	.000000	.000002	.000000
5.00	.000000	.000000	.000000	.000000	.000000	.000000
5.50	.000000	.000000	.000000	.000000	.000000	.000000
6.00	.000000	.000000	.000000	.000000	.000000	.000000

Table 23. Species Mass Fluxes With Respect to Stationary Coordinates. Multicomponent Fluxes Based on the High Diffusivity Profiles.

η	m_{O_2}	m_{N_2}	m_O	m_N	m_{CO_2}	m_{CO}
.00	.000000	-.002110	.000000	.000000	-.011203	.017337
.10	.000000	-.002581	.000000	.000000	-.011005	.016856
.20	.000000	-.004104	.000000	.000000	-.011228	.016420
.30	-.000001	-.006344	.000000	.000000	-.011703	.015861
.40	-.000017	-.009151	.000000	.000000	-.012520	.015391
.50	-.002344	-.011231	-.000001	.000000	-.008554	.011183
.60	-.006668	-.012692	.000000	.000000	-.000316	.003738
.70	-.008951	-.015355	.000001	.000000	.003276	.000079
.80	-.009334	-.019018	.000000	.000000	.002475	.000001
.90	-.009773	-.022601	.000000	.000000	.001764	.000000
1.00	-.010293	-.026094	.000000	.000000	.001209	.000000
1.10	-.010869	-.029443	.000000	.000000	.000791	.000000
1.20	-.011488	-.032665	.000000	.000000	.000478	.000000
1.30	-.012133	-.035758	.000000	.000000	.000251	.000000
1.40	-.012809	-.038778	.000000	.000000	.000085	.000000
1.50	-.013498	-.041695	.000000	.000000	-.000028	.000000
1.60	-.014200	-.044535	.000000	.000000	-.000103	.000000
1.70	-.014908	-.047298	.000000	.000000	-.000148	.000000
1.80	-.015632	-.050037	.000000	.000000	-.000173	.000000
1.90	-.016359	-.052717	.000000	.000000	-.000182	.000000
2.00	-.017091	-.055360	.000000	.000000	-.000180	.000000
2.10	-.017822	-.057959	.000000	.000000	-.000170	.000000
2.20	-.018566	-.060564	.000000	.000000	-.000157	.000000
2.30	-.019309	-.063134	.000000	.000000	-.000141	.000000
2.40	-.020054	-.065687	.000000	.000000	-.000124	.000000
2.50	-.020797	-.068213	.000000	.000000	-.000107	.000000
2.60	-.021551	-.070759	.000000	.000000	-.000091	.000000
2.70	-.022302	-.073281	.000000	.000000	-.000077	.000000
2.80	-.023054	-.075797	.000000	.000000	-.000064	.000000
2.90	-.023802	-.078291	.000000	.000000	-.000052	.000000
3.00	-.024561	-.080813	.000000	.000000	-.000042	.000000
3.50	-.028336	-.093304	.000000	.000000	-.000013	.000000
4.00	-.032115	-.105764	.000000	.000000	-.000003	.000000
4.50	-.035891	-.118202	.000000	.000000	-.000001	.000000
5.00	-.039676	-.130668	.000000	.000000	-.000001	.000000
5.50	-.043456	-.143118	.000000	.000000	.000000	.000000
6.00	-.047237	-.155568	.000000	.000000	.000000	.000000

Table 24. Elemental Mass Fluxes With Respect to the Mixture Mass Average Velocity and to Stationary Coordinates. Multicomponent Fluxes Based on the High Diffusivity Profiles.

η	$\tilde{J}_O$	$\tilde{J}_N$	$\tilde{J}_C$	$\tilde{m}_O$	$\tilde{m}_N$	$\tilde{m}_C$
.00	.000960	-.004738	.003778	.001758	-.002110	.004377
.10	.000968	-.004748	.003780	.001626	-.002581	.004224
.20	.000993	-.004836	.003843	.001215	-.004104	.003977
.30	.001003	-.004851	.003848	.000550	-.006344	.003607
.40	.000994	-.004791	.003797	-.000330	-.009151	.003183
.50	.000154	-.003553	.003399	-.002177	-.011231	.002461
.60	-.001330	-.001375	.002704	-.004763	-.012682	.001517
.70	-.001958	-.000320	.002278	-.006523	-.015355	.000928
.80	-.001842	-.000269	.002111	-.007534	-.019018	.000676
.90	-.001700	-.000238	.001937	-.008490	-.022601	.000482
1.00	-.001554	-.000207	.001761	-.009414	-.026094	.000330
1.10	-.001409	-.000179	.001588	-.010294	-.029443	.000216
1.20	-.001268	-.000153	.001421	-.011140	-.032665	.000130
1.30	-.001133	-.000130	.001263	-.011951	-.035758	.000068
1.40	-.001006	-.000110	.001116	-.012747	-.038778	.000023
1.50	-.000886	-.000093	.000980	-.013518	-.041695	-.000008
1.60	-.000776	-.000079	.000855	-.014275	-.044535	-.000028
1.70	-.000674	-.000067	.000741	-.015016	-.047298	-.000040
1.80	-.000582	-.000056	.000638	-.015758	-.050037	-.000047
1.90	-.000498	-.000047	.000546	-.016491	-.052717	-.000050
2.00	-.000424	-.000040	.000463	-.017221	-.055360	-.000049
2.10	-.000357	-.000033	.000391	-.017946	-.057959	-.000046
2.20	-.000299	-.000028	.000327	-.018681	-.060564	-.000043
2.30	-.000248	-.000023	.000271	-.019412	-.063134	-.000038
2.40	-.000205	-.000019	.000224	-.020145	-.065687	-.000034
2.50	-.000168	-.000015	.000183	-.020875	-.068213	-.000029
2.60	-.000136	-.000013	.000149	-.021618	-.070759	-.000025
2.70	-.000110	-.000010	.000120	-.022358	-.073281	-.000021
2.80	-.000088	-.000008	.000096	-.023100	-.075797	-.000017
2.90	-.000070	-.000006	.000076	-.023840	-.078291	-.000014
3.00	-.000055	-.000005	.000060	-.024591	-.080813	-.000011
3.50	-.000015	-.000001	.000016	-.028345	-.093304	-.000003
4.00	-.000003	.000000	.000004	-.032117	-.105764	-.000001
4.50	-.000001	.000000	.000001	-.035891	-.118202	.000000
5.00	.000000	.000000	.000000	-.039676	-.130668	.000000
5.50	.000000	.000000	.000000	-.043456	-.143118	.000000
6.00	.000000	.000000	.000000	-.047237	-.155568	.000000

Table 25. Species Mass Fluxes With Respect to the Mixture Mass Average Velocity. Multicomponent Fluxes Based on the Low Diffusivity Profiles.

η	J_{O_2}	J_{N_2}	J_O	J_N	J_{CO_2}	J_{CO}
.00	.000000	-.005243	.000000	.000000	-.012397	.017641
.10	.000000	-.005285	.000000	.000000	-.012437	.017722
.20	.000000	-.005384	.000000	.000000	-.012608	.017992
.30	.000000	-.005387	.000000	.000000	-.012552	.017940
.40	-.000087	-.005260	.000000	.000000	-.012099	.017447
.50	-.004611	-.002882	.000000	.000000	-.001457	.008950
.60	-.009024	-.000441	.000000	.000000	.009122	.000342
.70	-.008573	-.000314	.000000	.000000	.008883	.000004
.80	-.007849	-.000278	.000000	.000000	.008127	.000000
.90	-.007086	-.000242	.000000	.000000	.007328	.000000
1.00	-.006316	-.000207	.000000	.000000	.006524	.000000
1.10	-.005566	-.000175	.000000	.000000	.005742	.000000
1.20	-.004854	-.000147	.000000	.000000	.005001	.000000
1.30	-.004190	-.000122	.000000	.000000	.004312	.000000
1.40	-.003583	-.000100	.000000	.000000	.003683	.000000
1.50	-.003034	-.000082	.000000	.000000	.003116	.000000
1.60	-.002545	-.000067	.000000	.000000	.002612	.000000
1.70	-.002116	-.000054	.000000	.000000	.002169	.000000
1.80	-.001741	-.000043	.000000	.000000	.001785	.000000
1.90	-.001420	-.000035	.000000	.000000	.001454	.000000
2.00	-.001146	-.000028	.000000	.000000	.001174	.000000
2.10	-.000916	-.000022	.000000	.000000	.000938	.000000
2.20	-.000725	-.000017	.000000	.000000	.000743	.000000
2.30	-.000568	-.000014	.000000	.000000	.000582	.000000
2.40	-.000441	-.000011	.000000	.000000	.000451	.000000
2.50	-.000339	-.000008	.000000	.000000	.000347	.000000
2.60	-.000258	-.000006	.000000	.000000	.000264	.000000
2.70	-.000194	-.000005	.000000	.000000	.000198	.000000
2.80	-.000144	-.000004	.000000	.000000	.000148	.000000
2.90	-.000106	-.000003	.000000	.000000	.000109	.000000
3.00	-.000078	-.000002	.000000	.000000	.000080	.000000
3.50	-.000014	-.000000	.000000	.000000	.000014	.000000
4.00	-.000002	.000000	.000000	.000000	.000002	.000000
4.50	.000000	.000000	.000000	.000000	.000000	.000000
5.00	.000000	.000000	.000000	.000000	.000000	.000000
5.50	.000000	.000000	.000000	.000000	.000000	.000000
6.00	.000000	.000000	.000000	.000000	.000000	.000000

Table 26. Species Mass Fluxes With Respect to Stationary Coordinates. Multicomponent Fluxes Based on the Low Diffusivity Profiles.

η	m_{O_2}	m_{N_2}	m_O	m_N	m_{CO_2}	m_{CO}
.00	.000000	-.003041	.000000	.000000	-.012397	.018811
.10	.000000	-.003523	.000000	.000000	-.012274	.018451
.20	.000000	-.004989	.000000	.000000	-.012536	.018111
.30	.000000	-.007096	.000000	.000000	-.013007	.017610
.40	-.000087	-.009671	.000000	.000000	-.013619	.017035
.50	-.004618	-.010413	.000000	.000000	-.004573	.008925
.60	-.009527	-.011388	.000000	.000000	.005244	.000342
.70	-.009838	-.014781	.000000	.000000	.004581	.000004
.80	-.010070	-.018279	.000000	.000000	.003664	.000000
.90	-.010395	-.021712	.000000	.000000	.002912	.000000
1.00	-.010802	-.025092	.000000	.000000	.002300	.000000
1.10	-.011267	-.028358	.000000	.000000	.001812	.000000
1.20	-.011779	-.031519	.000000	.000000	.001423	.000000
1.30	-.012326	-.034568	.000000	.000000	.001115	.000000
1.40	-.012910	-.037557	.000000	.000000	.000869	.000000
1.50	-.013517	-.040450	.000000	.000000	.000675	.000000
1.60	-.014145	-.043272	.000000	.000000	.000522	.000000
1.70	-.014787	-.046016	.000000	.000000	.000403	.000000
1.80	-.015455	-.048741	.000000	.000000	.000308	.000000
1.90	-.016132	-.051407	.000000	.000000	.000235	.000000
2.00	-.016821	-.054035	.000000	.000000	.000178	.000000
2.10	-.017517	-.056618	.000000	.000000	.000135	.000000
2.20	-.018232	-.059209	.000000	.000000	.000101	.000000
2.30	-.018950	-.061765	.000000	.000000	.000075	.000000
2.40	-.019673	-.064295	.000000	.000000	.000056	.000000
2.50	-.020402	-.066817	.000000	.000000	.000041	.000000
2.60	-.021144	-.069351	.000000	.000000	.000030	.000000
2.70	-.021885	-.071864	.000000	.000000	.000021	.000000
2.80	-.022628	-.074369	.000000	.000000	.000015	.000000
2.90	-.023370	-.076854	.000000	.000000	.000011	.000000
3.00	-.024124	-.079368	.000000	.000000	.000008	.000000
3.50	-.027889	-.091836	.000000	.000000	.000001	.000000
4.00	-.031666	-.104286	.000000	.000000	-.000001	.000000
4.50	-.035441	-.116723	.000000	.000000	-.000001	.000000
5.00	-.039227	-.129189	.000000	.000000	-.000001	.000000
5.50	-.043008	-.141640	.000000	.000000	.000000	.000000
6.00	-.046788	-.154090	.000000	.000000	.000000	.000000

Table 27. Elemental Mass Fluxes With Respect to the Mixture Mass Average Velocity and to Stationary Coordinates. Multicomponent Fluxes Based on the Low Diffusivity Profiles.

η	$\tilde{J}_O$	$\tilde{J}_N$	$\tilde{J}_C$	$\tilde{m}_O$	$\tilde{m}_N$	$\tilde{m}_C$
.00	.001062	-.005243	.004181	.001731	-.003041	.004683
.10	.001080	-.005285	.004205	.001615	-.003523	.004562
.20	.001110	-.005384	.004274	.001230	-.004989	.004345
.30	.001120	-.005387	.004267	.000601	-.007096	.004001
.40	.001081	-.005260	.004179	-.000258	-.009671	.003588
.50	-.000558	-.002892	.003440	-.002845	-.010413	.002579
.60	-.002195	-.000441	.002636	-.005519	-.011388	.001578
.70	-.002112	-.000314	.002426	-.006505	-.014781	.001252
.80	-.001940	-.000278	.002218	-.007406	-.018279	.001000
.90	-.001758	-.000242	.002000	-.008278	-.021712	.000795
1.00	-.001573	-.000207	.001780	-.009129	-.025092	.000628
1.10	-.001392	-.000175	.001567	-.009949	-.028358	.000495
1.20	-.001218	-.000147	.001365	-.010744	-.031519	.000388
1.30	-.001055	-.000122	.001177	-.011515	-.034568	.000304
1.40	-.000905	-.000100	.001005	-.012279	-.037557	.000237
1.50	-.000769	-.000082	.000850	-.013026	-.040450	.000184
1.60	-.000646	-.000067	.000713	-.013765	-.043272	.000143
1.70	-.000538	-.000054	.000592	-.014495	-.046016	.000110
1.80	-.000444	-.000043	.000487	-.015230	-.048741	.000084
1.90	-.000362	-.000035	.000397	-.015961	-.051407	.000064
2.00	-.000293	-.000028	.000320	-.016692	-.054035	.000049
2.10	-.000234	-.000022	.000256	-.017419	-.056618	.000037
2.20	-.000185	-.000017	.000203	-.018158	-.059209	.000028
2.30	-.000145	-.000014	.000159	-.018896	-.061765	.000021
2.40	-.000113	-.000011	.000123	-.019632	-.064295	.000015
2.50	-.000087	-.000008	.000095	-.020373	-.066817	.000011
2.60	-.000066	-.000006	.000072	-.021122	-.069351	.000008
2.70	-.000050	-.000005	.000054	-.021869	-.071864	.000006
2.80	-.000037	-.000004	.000040	-.022617	-.074369	.000004
2.90	-.000027	-.000003	.000030	-.023362	-.076854	.000003
3.00	-.000020	-.000002	.000022	-.024119	-.079368	.000002
3.50	-.000003	.000000	.000004	-.027888	-.091836	.000000
4.00	-.000001	.000000	.000001	-.031667	-.104288	.000000
4.50	.000000	.000000	.000000	-.035442	-.116723	.000000
5.00	.000000	.000000	.000000	-.039227	-.129189	.000000
5.50	.000000	.000000	.000000	-.043008	-.141640	.000000
6.00	.000000	.000000	.000000	-.046788	-.154090	.000000

low diffusivity results.) A partial update of the mole fraction profiles (used to reduce the sensitivity of the $\tilde{D}_j$ on the mole fraction profiles), starting with the composition profiles resulting from the binary diffusivity solutions did converge in the innermost iterative loop of the numerical scheme. It is expected that the full multicomponent problem would converge to a solution; however, due to limitations on the available computation time, it was not possible to achieve such a solution in the present work.

Subsurface Heat Transfer Rate at the Carbon Surface

An energy balance at the surface (see Figure 8, page 112) results in:

$$q_s + \left(k \frac{\partial T}{\partial y}\right) - q_r + m_w H_s - \left(\sum_i m_i H_i\right)_w = 0 \qquad (5.5)$$

where q_s is the conductive heat flux from the interior of the solid towards the surface, H_s is the enthalpy of the solid carbon at the temperature T_w, and $(k\ \partial T/\partial y)_w$ represents the conductive heat flux from the gas phase to the surface. The contributions of each mode of energy transfer to the net heat transfer rate at the surface are presented in Table 28 (not including the radiant energy transfer). These contributions have been evaluated from the numerical solutions of the high diffusivity and low diffusivity runs.

Applicability of the Previous Results

The numerical results previously obtained apply to the stagnation streamline of any carbon body for which $\beta=1$, regardless of the value of

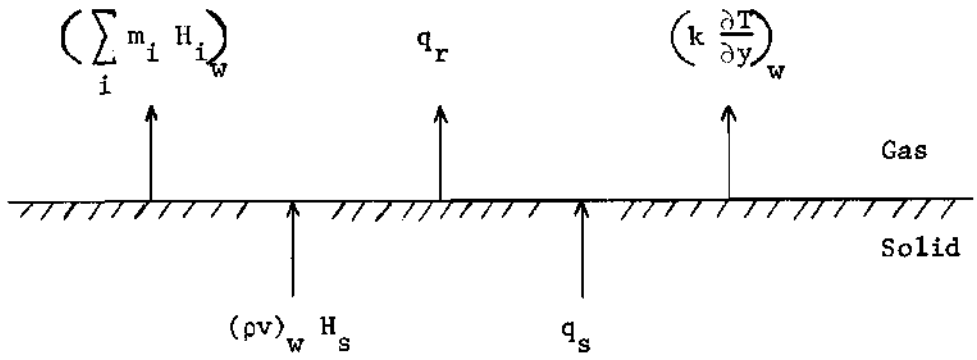

Figure 8. Heat Transfer Rate at the Surface

Table 28. Contributions of Energy Transfer Modes to the Heat Transfer Rate at the Surface

		High Diffusivity	Low Diffusivity
$\left(-k \frac{\partial T}{\partial y}\right)_w$	(cal/cm^2·sec)	-9.54	-6.45
$\left(\sum_i m_i H_i\right)_w$	(cal/cm^2·sec)	+15.74	+13.20
$-m_w H_s$	(cal/cm^2·sec)	-1.86	-1.56
q_s	(cal/cm^2·sec)	+4.34	+5.18

R_b and U_e (except for the limitation on U_e discussed below), provided that the boundary conditions T_e, T_w, all $(x_i)_e$, and P_e remain unchanged. If a solution is required for new values of U_e and R_b, say U_e^* and R_b^*, the fluxes must be multiplied by the ratio $(R_b\ U_e^*)^{\frac{1}{2}} \cdot (R_b^*\ U_e)^{-\frac{1}{2}}$ and the values of f, f', f'', T, and all compositions remain unchanged. The solutions presented in this work are for values of $(R_b/U_e)^{\frac{1}{2}} = (0.6/1500)^{\frac{1}{2}} = 0.02\ \text{sec}^{\frac{1}{2}}$.

The restriction on U_e mentioned above is that the term $U_e^2 \left[C(f'')^2 + f'\left(\frac{C_p T}{C_{pe} T_e} - \frac{\rho_e}{\rho}\right)\right]$ in the energy Equation (2.68) be negligible in comparison to the remaining energy equation terms. In the solutions presented in this work the term in question contributed less than one percent to the total energy equation; this can be shown to be the case for sufficiently low Mach number flows.

Approximate Solution for the Combustion Rate at the Carbon Surface

An approximate solution for the combustion rate at a carbon surface can be easily obtained if certain simplifying assumptions are made.

If the density and viscosity are assumed constant, the momentum Equation (2.47) becomes:

$$f''' + ff'' + \beta\left[1 - (f')^2\right] = 0 \qquad (5.6)$$

which is the constant property momentum equation. (Note that for geometries with $\beta \neq 0$, the assumption of $(\rho\mu)$ constant is not sufficient; indeed ρ and μ must be independently constant.)

If, in addition to constant density and viscosity, it is assumed that all the binary diffusivities are equal and constant across the boundary layer, the elemental conservation Equations (2.69) become:

$$\tilde{\omega}_j'' + \left(\frac{\mu}{\rho\mathcal{D}}\right) f \tilde{\omega}_j' = 0 \qquad (j=1, \ldots, K) \tag{5.7}$$

which is the constant property elemental conservation equation. From the boundary conditions at the wall, given by Equations (2.75, 2.84, and 2.85) it can be shown that Equation (5.1) follows.

For wall temperatures resulting in diffusion controlled combustion reactions at a carbon surface burning in an air stream, the only gas species present at the surface may be assumed to be N_2 and CO. At a surface temperature of 1500°K, the only other species at the wall is CO_2, and its mole fraction is only $9.1\text{x}10^{-5}$; at higher temperature, the equilibrium equations will favor the formation of CO at the wall, and therefore, the mole fraction of CO_2 at the wall would be even smaller. At higher temperatures, the dissociation reaction for O_2 begins to become appreciable, with the mole fraction of atomic oxygen approaching 0.001 at a wall temperature of about 2200°K; the N_2 dissociation is not appreciable until even higher wall temperatures are reached. As a result, the assumption of only N_2 and CO as the existing gas species at the wall is indeed very satisfactory in the range $1300 < T_w < 2200$°K.

If N_2 and CO are assumed to be the only species present at the wall, then Equation (5.1) can be solved for the gas composition at the surface. The resulting elemental mass fractions are: $\tilde{\omega}_{Ow} = 0.1983$, $\tilde{\omega}_{Nw} = 0.6529$, and $\tilde{\omega}_{Cw} = 0.1488$, which remain constant at those values for $1300 < T_w < 2200$°K.

From Equation (5.7) and the wall boundary conditions (Equations 2.75, 2.84, and 2.85) it can be shown that:

$$-f_w \, Sc = \left(\frac{\tilde{\omega}_{je} - \omega_{jw}}{\tilde{\omega}_{jw} - \alpha_{jw}} \right) \cdot \pi'(\eta=0, \beta=1, -f_w, Sc) \qquad (5.8)$$

where α_{jw} is the mass fraction of element j in the solid ($\alpha_{Ow} = \alpha_{Nw} = 0$, $\alpha_{Cw} = 1$), and $\pi'(\eta=0, \beta=1, -f_w, Sc)$ is the dimensionless profile gradient obtained from the solution of the constant property equations and given by standard tabulations, such as those of Elzy and Sisson (9).

For no mass transfer and a Schmidt number of unity the profile gradient, according to the data of Elzy and Sisson is:

$$\pi'(\eta=0, \beta=1, -f_w=0, Sc=1) = 0.57046 \qquad (5.9)$$

Correcting this value of the profile gradient for the Schmidt number dependence and for finite mass transfer rates at the surface:

$$\pi'(\eta=0, \beta=1, -f_w, Sc) = 0.57046 \, Sc^{1/3} \, \frac{\ell n(1+B)}{B} \qquad (5.10)$$

where

$$B = \left(\frac{\tilde{\omega}_{je} - \tilde{\omega}_{jw}}{\tilde{\omega}_{jw} - \alpha_{jw}} \right) \qquad (5.11)$$

and B is a constant equal for all of the elements. Substituting Equation (5.10) into (5.8) there results:

$$-f_w = 0.57046 \, Sc^{-2/3} \, \ell n(1+B) \qquad (5.12)$$

Combining Equation (2.75) and (5.10) a correlation is obtained for the prediction of the combustion rate at a carbon surface burning in air,

with a wall temperature in the range $1300 < T_w < 2200°K$:

$$\frac{m_w}{2\ \rho_e\ U_e} = C_1 \left[0.57046\ Sc^{-2/3}\ \ell n(1+B)\ Re^{-1/2}\right] \tag{5.13}$$

where C_1 is a free constant to be used in matching the approximate combustion rate calculated from Equation (5.13) (with $C_1 = 1$) to the numerical results obtained from the computer solutions. The Reynolds number, Re, is defined as:

$$Re = \frac{2\ R_b\ U_e\ \rho_e}{\mu_e} \tag{5.14}$$

and the Schmidt number is to be evaluated at the free stream conditions. Following the approach outlined above, with $C_1 = 1.0$, the calculated combustion rate at the surface for the high diffusivity assumption was 0.003626 g /cm^2·sec, or 90.06 percent of the value calculated in the computer solution. To match the computer results with the approximate results of Equation (5.13) (with $C_1 = 1$) the value of the free constant must be $C_1 = 1.1103$. Estimating the combustion rate at the surface from Equation (5.13) with $C_1 = 1.1103$ for the low diffusivity assumption, the result is 0.003317 g /cm^2·sec, which deviates by about 1.8 percent from the computer result of 0.003376 g /cm^2·sec. The correlation equation, therefore, can be taken as:

$$\frac{m_w}{2\ \rho_e\ U_e} = 0.6334\ Sc^{-2/3}\ \ell n(1+B)\ Re^{-1/2} \tag{5.15}$$

where the dimensionless profile gradient obtained from the solution of the constant property boundary layer equations has been multiplied by a

"correcting factor," $C_1 = 1.1103$, to match the results with the variable physical property numerical solution.

Some comments are in order regarding the applicability of Equation (5.15). As stated above, the value of B is a constant equal for all the elements (this follows from the assumption of equal binary diffusivities and the boundary conditions for the elemental conservation equations). Furthermore, for carbon combustion in an <u>air</u> stream, when the wall temperature is such that essentially only N_2 and CO are present in the vicinity of the wall ($1300 < T_w < 2200°K$), the value of B is approximately 0.1748. The Schmidt number can be shown to be, to a first approximation, independent of temperature. Since the Reynolds number varies approximately with the -3/2 power of the temperature and density varies inversely with temperature, it is expected that the combustion rate would vary with the -1/4 power of the free stream temperature, and be essentially independent of the wall temperature in the diffusion controlled regime. It is also expected that the combustion rate will vary with the -1/2 power of the body radius and with the 1/2 power of the approach velocity.

The excellent agreement obtained in predicting the low diffusivity combustion rate after matching the approximate equation to the results of the high diffusivity combustion rate, demonstrates that the differences between the two combustion rates calculated from the numerical solutions are attributable to differences in Schmidt numbers.

Approximate Solution for the Subsurface Heat Transfer Rate at the Carbon Surface

With the assumption of equal binary diffusivities, the energy Equation (2.20) applicable along the stagnation streamline of a cylinder can be written in terms of the mixture enthalpy as:

$$\rho u \frac{\partial H}{\partial x} + \rho v \frac{\partial H}{\partial y} = \frac{\partial}{\partial y}\left[\frac{\mu}{Pr}\frac{\partial H}{\partial y} + \left(\frac{1}{Le} - 1\right)\rho \sum_i \left(H_i \frac{\partial \omega_i}{\partial y}\right)\right] \qquad (5.16)$$

If ρ, μ, $\mathcal{D}$, k, C_p are assumed constant and, in addition, $Pr = Sc$, $(Le = 1)$, then the energy equation becomes:

$$\rho u \frac{\partial H}{\partial x} + \rho v \frac{\partial H}{\partial y} = \frac{k}{\rho C_p}\frac{\partial^2 H}{\partial y^2} \qquad (5.17)$$

which is the usual form of the constant property energy equation but with the temperature replaced by the mixture enthalpy as the independent variable (thus including chemical reaction effects). The profile gradient is given by:

$$\pi'(\eta=0,\ \beta=1,\ -f_w,\ Pr) = \frac{d}{d\eta}\left[\frac{H - H_w}{H_e - H_w}\right]_w \qquad (5.18)$$

It can be shown that:

$$\frac{-\left(\frac{k}{C_p}\frac{\partial H}{\partial y}\right)_w}{2\,\rho_e U_e (H_e - H_w)} = \pi'(\eta=0,\ \beta=1,\ -f_w,\ Pr)\ Re^{-\frac{1}{2}}\ Pr \qquad (5.19)$$

Following a procedure similar to that used in obtaining Equation (5.13):

$$\frac{-\left(\frac{k}{C_p}\frac{\partial H}{\partial y}\right)_w}{2\,\rho_e\,U_e\,(H_e - H_w)} = C_2\left[0.57046\,Pr^{-2/3}\,\frac{\ell n(1+B)}{B}\,Re^{-1/2}\right] \qquad (5.20)$$

Similarly, it can be shown that for the case of Le = 1, and constant physical properties, Equation (5.5) becomes:

$$q_s = -\left(\frac{k}{C_p}\frac{\partial H}{\partial y}\right)_w + m_w\,(H_w - H_s) + q_r \qquad (5.21)$$

Substitution of Equations (5.15) and (5.20) into Equation (5.21) yields an approximate expression for the subsurface heat transfer rate (assuming the value of the constant $C_2 = C_1$):

$$\frac{q_s}{2\,\rho_e\,U_e\,(H_e - H_w)} = 0.6334\,Pr^{-2/3}\,\ell n(1+B)\,Re^{-1/2}\left[1 + B\left(\frac{H_w - H_s}{H_e - H_w}\right)\right] \qquad (5.22)$$

$$+\frac{q_r}{2\,\rho_e\,U_e\,(H_e - H_w)}$$

The enthalpies of the gas species in the numerical solutions were calculated by integrating the species heat capacity Equations (3.18), with the mixture enthalpy being calculated from the species enthalpies and their mass fractions in the mixture. Because of the fortuitous choice of the reference temperature employed, the quantities H_e and H_w are numerically close together. By subtracting these two quantities, considerable accuracy is lost and the results obtained from Equation (5.22) are poor. It should be emphasized that this problem can be avoided by employing a different reference temperature in the calculation of the species enthalpies.

CHAPTER VI

CONCLUSIONS AND RECOMMENDATIONS

Conclusions

Based on the results of this investigation, the following conclusions were made:

1. The use of the effective elemental diffusivities provides a straightforward numerical technique for the solution of the elemental conservation equations. However, due to the sensitivity of the effective elemental diffusivities to the composition profiles from which they are calculated, an iterative numerical solution of the elemental conservation equations for the system studied would require a large amount of computer time.

2. Computer solutions for assumed equal binary diffusivities show that the differences in the results between the assumed high diffusivity and low diffusivity are slight and can be explained by arguments involving the Schmidt number for the gas mixture. The high diffusivity solution results in higher boundary layer velocity ratios and higher temperatures than those resulting from the low diffusivity solution. Composition profiles for both solutions were not only similar but also numerically close together. The high diffusivity assumption resulted in a burning rate approximately 20 percent higher than that obtained with the low diffusivity assumption, and a subsurface heat transfer rate approximately 16 percent lower.

3. Approximate equations for predicting combustion rates and subsurface heat transfer rates were obtained based on available solutions of the constant property boundary layer equations. The approximate equation predicted a combustion rate corresponding to the high diffusivity assumption that was ten percent low. Matching the approximate equation to the numerical solution for the high diffusivity assumption permitted the prediction of the combustion rate for the low diffusivity assumption to within two percent. The approximate equations developed should prove useful in predicting the results of carbon combustion taking place under conditions different from those in this investigation.

4. The iterative scheme developed in the present work can be used to parametrically study the combustion of carbon for other free stream temperatures, compositions and approach gas velocities, as well as for different wall temperatures and body geometries. Only minor modifications of the details of the numerical technique will be necessary to study many different systems with interfacial mass transfer.

Recommendations

The following recommendations for future work are the result of the experience gained in this investigation:

1. The numerical techniques used in the investigation should be employed in an effort to attain the solution of the fully multicomponent, variable property, carbon combustion problem. The suggestions listed below should prove valuable in realizing savings in computer time:

a. The evaluation of physical properties accounts for about 75-80 percent of the total computation time. A 15-20 percent savings in computer time should be realized by breaking up the calculations according to their temperature and/or composition dependence. Thus, it would be desirable to account for the temperature dependence of the species properties only when temperature has been updated, instead of when either temperature or composition has been updated (as in the present work).

b. At the temperatures involved in this study, the effect of air species dissociation on the overall process is negligible. Thus, at these temperatures, the deletion of O and N from the considered species would also reduce the computation time. However, it is felt that for wall temperatures above 1800°K, the dissociation of O_2 in the vicinity of the temperature maximum would be significant and the equilibrium model would no longer be valid without consideration of elemental O. (The same comment applies to the dissociation of N_2, which is significant at higher temperatures than those for O_2.)

APPENDIX

COMPUTER PROGRAMS

The numerical calculations presented in this work were made on the UNIVAC 1108 Digital Computer operated by the Rich Electronic Computer Center at the Georgia Institute of Technology. All programs were written in FORTRAN V source language. Chapter IV discusses the computer programs in detail. The nomenclature which applies to the programs is presented in the following pages, as well as a schematic of the program arrangement showing counter variables, upper limits for these counters, convergence tolerances and logical variables used to denote convergence. A flowchart indicating the interactions among the various subroutines was presented in Chapter IV.

Nomenclature for Computer Programs

Real Variables

A(I,J)	J^{th} coefficient in the heat capacity equation of specie I
B(I,J)	J^{th} coefficient in the I^{th} chemical equilibrium equation
BURNM	mass transfer rate at the wall
C(L)	dimensionless density-viscosity product
CD(L)	derivative of C(L)
COEFF(J,L)	coefficient in the J^{th} elemental conservation equation at location L
CP(I,L)	heat capacity of specie I at location L
CPM(L)	mixture heat capacity at location L
DB(I,J,L)	binary diffusivity of species I and J at location L
DE(J,L)	effective elemental diffusivity of element J at location L
DELTA	constant step size in the transformed coordinate plane
DEN(L)	array used in the calculation of VISM(L) and THCM(L)
DM(I,J,L)	multicomponent diffusivity of species I and J at location L
DS(I,J)	accumulators and/or temporary storage
E(I,J)	mass of element J per unit mass of specie I
EK(I)	Lennard-Jones energy of interaction of specie I
EKP(I,J)	Lennard-Jones energy of interaction of species I and J
EQ(K,L)	K^{th} chemical equilibrium constant at location L ($K=1, K_{CO}$ $K=2, K_O$ $K=3, K_N$ $K=4, K_S$)
ER(I,L)	error in X(I,L,K) in subroutines EQUIL and CONWAL
ERRELE(J,L)	error in WE(J,L,K) in subroutine ELEMT

ERRFPP(K)	error in FPP(1) in subroutine MOMT
ERRT(L)	error in T(L,K) in subroutine ENERGY
ERRVEL(L)	error in FP(L,K) in subroutine MOMT
ETA(L)	value of the transformed coordinate at location L
F(L,K)	integral of FP(L,K) at location L, K^{th} iteration
FBURN	mass transfer rate at the wall
FFO(I,J)	array used in the calculation of DM(I,J,L)
FJE(J,L)	elemental mass flux of element J with respect to the mixture mass average velocity at location L
FJS(I,L)	mass flux of specie I with respect to the mixture mass average velocity at location L
FNE(J,L)	elemental mass flux of element J with respect to stationary coordinates at location L
FNO(I,J)	array used in the calculation of DM(I,J,L)
FNS(I,L)	mass flux of specie I with respect to stationary coordinates at location L
FNT(I,J)	array used in the calculation of DM(I,J,L)
FO(I,J)	array used in the calculation of DM(I,J,L)
FP(L,K)	velocity ratio at location L, K^{th} iteration index
FPP(L,K)	derivative of FP(L,K)
FPPW(K)	value of FPP(1,K), K^{th} iteration index
FW1	value of FBURN calculated from element O
FW2	value of FBURN calculated from element N
FW3	value of FBURN calculated from element C
FWBAR	arithmetic average of FW1, FW2, and FW3
GEN(I,L)	rate of generation of specie I at location L
H(I,L)	enthalpy of specie I at location L
HB(I)	enthalpy of specie I at base temperature

HMIX(L)	mixture enthalpy at location L
HRAT(L)	dimensionless mixture enthalpy ratio at location L
P	pressure
PHI(I,J)	mixture rule parameter for VISM(L) and THCM(L)
PR(L)	mixture Prandtl number at location L
RB	principal body radius of curvature
RHOM(L)	mixture density at location L
RR(L)	RHOM(NETA)/RHOM(L)
RT(L)	dimensionless temperature ratio at location L
RU	universal gas constant (82.0560 atm cm^3/gr.mole K)
SC(L)	mixture Schmidt number at location L
SDEN(I)	array used in the calculation of VISM(L) and THCM(L)
SIG(I)	Lennard-Jones collision diameter of specie I
SIGP(I,J)	Lennard-Jones collision diameter of species I and J
T(L,K)	absolute temperature at location L, K^{th} iteration index
THC(I,L)	thermal conductivity of specie I at location L
THCM(L)	mixture thermal conductivity at location L
TLCONC	maximum allowable value of ER(I,L)
TLELEM	maximum allowable value of ERRELE(J,L)
TLENER	maximum allowable value of ERRT(L)
TLMOML	maximum allowable error in momentum and elemental conservation equations boundary conditions at the wall (in subroutine MOMLUP)
TLMOMT	maximum allowable value of ERRVEL(L) and ERRFPP(K)
UE	approach velocity (along stagnation streamline)
VIS(I,L)	viscosity of specie I at location L
VISM(L)	mixture viscosity at location L

VV(M)	array used for input/output in subroutine GJR
W(I,L,K)	mass fraction of specie I at location L, K^{th} iteration index
WE(J,L,K)	mass fraction of element J at location L, K^{th} iteration index
WEP(J,L)	derivative of WE(J,L,K)
WP(I,L)	derivative of W(I,L,K)
WT(I)	molecular weight of specie I
WTM(L)	mixture molecular weight at location L
WTP(I,J)	pseudo-molecular weight of species I and J
X(I,L,K)	mole fraction of specie I at location L, K^{th} iteration index
XEDGE(I)	mole fraction of specie I in the approach gas stream
XP(I,L)	derivative of X(I,L,K)
Y	distance from the body surface along the stagnation streamline

Integer Variables

IENRG	counter in subroutine ENGLUP
IKOUNT	on input: IKOUNT=0 generates WE(J,L,K), T(L,K), and FP(L,K) profiles IKOUNT=1 reads in WE(J,L,K), T(L,K), and FP(L,K) profiles
IMOMT	counter in subroutine MOMT
IPC	print control index in subroutine PROP
IPROP	counter in subroutine PROP
ISPEC	counter in subroutine SPCLUP
ITN(L)	counter in subroutines EQUIL and CONWAL
JC(I)	array used in subroutine GJR

MENERG	counter in subroutine ENERGY
MITN	upper limit on ITN(L)
MNELEM	upper limit on NELEM
MNMOMT	upper limit on NMOMT
MXMOMT	upper limit on IMOMT
MXSPEC	upper limit on ISPEC
MXTEMP	upper limit on IENRG
NELEM	counter in subroutine ELEMT
NENERG	counter in subroutine ENERGY
NETA	number of finite difference locations
NMOMT	counter in subroutine MOMT

Logical Variables

CVCONW	denotes convergence of the chemical equilibrium equations at the gas-solid interphase
CVELEM	denotes convergence of elemental conservation equations
CVENER	denotes convergence of energy equation
CVENGL	denotes convergence of entire solution
CVEQUI	denotes convergence of the chemical equilibrium equations in the gas phase
CVMOML	denotes convergence of mass transfer rate and of flux ratios at the surface
CVMOMT	denotes convergence of momentum equation
CVSPCL	denotes convergence of elemental mass fraction profiles and of flux ratios at the surface

Index of Species	Index of Elements
1 = O_2	1 = O
2 = N_2	2 = N
3 = O	3 = C
4 = N	
5 = CO_2	
6 = CO	

Schematic of Program Arrangement

Subroutine Name	Counter	Upper Limit of Counter	Tolerance Criteria	Convergence Indicator
DRIVER	******	******	******	******
INIT	******	******	******	******
PROP	IPROP	******	******	******
ENGLUP	IENRG	MXTEMP	******	CVENGL
MOMLUP	IMOMT	MXMOMT	TLMOML	CVMOML
SPCLUP	ISPEC	MXSPEC	TLSPCL	CVSPCL
MOMT	NMOMT	MNMOMT	TLMOMT	CVMOMT
ELEMT	NELEM	MNELEM	TLELEM	CVELEM
EQUIL	ITN(L)	MITN	TLCONC	CVEQUI
CONWAL	ITN(1)	MITN	TLCONC	CVCONW
GENER	******	******	******	******
ENERGY	NENERG	MNENER	TLENER	CVENER
OUTPUT	******	******	******	******

LISTING OF COMPUTER PROGRAMS

Main Program: Driver

```
C*************************************************************************
C**** ALL QUANTITIES HAVE UNITS CONSISTENT WITH THE  C.G.S SYSTEM
C**** DECLARATION STATEMENTS
C*************************************************************************
      LOGICAL CVENGL,CVMOML,CVSPCL,CVMOMT,CVELEM,CVEQUI,CVCONW,CVENER
      COMMON   SIG(6),EK(6),A(6,5),CP(6,101),HB(6),B(4,2),EQ(4,101),
     1 WT(6),FP(101,2),ETA(101),T(101,2),X(6,101,2),E(6,3),UE(3,101),
     2 WE(3,101,2),DS(6,101),WTM(101),RHOM(101),W(6,102,2),CPM(101),
     3 SIGP(6,6),EKP(6,6),WTP(6,6),VIS(6,101),THC(6,101),DB(6,6,101),
     4 PHI(6,6),VISM(101),THCM(101),DEN(6),SDEN(6),FO(6,6),FFO(6,6),
     5 FNO(5,5),FNT(5,5),JC(6),VV(2),DM(6,6,101),H(6,101),C(101),
     6 PR(101),F(101,2),ERRVEL(101),FPPW(2),ERRFPP(2),ERRELE(3,101),
     7 ER(6,101),XEDGE(6),GEN(6,101),WP(6,101),WPP(6,101),ERRT(101),
     8 P,NETA,DELTA,RU,BURNM,FBURN,RB,UE,FWBAR,IPROP,IENRG,IMOMT,
     9 ISPEC,NMOMT,NELEM,ITN(101),NENERG,MXTEMP,MXMOMT,MXSPEC,MNMOMT,
     0 MNELEM,MITN,MENERG,TLMOML,TLSPCL,TLMOMT,TLELEM,TLCONC,TLENER,
     1 CVENGL,CVMOML,CVSPCL,CVMOMT,CVELEM,CVEQUI,CVCONW,CVENER,FPP(101),
     2 IPC,FW1,FW2,FW3,CD(101),RR(101),XP(6,101),WEP(3,101),FJS(6,101),
     3 FJE(3,101),FHE(3,101),IKOUNT,HMIX(101),FNS(6,101),FNE(3,101)
      DIMENSION TITLE(12)
C*************************************************************************
C**** READ CARD INPUT DATA
C*************************************************************************
      READ 8,TITLE
    8 FORMAT (12A6)
   10 FORMAT ( )
      READ 10,NETA,DELTA,P,T(NETA,1),RB,UE,T(1,1),BURNM
      READ 10,(XEDGE(I),I=1,6)
      READ 10,MXTEMP,MXMOMT,MXSPEC,MNMOMT,MNELEM,MITN,MENERG,IPC,IKOUNT
      READ 10,TLMOML,TLSPCL,TLMOMT,TLELEM,TLCONC,TLENER
C*************************************************************************
C**** PRINT CARD INPUT DATA
C*************************************************************************
      PRINT 9,TITLE
    9 FORMAT(1H1,///,30X,12A6)
      PRINT 11,XEDGE(1),P,TLMOML,MXMOMT,XEDGE(2),T(1,1),TLSPCL,MXSPEC,
     1         XEDGE(3),T(NETA,1),TLMOMT,MNMOMT,XEDGE(4),UE,TLELEM,
     2         MNELEM,XEDGE(5),RB,TLCONC,MITN,XEDGE(6),BURNM,TLENER,
     3         MENERG,MXTEMP,DELTA,NETA
   11 FORMAT(///,
     1   6X,'XEDGE(O2)  =',E13.6,5X,'PRESSURE   =',E13.6,5X,'TLMOML =',
     2   E13.6,9X,'MXMOMT =',I6,/,
     3   6X,'XEDGE(N2)  =',E13.6,5X,'TEMP(WALL) =',E13.6,5X,'TLSPCL =',
     4   E13.6,9X,'MXSPEC =',I6,/,
     5   6X,'XEDGE(O)   =',E13.6,5X,'TEMP(EDGE) =',E13.6,5X,'TLMOMT =',
     6   E13.6,9X,'MNMOMT =',I6,/,
     7   6X,'XEDGE(N)   =',E13.6,5X,'VELOC EDGE =',E13.6,5X,'TLELEM =',
     8   E13.6,9X,'MNELEM =',I6,/,
     9   6X,'XEDGE(CO2) =',E13.6,5X,'RADIUS     =',E13.6,5X,'TLCONC =',
     0   E13.6,9X,'MITN   =',I6,/,
     1   6X,'XEDGE(CO)  =',E13.6,5X,'BURN RATE  =',E13.6,5X,'TLENER =',
     2   E13.6,9X,'MENERG =',I6,/,96X,'MXTEMP =',I6,//,
     3   50X,'GRID SIZE =',F6.3,/,46X,'NO. OF POINTS =',I6)
      CALL INIT
      CALL ENGLUP
      CALL OUTPUT
      CONTINUE
      END
```

NO DIAGNOSTICS.

```
      SUBROUTINE INIT
C*****************************************************************
C**** ALL QUANTITIES HAVE UNITS CONSISTENT WITH THE  C.G.S SYSTEM
C**** DECLARATION STATEMENTS
C*****************************************************************
      LOGICAL CVENGL,CVMOML,CVSPCL,CVMOMT,CVELEM,CVEQUI,CVCONW,CVENER
      COMMON   SIG(6),EK(6),A(6,5),CP(6,101),HB(6),B(4,2),EQ(4,101),
     1 WT(6),FP(101,2),ETA(101),T(101,2),X(6,101,2),E(6,3),DE(3,101),
     2 WE(3,101,2),DS(6,101),WTM(101),RHOM(101),W(6,102,2),CPM(101),
     3 SIGP(6,6),EKP(6,6),WTP(6,6),VIS(6,101),THC(6,101),DB(6,6,101),
     4 PHI(6,6),VISM(101),THCM(101),DEN(6),SDEN(6),FO(6,6),FFO(6,6),
     5 FNO(5,5),FNT(5,5),JC(6),VV(2),DM(6,6,101),H(6,101),C(101),
     6 PR(101),F(101,2),ERRVEL(101),FPPW(2),ERRFPP(2),ERRELE(3,101),
     7 ER(6,101),XEDGE(6),GEN(6,101),WP(6,101),WPP(6,101),ERRT(101),
     8 P,NETA,DELTA,RU,BURNM,FBURN,RB,UE,FWBAR,IPROP,IENRG,IMOMT,
     9 ISPEC,NMOMT,NELEM,ITN(101),NENERG,MXTEMP,MXMOMT,MXSPEC,MNMOMT,
     0 MNELEM,MITN,MENERG,TLMOML,TLSPCL,TLMOMT,TLELEM,TLCONC,TLENER,
     1 CVENGL,CVMOML,CVSPCL,CVMOMT,CVELEM,CVEQUI,CVCONW,CVENER,FPP(101),
     2 IPC,FW1,FW2,FW3,CD(101),RR(101),XP(6,101),WEP(3,101),FJS(6,101),
     3 FJE(3,101),FHE(3,101),IKOUNT,HMIX(101),FNS(6,101),FNE(3,101)
      DIMENSION RT(101)
C*****************************************************************
C**** SET UP DATA FOR SYSTEM UNDER CONSIDERATION
C*****************************************************************
      WT(1)=31.9988
      WT(2)=28.0134
      WT(3)=15.9994
      WT(4)=14.0067
      WT(5)=44.0099
      WT(6)=28.0105
      SIG(1)=3.433
      SIG(2)=3.681
      SIG(3)=7.990
      SIG(4)=7.940
      SIG(5)=3.996
      SIG(6)=3.590
      EK(1)=113.0
      EK(2)=91.5
      EK(3)=113.0
      EK(4)=91.5
      EK(5)=190.0
      EK(6)=110.0
      RU=82.0560
      A(1,1)=6.732/WT(1)
      A(1,2)=0.1515E-2/WT(1)
      A(1,3)=-0.01791E-5/WT(1)
      A(1,4)=0.0
      A(1,5)=0.0
      A(2,1)=6.529/WT(2)
      A(2,2)=0.1488E-2/WT(2)
      A(2,3)=-0.02271E-5/WT(2)
      A(2,4)=0.0
      A(2,5)=0.0
      A(3,1)=5.691554/WT(3)
      A(3,2)=-1.556717E-3/WT(3)
      A(3,3)=1.039789E-6/WT(3)
      A(3,4)=-2.154961E-10/WT(3)
```

```
      A(3,5)=0.0
      A(4,1)=4.954516/WT(4)
      A(4,2)=5.701184E-5/WT(4)
      A(4,3)=-5.351194E-8/WT(4)
      A(4,4)=1.373779E-11/WT(4)
      A(4,5)=0.0
      A(5,1)=[illegible]/WT(5)
      A(5,2)=-4.474E-5/WT(5)
      A(5,3)=0.0
      A(5,4)=0.0
      A(5,5)=-1.5[illegible]/WT(5)
      A(6,1)=6.[illegible]/WT(6)
      A(6,2)=0.1566E-2/WT(6)
      A(6,3)=-0.[illegible]87E-5/WT(6)
      A(6,4)=0.0
      A(6,5)=0.0
      HB(1)=-2.075E3/WT(1)
      HB(2)=-2.072E3/WT(2)
      HB(3)=5.7991E4/WT(3)
      HB(4)=1.11519E5/WT(4)
      HB(5)=-9.[illegible]2[illegible]4/WT(5)
      HB(6)=-2.84985E4/WT(6)
      B(1,1)=10.330380
      B(1,2)=-0.3394896E5
      B(2,1)=[illegible].097839
      B(2,2)=-0.3002069E5
      B(3,1)=7.419445
      B(3,2)=-0.5687790E5
      B(4,1)=10.558601
      B(4,2)=1.3395959E4
C*****************************************************************
C**** CALCULATE E(I,J)=MASS OF ELEMENT J/UNIT MASS OF SPECIES I
C**** ELEMENTS:1=O 2=N 3=C  SPECIES:1=O2 2=N2 3=O 4=N 5=CO2 6=CO
C*****************************************************************
      E(1,1)=1.0
      E(1,2)=0.0
      E(1,3)=0.0
      E(2,1)=0.0
      E(2,2)=1.0
      E(2,3)=0.0
      E(3,1)=1.0
      E(3,2)=0.0
      E(3,3)=0.0
      E(4,1)=0.0
      E(4,2)=1.0
      E(4,3)=0.0
      E(5,1)=WT(1)/WT(5)
      E(5,2)=0.0
      E(5,3)=1.0-E(5,1)
      E(6,1)=WT(3)/WT(6)
      E(6,2)=0.0
      E(6,3)=1.0-E(6,1)
C**** CALCULATE ETA
      DO 1303 I=1,NETA
         ETA(I)=(I-1)*DELTA
 1303 CONTINUE
C*****************************************************************
```

```
C**** IF IKOUNT=1 READ INPUT WE, FP AND T PROFILES
C*************************************************************************
      IF (IKOUNT.EQ.1) GO TO 9000
C*************************************************************************
C**** FEED IN FALKNER-SKAN VELOCITY PROFILE
C*************************************************************************
      FP(1,1)  =0.0000
      FP(2,1)  =0.1183
      FP(3,1)  =0.2266
      FP(4,1)  =0.3252
      FP(5,1)  =0.4145
      FP(6,1)  =0.4946
      FP(7,1)  =0.5663
      FP(8,1)  =0.6299
      FP(9,1)  =0.6859
      FP(10,1) =0.7351
      FP(11,1) =0.7779
      FP(12,1) =0.8149
      FP(13,1) =0.8467
      FP(14,1) =0.8738
      FP(15,1) =0.8968
      FP(16,1) =0.9162
      FP(17,1) =0.9323
      FP(18,1) =0.9458
      FP(19,1) =0.9568
      FP(20,1) =0.9659
      FP(21,1) =0.9732
      FP(22,1) =0.9791
      FP(23,1) =0.9839
      FP(24,1) =0.9876
      FP(25,1) =0.9905
      FP(26,1) =0.9929
      FP(27,1) =0.9946
      FP(28,1) =0.9960
      FP(29,1) =0.9970
      FP(30,1) =0.9978
      FP(31,1) =0.9984
      FP(32,1) =0.9989
      FP(33,1) =0.9992
      FP(34,1) =0.9994
      FP(35,1) =0.999608
      FP(36,1) =0.999729
      FP(37,1) =0.999816
      FP(38,1) =0.999877
      FP(39,1) =0.999919
      FP(40,1) =0.999949
      FP(41,1) =0.999970
      FP(42,1) =0.999985
      FP(43,1) =0.999993
      DO 1304 I=44,NETA
         FP(I,1)= 1.0
 1304 CONTINUE
 1302 FPPW(1)=1.232588
C*************************************************************************
C**** GENERATE TEMPERATURE PROFILE FOR THE FIRST ITERATION
C*************************************************************************
      RT(1) =1.000
```

```
      RT(2) =1.099308
      RT(3) =1.199042
      RT(4) =1.298583
      RT(5) =1.394675
      RT(6) =1.448383
      RT(7) =1.362733
      RT(8) =1.126475
      RT(9) =0.864733
      RT(10)=0.655033
      RT(11)=0.491611
      RT(12)=0.366460
      RT(13)=0.271748
      RT(14)=0.200551
      RT(15)=0.147295
      RT(16)=0.107626
      RT(17)=0.078033
      RT(18)=0.055786
      RT(19)=0.039282
      RT(20)=0.027449
      RT(21)=0.018962
      RT(22)=0.012898
      RT(23)=0.008602
      RT(24)=0.005594
      RT(25)=0.003524
      RT(26)=0.002167
      RT(27)=0.001205
      RT(28)=0.000617
      RT(29)=0.000242
      RT(30)=0.000018
      RT(31)=0.0
      DO 1305 L=32,NETA
 1305 RT(L)=0.0
      DO 1306 L=1,NETA
 1306 T(L,1)=RT(L)*(T(1,1)-T(NETA,1)) + T(NETA,1)
C*****************************************************************
C**** CALCULATE ELEMENTAL MASS FRACTIONS AT THE EDGE
C*****************************************************************
      WTM(NETA)=WT(1)*XEDGE(1)+WT(2)*XEDGE(2)+WT(3)*XEDGE(3)+
     1          WT(4)*XEDGE(4)+WT(5)*XEDGE(5)+WT(6)*XEDGE(6)
      DO 1351 I=1,6
         W(I,NETA,1)=XEDGE(I)*WT(I)/WTM(NETA)
 1351 CONTINUE
      DO 1353 J=1,3
         WE(J,NETA,1)=0.
         DO 1352 I=1,6
            VAR=0.
            VAR=E(I,J)*W(I,NETA,1)
            WE(J,NETA,1)=WE(J,NETA,1)+VAR
 1352    CONTINUE
 1353 CONTINUE
C*****************************************************************
C**** ESTIMATE ELEMENTAL MASS FRACTIONS AT THE WALL
C*****************************************************************
      WECMAX   =(WE(2,NETA,1)+WE(3,NETA,1)-1.)/
     1          (WE(2,NETA,1)+((WE(3,NETA,1)-1.)/E(6,3)))
      PRCT=1.0
 1700 WE(3,1,1)=PRCT*WECMAX
```

```
      WE(1,1,1)=WE(1,NETA,1)*(WE(3,1,1)-1.0)/(WE(3,NETA,1)-1.0)
      WE(2,1,1)=WE(2,NETA,1)*(WE(3,1,1)-1.0)/(WE(3,NETA,1)-1.0)
C*****************************************************************
C**** GENERATE ELEMENTAL MASS FRACTION PROFILES
C*****************************************************************
      DO 1354 L=1,NETA
         VAR=FP(L,1)
         DO 1355 J=1,3
            WE(J,L,1)=WE(J,1,1) + VAR*(WE(J,NETA,1)-WE(J,1,1))
 1355    CONTINUE
 1354 CONTINUE
C*****************************************************************
C**** IF IKOUNT=1 READ INPUT WE, FP AND T PROFILES
C*****************************************************************
      IF (IKOUNT.EQ.0) GO TO 9500
 9000 DO 1500 L=1,NETA
 1500 READ 1501,(WE(J,L,1),J=1,3),FP(L,1),T(L,1),F(L,1)
 1501 FORMAT(6(E13.6))
      WTM(NETA)= WT(1)*XEDGE(1) + WT(2)*XEDGE(2) + WT(3)*XEDGE(3) +
     1           WT(4)*XEDGE(4) + WT(5)*XEDGE(5) + WT(6)*XEDGE(6)
      FBURN=F(1,1)
      FPPW(1)=(FP(2,1)-FP(1,1))/DELTA
C*****************************************************************
C**** CALCULATE EQUILIBRIUM CONSTANTS
C*****************************************************************
 9500 DO 1358 L=1,NETA
         DO 1359 K=1,4
            EQ(K,L)=EXP(B(K,1)+B(K,2)/T(L,1))
 1359    CONTINUE
 1358 CONTINUE
C*****************************************************************
C**** CALCULATE SPECIES MOLE FRACTIONS IN THE FLOWFIELD AND AT THE WALL
C*****************************************************************
      DO 1356 I=1,6
         X(I,NETA,1)=XEDGE(I)
 1356 CONTINUE
      DO 1357 L=1,NETA
         WTM(L)=WTM(NETA)
         ITN(L)=0
 1357 CONTINUE
      CALL EQUIL
      IF (.NOT.CVEQUI) GO TO 1399
      IF (IKOUNT.EQ.1) GO TO 1360
      WE(1,1,1)=WE(1,NETA,1)
      WE(2,1,1)=WE(2,NETA,1)
 1360 IKOUNT=3
      CALL CONWAL
      IF (.NOT.CVCONW) GO TO 1399
C*****************************************************************
C**** CALL 'PROP' TO CALCULATE THERMODYNAMIC AND TRANSPORT PROPERTIES
C**** ACROSS THE FLOWFIELD. THIS IS THE FIRST APPROXIMATION.
C*****************************************************************
      IPROP=0
      CALL PROP
C**** CALCULATE BURNING RATE FROM ASSUMED MASS LOSS RATE
 1702 BURNM1= -FJE(1,1)/WE(1,1,1)
      BURNM2= -FJE(2,1)/WE(2,1,1)
```

```
      BURNM3= -FJE(3,1)/(WE(3,1,1)-1.0)
      BURNM=(BURNM1+BURNM2+BURNM3)/3.0
      FBURN=-BURNM3*(SQRT(RB/(2.*RHOM(NETA)*VISM(NETA)*UE)))
 1399 CONTINUE
      RETURN
      END
```

NO DIAGNOSTICS.

```
      SUBROUTINE PROP
C*****************************************************************
C**** ALL QUANTITIES HAVE UNITS CONSISTENT WITH THE  C.G.S SYSTEM
C**** DECLARATION STATEMENTS
C*****************************************************************
      LOGICAL CVENGL,CVMOML,CVSPCL,CVMOMT,CVELEM,CVEQUI,CVCONW,CVENER
      COMMON   SIG(6),EK(6),A(6,5),CP(6,101),HB(6),B(4,2),EQ(4,101),
     1 WT(6),FP(101,2),ETA(101),T(101,2),X(6,101,2),E(6,3),DE(3,101),
     2 WE(3,101,2),DS(6,101),WTM(101),RHOM(101),W(6,102,2),CPM(101),
     3 SIGP(6,6),EKP(6,6),WTP(6,6),VIS(6,101),THC(6,101),DB(6,6,101),
     4 PHI(6,6),VISM(101),THCM(101),DEN(6),SDEN(6),FO(6,6),FFO(6,6),
     5 FNO(5,5),FNT(5,5),JC(6),VV(2),DM(6,6,101),H(6,101),C(101),
     6 PR(101),F(101,2),ERRVEL(101),FPPW(2),ERRFPP(2),ERRELE(3,101),
     7 ER(6,101),XEDGE(6),GEN(6,101),WP(6,101),WPP(6,101),ERRT(101),
     8 P,NETA,DELTA,RU,BURNM,FBURN,RB,UE,FWBAR,IPROP,IENRG,IMOMT,
     9 ISPEC,NMOMT,NELEM,ITN(101),NENERG,MXTEMP,MXMOMT,MXSPEC,MNMOMT,
     0 MNELEM,MITN,MENERG,TLMOML,TLSPCL,TLMOMT,TLELEM,TLCONC,TLENER,
     1 CVENGL,CVMOML,CVSPCL,CVMOMT,CVELEM,CVEQUI,CVCONW,CVENER,FPP(101),
     2 IPC,FW1,FW2,FW3,CO(101),RR(101),XP(6,101),WEP(3,101),FJS(6,101),
     3 FJE(3,101),FHE(3,101),IKOUNT,HMIX(101),FNS(6,101),FNE(3,101)
C*****************************************************************
C**** SWEEP FLOWFIELD AND EVALUATE THERMODYNAMIC AND TRANSPORT
C**** PROPERTIES OF THE MULTICOMPONENT MIXTURE AT EACH LOCATION
C*****************************************************************
      IPROP=IPROP+1
      K=1
      DO 5980  L=1,NETA
C*****************************************************************
C**** CALCULATE MIXTURE MOLECULAR WEIGHT, DENSITY (GR/CC) AND MASS
C**** FRACTIONS
C*****************************************************************
      WTM(L)=0.
      DO 5301 I1=1,6
         WTM(L)=WTM(L)+X(I1,L,K)*WT(I1)
 5301 CONTINUE
      RHOM(L)=P*WTM(L)/(RU*T(L,K))
      DO 5303 I1=1,6
         W(I1,L,K)=X(I1,L,K)*WT(I1)/WTM(L)
 5303 CONTINUE
C*****************************************************************
C**** CALCULATION OF SPECIES AND MIXTURE HEAT CAPACITIES (CAL/GR.K)
C*****************************************************************
      CPM(L)=0.
      DO 5305 I1=1,6
         CP(I1,L)=0.
         CP(I1,L)=A(I1,1)+A(I1,2)*T(L,K)+A(I1,3)*T(L,K)**2+A(I1,4)*T(L,K
     1   )**3+A(I1,5)/SQRT(T(L,K))
         CPM(L)=CPM(L)+W(I1,L,K)*CP(I1,L)
 5305 CONTINUE
C*****************************************************************
C**** CALCULATE MOLECULAR PARAMETERS FOR PAIRS OF SPECIES
C*****************************************************************
      DO 5309 I1=1,6
         DO 5311 I2=1,6
            SIGP(I1,I2)=0.5*(SIG(I1)+SIG(I2))
            EKP(I1,I2)=SQRT(EK(I1)*EK(I2))
            WTP(I1,I2)=(WT(I1)+WT(I2))/(WT(I1)*WT(I2))
 5311    CONTINUE
 5309 CONTINUE
```

```
C*****************************************************************
C**** CALCULATE SINGLE SPECIES COLLISION INTEGRAL, VISCOSITY (GR/CM.SEC)
C**** AND THERMAL CONDUCTIVITY (CAL/CM.SEC.K)
C*****************************************************************
      DO 5313 I1=1,6
         VIS(I1,L)=0.
         THC(I1,L)=0.
         TR=T(L,K)/EK(I1)
         CI1=1.43472/(1.+0.323*ALOG(TR))
         VIS(I1,L)=2.6693E-5*SQRT(T(L,K)*WT(I1))/((SIG(I1)**2)*CI1)
         THC(I1,L)=(CP(I1,L)+(2.484/WT(I1)))*VIS(I1,L)
 5313 CONTINUE
C*****************************************************************
C**** CALCULATE BINARY PAIR COLLISION INTEGRAL AND BINARY DIFFUSIVITIES
C**** (CM.CM/SEC)
C*****************************************************************
      DO 5315 I1=1,6
         DO 5317 I2=1,6
            TR=T(L,K)/EKP(I1,I2)
            CI2=1.32468/(1.+0.3478*ALOG(TR))
            TEMPOR=1.8583E-3*(SQRT((T(L,K)**3)*WTP(I1,I2)))/(P*CI2*SIG
     1      P(I1,I2)**2)
            DB(I1,I2,L)=TEMPOP
 5317    CONTINUE
 5315 CONTINUE
      DO 5316 I1=1,6
      DO 5316 I2=1,6
 5316 DB(I1,I2,L)=DB(1,6,L)
C*****************************************************************
C**** CALCULATE VISCOSITY AND THERMAL CONDUCTIVITY MIXTURE RULE
C**** PARAMETER (PHI)
C*****************************************************************
      DO 5319 I1=1,6
         DO 5321 I2=1,6
            TEM1=SQRT(WT(I1)/WT(I2))
            TEM2=SQRT(VIS(I1,L)/VIS(I2,L))*SQRT(TEM1)
            TEM3=(1.+TEM2)**2
            TEM4=SQRT(1.+(WT(I1)/WT(I2)))
            PHI(I1,I2)=(1.0/SQRT(8.))*TEM3/TEM4
 5321    CONTINUE
 5319 CONTINUE
C*****************************************************************
C**** CALCULATE MIXTURE VISCOSITY, VISM(GR/CM,SEC) AND THERMAL CONDUCTI-
C**** VITY, THCM (CAL/CM,SEC,K)
C*****************************************************************
      VISM(L)=0.
      THCM(L)=0.
      DO 5323 I1=1,6
         DEN(I1)=0.0
         SDEN(I1)=0.0
 5323 CONTINUE
      DO 5325 I1=1,6
         DO 5327 I2=1,6
            DEN(I1)=X(I2,L,K)*PHI(I1,I2)
            SDEN(I1)=SDEN(I1)+DEN(I1)
 5327    CONTINUE
 5325 CONTINUE
      DO 5329 I1=1,6
         VISM(L)=VISM(L)+(X(I1,L,K)*VIS(I1,L)/SDEN(I1))
```

```
      THCM(L)=THCM(L)+(X(I1,L,K)*THC(I1,L)/SDEN(I1))
 5329 CONTINUE
C*****************************************************************
C**** CALCULATE FO(I,J) IN THE MULTICOMPONENT DIFFUSIVITY EQUATIONS
C*****************************************************************
      DO 5331 I1=1,6
         DO 5333 I2=1,6
            FO(I1,I2)=0.0
 5333    CONTINUE
 5331 CONTINUE
      DO 5335 I1=1,6
         TEMP1=0.0
         DO 5337 I2=1,6
            IF (I1-I2)5332,5334,5332
 5332       TEMP1=TEMP1+(X(I2,L,K)/DB(I1,I2,L))
 5334       CONTINUE
 5337    CONTINUE
         DO 5339 I3=1,6
            IF (I1-I3)5336,5338,5336
 5338       FO(I1,I3)=0.0
            FFO(I1,I3)=0.0
            GO TO 5339
 5336       FO(I1,I3)=((X(I1,L,K)/DB(I1,I3,L))+(TEMP1*WT(I3)/WT(I1)))
            FFO(I1,I3)=FO(I1,I3)
 5339    CONTINUE
 5335 CONTINUE
      VV(1)=2.0
      CALL GJR(FFO,6,6,6,6,$5990,JC,VV)
      DETD=VV(1)*EXP(VV(2))
      GO TO 5341
 5990 PRINT 5201,L,JC(1),IPROP
 5201 FORMAT(5X,'TROUBLE WITH GJR IN DM CALCULATION AT LOCATION',I4,'ERR
     1OR CODE JC(1)=',I4,'IPROP=',I4)
 5341 CONTINUE
C*****************************************************************
C**** CONVERT MATRIX FO INTO FNO AND FNT BY ELIMINATION OF APPROPRIATE
C**** ROWS AND/OR COLUMNS
C**** CALCULATE DETERMINANTS USING GJR SUBROUTINE
C**** CALCULATE MULTICOMPONENT DIFFUSIVITIES, DM(I,J) (CM,CM/SEC)
C*****************************************************************
      DO 5453 I1=1,6
         DO 5452 I2=1,6
            DETN1=0.0
            DETN2=0.0
            IF (I1-I2)5351,5451,5351
 5351       DO 5450 I3=1,6
               DO 5449 I4=1,6
                  IF (I3-I1)5352,5390,5372
 5352             II1=I3
                  IF (I4-I1)5354,5390,5356
 5354             JJ1=I4
                  GO TO 5380
 5356             JJ1=I4-1
                  GO TO 5380
 5372             II1=I3-1
                  IF (I4-I1)5374,5390,5376
 5374             JJ1=I4
                  GO TO 5380
 5376             JJ1=I4-1
 5380             FNO(II1,JJ1)=FO(I3,I4)
```

```
 5390              IF (I3-I2)5402,5449,5422
 5402              II1=I3
                   IF (I4-I1)5404,5449,5406
 5404              JJ1=I4
                   GO TO 5430
 5406              JJ1=I4-1
                   GO TO 5430
 5422              II1=I3-1
                   IF (I4-I1)5424,5449,5426
 5424              JJ1=I4
                   GO TO 5430
 5426              JJ1=I4-1
 5430              FNT(II1,JJ1)=FO(I3,I4)
 5449           CONTINUE
 5450        CONTINUE
C*************************************************************************
C**** NOW WE NEED TO CALCULATE THE DETERMINANTS OF THE MATRICES FNO
C**** AND FNT USING THE GJR SUBROUTINE FROM THE UNIVAC 1108 MATHPACK
C*************************************************************************
            VV(1)=2.0
            CALL GJR(FNO,5,5,5,5,$5992,JC,VV)
            DETN1=VV(1)*EXP(VV(2))
            GO TO 5400
 5992       PRINT 5201,L,JC(1),IPROP
 5400       VV(1)=2.0
            CALL GJR(FNT,5,5,5,5,$5996,JC,VV)
            DETN2=VV(1)*EXP(VV(2))
            GO TO 5403
 5996       PRINT 5201,L,JC(1),IPROP
 5403       RATIO=((DETN1+((-1.0)**(I1+I2+1))*DETN2)/DETD)
            DM(I1,I2,L)=-(WTM(L)/WT(I2))*RATIO
            GO TO 5452
 5451       DM(I1,I2,L)=0.0
 5452    CONTINUE
 5453 CONTINUE
C*************************************************************************
C**** CALCULATE SPECIES ENTHALPIES (CAL/GR), AND MIXTURE ENTHALPY
C**** H(I)=HB(I)+A1*T+1/2*A2*T**2+1/3*A3*T**3+1/4*A4*T**4+2*A5*SQRT(T)
C*************************************************************************
      DO 5477 I1=1,6
         H(I1,L)=0.0
         QUA=0.
         QUA=A(I1,1)*T(L,K)+(1./2.)*A(I1,2)*(T(L,K)**2)+(1./3.)*A(I1,3)*
     1   (T(L,K)**3)+(1./4.)*A(I1,4)*(T(L,K)**4)+(2.)*A(I1,5)*SQRT(T(L,K
     2   ))
         H(I1,L)=HB(I1)+QUA
 5477 CONTINUE
      HMIX(L)=H(1,L)*W(1,L,1)+H(2,L)*W(2,L,1)+H(3,L)*W(3,L,1)+
     1        H(4,L)*W(4,L,1)+H(5,L)*W(5,L,1)+H(6,L)*W(6,L,1)
C*************************************************************************
C**** CALCULATE EQUILIBRIUM CONSTANTS
C**** EQ(I,L)=EXP(B(I,1)+(B(I,2)/T(L,K))) ,  T IN DEGREES KELVIN
C*************************************************************************
      DO 5479 I1=1,4
         EQ(I1,L)=EXP(B(I1,1)+(B(I1,2)/T(L,K)))
 5479 CONTINUE
C*************************************************************************
C**** CALCULATE ELEMENTAL MASS FRACTIONS, WE.
C*************************************************************************
```

```
      DO 5481 I1=1,3
         WE(I1,L,K)=E(1,I1)*W(1,L,K)+E(2,I1)*W(2,L,K)+E(3,I1)*W(3,L,K)
     1   +E(4,I1)*W(4,L,K)+E(5,I1)*W(5,L,K)+E(6,I1)*W(6,L,K)
 5481 CONTINUE
C*************************************************************************
C**** CALCULATE MIXTURE PRANDTL NUMBER
C*************************************************************************
      PR(L)=CPM(L)*VISM(L) /THCM(L)
 5980 CONTINUE
C*************************************************************************
C**** CALCULATE RHOM*VISM RATIO
C*************************************************************************
      DO 5483 L=1,NETA
      C(L)=(RHOM(L)*VISM(L))/(RHOM(NETA)*VISM(NETA))
 5483 CONTINUE
C*************************************************************************
C**** CALCULATE SPECIES AND ELEMENTAL FLUXES IN THE TRANSFORMED PLANE
C**** CALCULATE SPECIES MOLE FRACTION GRADIENTS
C*************************************************************************
      DO 7302 L=1,NETA
      DO 7304 I=1,6
      IF (L.EQ.1) GO TO 7301
      IF (L.EQ.NETA) GO TO 7303
      XP(I,L)=(X(I,L+1,1)-X(I,L-1,1))/(2.*DELTA)
      GO TO 7304
 7301 XP(I,1)=(X(I,2,1)-X(I,1,1))/DELTA
      GO TO 7304
 7303 XP(I,NETA)=(X(I,NETA,1)-X(I,NETA-1,1))/DELTA
 7304 CONTINUE
 7302 CONTINUE
C*************************************************************************
C**** CALCULATE ELEMENTAL MASS FRACTION GRADIENTS
C*************************************************************************
      DO 7306 L=1,NETA
      DO 7308 J=1,3
      IF (L.EQ.1) GO TO 7307
      IF (L.EQ.NETA) GO TO 7309
      WEP(J,L)=(WE(J,L+1,1)-WE(J,L-1,1))/(2.*DELTA)
      GO TO 7308
 7307 WEP(J,1)=(WE(J,2,1)-WE(J,1,1))/DELTA
      GO TO 7308
 7309 WEP(J,NETA)=(WE(J,NETA,1)-WE(J,NETA-1,1))/DELTA
 7308 CONTINUE
 7306 CONTINUE
C*************************************************************************
C**** CALCULATE FJS(I,L) AND ADD UP ALL XP(I,L) AND ALL FJS(I,L)
C*************************************************************************
      DO 7406 L=1,NETA
      PRE=((RHOM(L)**2.)/(WTM(L)**2.))*SQRT((2.*UE)/(RHOM(NETA)*
     1    VISM(NETA)*RB))
      DO 7408 I=1,6
      FJS(I,L)=(WT(1)*DM(I,1,L)*XP(1,L) + WT(2)*DM(I,2,L)*XP(2,L) +
     1          WT(3)*DM(I,3,L)*XP(3,L) + WT(4)*DM(I,4,L)*XP(4,L) +
     2          WT(5)*DM(I,5,L)*XP(5,L) + WT(6)*DM(I,6,L)*XP(6,L) )
     3          *PRE*WT(I)
 7408 CONTINUE
      DS(1,L)=XP(1,L)+XP(2,L)+XP(3,L)+XP(4,L)+XP(5,L)+XP(6,L)
      DS(2,L)=FJS(1,L)+FJS(2,L)+FJS(3,L)+FJS(4,L)+FJS(5,L)+FJS(6,L)
 7406 CONTINUE
```

```
C*****************************************************************
C**** CALCULATE FJE(J,L) AND ADD UP ALL WEP(J,L) AND ALL FJE(J,L)
C*****************************************************************
      DO 7416 L=1,NETA
      DO 7418 J=1,3
      FJE(J,L)=E(1,J)*FJS(1,L)   + E(2,J)*FJS(2,L)   + E(3,J)*FJS(3,L) +
     1         E(4,J)*FJS(4,L)   + E(5,J)*FJS(5,L)   + E(6,J)*FJS(6,L)
 7418 CONTINUE
      DS(3,L)=WEP(1,L)+WEP(2,L)+WEP(3,L)
      DS(4,L)=FJE(1,L)+FJE(2,L)+FJE(3,L)
 7416 CONTINUE
C*****************************************************************
C**** CALCULATE DE(J,L)
C*****************************************************************
      DO 7422 L=1,NETA
      PRE=RHOM(L)*SQRT((2.*UE)/(RHOM(NETA)*VISM(NETA)*RB))
      DO 7424 J=1,3
      DE(J,L)=0.0
      IF (ABS(WEP(J,L)).LT.1.0E-08) GO TO 7424
 7434 DE(J,L)=FJE(J,L)/(-RHOM(L)*WEP(J,L)*PRE)
 7424 CONTINUE
 7422 CONTINUE
C*****************************************************************
C**** SUM ALL X(I,L,1) AND WE(J,L,1) AT EACH LOCATION L.
C*****************************************************************
      DO 7426 L=1,NETA
      DS(5,L)=X(1,L,1)+X(2,L,1)+X(3,L,1)+X(4,L,1)+X(5,L,1)+X(6,L,1)
      DS(6,L)=WE(1,L,1)+WE(2,L,1)+WE(3,L,1)
 7426 CONTINUE
C*****************************************************************
C**** CALCULATE SPECIES AND ELEMENTAL FLUXES WRT STATIONARY COORDINATES
C*****************************************************************
      IF (IPROP.EQ.1) GO TO 7505
      PRE=SQRT(2.*RHOM(NETA)*VISM(NETA)*UE/RB)
      DO 7501 L=1,NETA
      DO 7501 I=1,6
 7501 FNS(I,L)=FJS(I,L)-PRE*W(I,L,1)*F(L,1)
      DO 7503 L=1,NETA
      DO 7503 J=1,3
 7503 FNE(J,L)= E(1,J)*FNS(1,L) + E(2,J)*FNS(2,L) + E(3,J)*FNS(3,L)
     1        + E(4,J)*FNS(4,L) + E(5,J)*FNS(5,L) + E(6,J)*FNS(6,L)
 7505 CONTINUE
C*****************************************************************
C**** PRINT OUTPUT OF PROP S/P
C*****************************************************************
      PRINT 5002
 5002 FORMAT(1H1,46X,'TRANSPORT AND THERMODYNAMIC PROPERTIES')
      PRINT 5003,IPROP,P
 5003 FORMAT(///,50X,'IPROP=',I6,6X,'P=',E11.4)
      PRINT 5004
 5004 FORMAT(//,3X,'L',4X,'ETA(L)',6X,'X(O2,L)',12X,'X(N2,L)',13X,'X(O
     1,L)',13X,'X(N,L)',11X,'X(CO2,L)',12X,'X(CO,L)')
      DO 5005 L=1,NETA,IPC
 5005 PRINT 5006,L,ETA(L),(X(I,L,1),I=1,6)
 5006 FORMAT (2X,I3,2X,F6.2,4X,E13.6,5(6X,E13.6))
      PRINT 5007
 5007 FORMAT(//,3X,'L',4X,'ETA(L)',6X,'W(O2,L)',12X,'W(N2,L)',13X,'W(O
     1,L)',13X,'W(N,L)',11X,'W(CO2,L)',12X,'W(CO,L)')
      DO 5008 L=1,NETA,IPC
 5008 PRINT 5006,L,ETA(L),(W(I,L,1),I=1,6)
```

```
      PRINT 5009
 5009 FORMAT(//,3X,'L',4X,'ETA(L)',5X,'CP(O2,L)',11X,'CP(N2,L)',12X,'  C
     1P(O,L)',12X,'CP(N,L)',10X,'CP(CO2,L)',11X,'CP(CO,L)')
      DO 5010 L=1,NETA,IPC
 5010 PRINT 5006,L,ETA(L),(CP(I,L),I=1,6)
      PRINT 5011
 5011 FORMAT(//,3X,'L',4X,'ETA(L)',4X,'VIS(O2,L)',10X,'VIS(N2,L)',11X,
     1       'VIS(O,L)',11X,'VIS(N,L)',9X,'VIS(CO2,L)',10X,'VIS(CO,L)')
      DO 5012 L=1,NETA,IPC
 5012 PRINT 5006,L,ETA(L),(VIS(I,L),I=1,6)
      PRINT 5013
 5013 FORMAT(//,3X,'L',4X,'ETA(L)',4X,'THC(O2,L)',10X,'THC(N2,L)',11X,
     1       'THC(O,L)',11X,'THC(N,L)',9X,'THC(CO2,L)',10X,'THC(CO,L)')
      DO 5014 L=1,NETA,IPC
 5014 PRINT 5006,L,ETA(L),(THC(I,L),I=1,6)
      PRINT 5015
 5015 FORMAT(//,3X,'L',4X,'ETA(L)',6X,'H(O2,L)',12X,'H(N2,L)',13X,
     1       'H(O,L)',13X,'H(N,L)',11X,'H(CO2,L)',12X,'H(CO,L)')
      DO 5016 L=1,NETA,IPC
 5016 PRINT 5006,L,ETA(L),(H(I,L),I=1,6)
C*************************************************************************
      PRINT 5028
 5028 FORMAT(///,3X,'MIXTURE PROPERTIES')
C*************************************************************************
      PRINT 5024
 5024 FORMAT(//,3X,'L',4X,'ETA(L)',5X,'FJS(O2,L)',10X,'FJS(N2,L)',11X,
     1       'FJS(O,L)',11X,'FJS(N,L)',9X,'FJS(CO2,L)',10X,'FJS(CO,L)')
      DO 5025 L=1,NETA,IPC
 5025 PRINT 5006,L,ETA(L),(FJS(I,L),I=1,6)
      PRINT 5070
 5070 FORMAT(//,3X,'L',4X,'ETA(L)',5X,'FNS(O2,L)',10X,'FNS(N2,L)',11X,
     1       'FNS(O,L)',11X,'FNS(N,L)',9X,'FNS(CO2,L)',10X,'FNS(CO,L)')
      DO 5071 L=1,NETA,IPC
 5071 PRINT 5006,L,ETA(L),(FNS(I,L),I=1,6)
      PRINT 5026
 5026 FORMAT(//,3X,'L',4X,'ETA(L)',5X,'WE(O,L)',12X,'WE(N,L)',13X,
     1'WE(C,L)',12X,'DE(O,L)',11X,'DE(N,L)',12X,'DE(C,L)')
      DO 5027 L=1,NETA,IPC
 5027 PRINT 5006,L,ETA(L),(WE(J,L,1),J=1,3),(DE(J,L),J=1,3)
      PRINT 5050
 5050 FORMAT(//,3X,'L',4X,'ETA(L)',12X,'FJE(O,L)',15X,'FJE(N,L)',15X,'FJ
     1E(C,L)',15X,'HMIX(L)',15X,'HRAT(L)')
      DO 5051 L=1,NETA
      RAT=(HMIX(L)-HMIX(NETA))/(HMIX(1)-HMIX(NETA))
 5051 PRINT 5052,L,ETA(L),(FJE(J,L),J=1,3),HMIX(L),RAT
 5052 FORMAT(2X,I3,2X,F6.2,5(10X,E13.6))
      PRINT 5072
 5072 FORMAT(//,3X,'L',4X,'ETA(L)',12X,'FNE(O,L)',15X,'FNE(N,L)',15X,
     1       'FNE(C,L)')
      DO 5073 L=1,NETA,IPC
 5073 PRINT 5074,L,ETA(L),(FNE(J,L),J=1,3)
 5074 FORMAT(2X,I3,2X,F6.2,3(10X,E13.6))
      PRINT 5053
 5053 FORMAT(//,3X,'L',4X,'ETA(L)',5X,'SUMX(I,L)',11X,'SUMXP(I,L)',9X,'S
     1UMFJS(I,L)',8X,'SUMWE(J,L)',9X,'SUMWEP(J,L)',8X,'SUMFJE(J,L)')
      DO 5054 L=1,NETA
 5054 PRINT 5006,L,ETA(L),DS(5,L),DS(1,L),DS(2,L),DS(6,L),DS(3,L),DS(4,L
     1)
      PRINT 5029
```

```
5029 FORMAT(//,3X,'L',4X,'ETA(L)',7X,'T(L)',14X,'WTM(L)',12X,'RHOM(L)',
    1       13X,'VISM(L)',10X,'THCM(L)',14X,'CPM(L)')
     DO 5030 L=1,NETA,IPC
5030 PRINT 5006,L,ETA(L),T(L,1),WTM(L),RHOM(L),VISM(L),THCM(L),CPM(L)
     PRINT 5031
5031 FORMAT(//,3X,'L',4X,'ETA(L)',7X,'C(L)',15X,'PR(L)',12X,'EQ(CO,L)',
    1       12X,'EQ(O,L)',10X,'EQ(N,L)',15X,'EQ(S,L)')
     DO 5032 L=1,NETA,IPC
5032 PRINT 5006,L,ETA(L),C(L),PR(L),(EQ(I,L),I=1,4)
     CONTINUE
     RETURN
     END
```

NO DIAGNOSTICS.

```
      SUBROUTINE ENGLUP
C*************************************************************************
C**** ALL QUANTITIES HAVE UNITS CONSISTENT WITH THE  C.G.S SYSTEM
C**** DECLARATION STATEMENTS
C*************************************************************************
      LOGICAL CVENGL,CVMOML,CVSPCL,CVMOMT,CVELEM,CVEQUI,CVCONW,CVENER
      COMMON   SIG(6),EK(6),A(6,5),CP(6,101),HB(6),B(4,2),EQ(4,101),
     1 WT(6),FP(101,2),ETA(101),T(101,2),X(6,101,2),E(6,3),DE(3,101),
     2 WE(3,101,2),DS(6,101),WTM(101),RHOM(101),W(6,102,2),CPM(101),
     3 SIGP(6,6),EKP(6,6),WTP(6,6),VIS(6,101),THC(6,101),DB(6,6,101),
     4 PHI(6,6),VISM(101),THCM(101),DEN(6),SDEN(6),FO(6,6),FFO(6,6),
     5 FNO(5,5),FNT(5,5),JC(6),VV(2),DM(6,6,101),H(6,101),C(101),
     6 PR(101),F(101,2),ERRVEL(101),FPPW(2),ERRFPP(2),ERRELE(3,101),
     7 ER(6,101),XEDGE(6),GEN(6,101),WP(6,101),WPP(6,101),ERRT(101),
     8 P,NETA,DELTA,RU,BURNM,FBURN,RB,UE,FWBAR,IPROP,IENRG,IMOMT,
     9 ISPEC,NMOMT,NELEM,ITN(101),NENERG,MXTEMP,MXMOMT,MXSPEC,MNMOMT,
     0 MNELEM,MITN,MENERG,TLMOML,TLSPCL,TLMOMT,TLELEM,TLCONC,TLENER,
     1 CVENGL,CVMOML,CVSPCL,CVMOMT,CVELEM,CVEQUI,CVCONW,CVENER,FPP(101),
     2 IPC,FW1,FW2,FW3,CD(101),RR(101),XP(6,101),WEP(3,101),FJS(6,101),
     3 FJE(3,101),FHE(3,101),IKOUNT,HMIX(101),FNS(6,101),FNE(3,101)
      IENRG=0
  101 CVENGL=.FALSE.
      IENRG=IENRG+1
         IMOMT=0
         CALL MOMLUP
         IF (CVMOML) GO TO 103
         GO TO 1130
  103    CALL GENER
         NENERG=0
         CALL ENERGY
         IF (CVENER) GO TO 105
         GO TO 1130
  105    IF(NENERG.EQ.1) GO TO 109
         GO TO 113
  109    CVENGL=.TRUE.
  113    CONTINUE
C*************************************************************************
C**** PRINT OUT STATE OF ENERGY LOOP ITERATIONS
C*************************************************************************
      PRINT 130
  130 FORMAT(1H1,54X,'ENERGY LOOP ITERATIONS')
      PRINT 131,CVMOML,CVENER,CVENGL,CVENGL
  131 FORMAT(///,5X,'IF THE INTERMEDIATE MOMENTUM LOOP CONVERGED',3X,L6,
     1/,5X,'IF THE ENERGY EQUATION CONVERGED',3X,L6,' IN ITS FIRST ITERA
     2TION',3X,L6,/,9X,'THEN THE OUTERMOST ENERGY LOOP IS CONSIDERED CON
     3VERGENT',5X,L6,/,9X,'OTHERWISE, ENGLUP CALLS PROP TO UPDATE THE PH
     4YSICAL PROPERTIES AND ANOTHER PASS THRU',/,20X,'ENGLUP IS MADE')
      PRINT 132,IENRG,CVENGL
  132 FORMAT(///,5X,'THE CURRENT PASS (',I4,') THRU THE OUTERMOST ENERGY
     1 LOOP CONVERGED',5X,L6)
      IF ((.NOT.CVENGL).AND.(IENRG.LT.MXTEMP)) GO TO 107
      GO TO 111
  107 CALL PROP
      GO TO 101
  111 CONTINUE
 1130 CONTINUE
      RETURN
      END
```

NO DIAGNOSTICS.

```
      SUBROUTINE MOMLUP
C*****************************************************************
C**** ALL QUANTITIES HAVE UNITS CONSISTENT WITH THE  C.G.S SYSTEM
C**** DECLARATION STATEMENTS
C*****************************************************************
      LOGICAL CVENGL,CVMOML,CVSPCL,CVMOMT,CVELEM,CVEQUI,CVCONW,CVENER
      COMMON   SIG(6),EK(6),A(6,5),CP(6,101),HB(6),B(4,2),EQ(4,101),
     1 WT(6),FP(101,2),ETA(101),T(101,2),X(6,101,2),E(6,3),DE(3,101),
     2 WE(3,101,2),DS(6,101),WTM(101),RHOM(101),W(6,102,2),CPM(101),
     3 SIGP(6,6),EKP(6,6),WTP(6,6),VIS(6,101),THC(6,101),DB(6,6,101),
     4 PHI(6,6),VISM(101),THCM(101),GEN(6),SGEN(6),FO(6,6),FFO(6,6),
     5 FNO(5,5),FNT(5,5),JC(6),VV(2),DM(6,6,101),H(6,101),C(101),
     6 PR(101),F(101,2),ERRVEL(101),FPPW(2),ERRFPP(2),ERRELE(3,101),
     7 ER(6,101),XEDGE(6),GEN(6,101),WP(6,101),WPP(6,101),ERRT(101),
     8 P,NETA,DELTA,RU,BURNM,FBURN,RB,UE,FWBAR,IPROP,IENRG,IMOMT,
     9 ISPEC,NMOMT,NELEM,ITN(101),NENERG,MXTEMP,MXMOMT,MXSPEC,MNMOMT,
     0 MNELEM,MITN,MENERG,TLMOML,TLSPCL,TLMOMT,TLELEM,TLCONC,TLENER,
     1 CVENGL,CVMOML,CVSPCL,CVMOMT,CVELEM,CVEQUI,CVCONW,CVENER,FPP(101),
     2 IPC,FW1,FW2,FW3,CD(101),RR(101),XP(6,101),WEP(3,101),FJS(6,101),
     3 FJE(3,101),FHE(3,101),IKOUNT,HMIX(101),FNS(6,101),FNE(3,101)
      COMMON/BLK1/EMFO,EMFN,EMFC,ELEMRT(101),FLUXRT(101)
  900 CVMOML=.FALSE.
      IMOMT=IMOMT+1
      VR10=WE(1,1,1)
      VR20=WE(2,1,1)
      VR30=WE(3,1,1)
      VR40=FBURN
C*****************************************************************
C**** SOLVE MOMENTUM EQUATION
C*****************************************************************
      NMOMT=0
      CALL MOMT
      IF (CVMOMT) GO TO 905
      GO TO 9270
  905 ISPEC=0
C*****************************************************************
      CALL SPCLUP
C*****************************************************************
      IF (CVSPCL) GO TO 307
      GO TO 9270
  307 IKOUNT=1
      ELEMRT(IMOMT)=WE(1,1,1)/WE(2,1,1)
      FLUXRT(IMOMT)=FJE(1,1)/FJE(2,1)
C*****************************************************************
C**** UPDATE ELEMENTAL MASS FRACTION RATIOS TO OBTAIN THE NEW
C**** PSEUDO-BOUNDARY CONDITION AT THE WALL
C*****************************************************************
      ITN(1)=0
      CALL CONWAL
      IF (CVCONW) GO TO 9130
      GO TO 9270
C*****************************************************************
C**** ADJUST ELEMENTAL MASS FRACTION PROFILES TO ACCOUNT FOR THE
C**** UPDATE OF THE PSEUDO-BOUNDARY CONDITION AT THE WALL
C*****************************************************************
 9130 FACT=(WE(1,NETA,1)-EMFO)/(WE(1,NETA,1)-VR10)
      DO 9135 L=1,NETA
 9135 WE(1,L,1)=EMFO + FACT*(WE(1,L,1)-VR10)
```

```
      FACT=(WE(2,NETA,1)-EMFN)/(WE(2,NETA,1)-VR20)
      DO 9136 L=1,NETA
 9136 WE(2,L,1)=EMFN + FACT*(WE(2,L,1)-VR20)
      FACT=(WE(3,NETA,1)-EMFC)/(WE(3,NETA,1)-VR30)
      DO 9137 L=1,NETA
 9137 WE(3,L,1)=EMFC + FACT*(WE(3,L,1)-VR30)
      DO 9138 L=1,NETA
      SUM = WE(1,L,1) + WE(2,L,1) + WE(3,L,1)
      DO 9138 J=1,3
 9138 WE(J,L,1) = WE(J,L,1)/SUM
      DO 9132 L=1,NETA
C*************************************************************************
C**** RESOLVE THE CHEMICAL EQUILIBRIUM EQUATIONS IN THE FLOWFIELD
C*************************************************************************
 9132 ITN(L)=0
      CALL EQUIL
      IF (CVEQUI) GO TO 913
      GO TO 9270
C*************************************************************************
  913 CALL PROP
C*************************************************************************
      VR1N=WE(1,1,1)
      VR2N=WE(2,1,1)
      VR3N=WE(3,1,1)
C*************************************************************************
C**** CALCULATE NEW BURNING RATE AT THE WALL
C*************************************************************************
      PRE=SQRT(RB/(2.*RHOM(NETA)*VISM(NETA)*UE))
      FW1=PRE*FUE(1,1)/WE(1,1,1)
      FW2=PRE*FUE(2,1)/WE(2,1,1)
      FW3=PRE*FUE(3,1)/(WE(3,1,1)-1.0)
C*************************************************************************
C**** AVERAGE TO OBTAIN NEW WALL BURNING RATE
C*************************************************************************
      FWBAR=(FW1+FW2+FW3)/3.
      VR4N=FWBAR
      VR5N=FW1
      VR6N=FW2
      VR7N=FW3
C*************************************************************************
C**** DETERMINE IF CONVERGENCE OF THE MOMLUP HAS BEEN ACHIEVED
C*************************************************************************
      EVR1=ABS(VR1N/VR10 -1.)
      EVR2=ABS(VR2N/VR20 -1.)
      EVR3=ABS(VR3N/VR30 -1.)
      EVR4=ABS(VR4N/VR40 -1.)
      EVR5=ABS(VR5N/VR4N -1.)
      EVR6=ABS(VR6N/VR4N -1.)
      EVR7=ABS(VR7N/VR4N -1.)
      IF (EVR1.GE.TLSPCL) GO TO 951
      IF (EVR2.GE.TLSPCL) GO TO 951
      IF (EVR3.GE.TLSPCL) GO TO 951
      IF (EVR4.GE.TLMOML) GO TO 951
      IF (EVR5.GE.TLMOML) GO TO 951
      IF (EVR6.GE.TLMOML) GO TO 951
      IF (EVR7.GE.TLMOML) GO TO 951
      CVMOML=.TRUE.
      GO TO 999
  951 IF (IMOMT.LT.MXMOMT) GO TO 953
```

```
      GO TO 999
  953 WE(1,1,1)=VR1N
      WE(2,1,1)=VR2N
      WE(3,1,1)=VR3N
      FBURN=VR4N
  999 CONTINUE
C*********************************************************************
C**** PRINT OUT INTERMEDIATE MOMENTUM LOOP ITERATIONS
C*********************************************************************
      PRINT 9100
 9100 FORMAT(1H1,///,48X,'STATE OF MOMENTUM LOOP ITERATIONS')
      LPROP=IPROP-1
      PRINT 9102,IENRG,MXTEMP,IMOMT,MXMOMT,LPROP
 9102 FORMAT(///,5X,'THIS IS THE ',I4,' PASS THRU THE OUTERMOST ENERGY L
     1OOP.  MAXIMUM NUMBER OF PASSES IS ',I4,/,5X,'THIS IS THE ',I4,' PA
     2SS THRU THE INTERMEDIATE MOMENTUM LOOP.  MAXIMUM NUMBER OF PASSES
     3IS ',I4,/,5X,'THE PHYSICAL PROPERTIES USED ARE FROM THE ',I4,' PAS
     4S THRU THE PROP SUBROUTINE')
      PRINT 9104,CVMOMT,NMOMT,TLMOMT,F(1,1),CVELEM,NELEM,TLELEM,VR10,VR2
     10,VR30
 9104 FORMAT(/,10X,'THE MOMENTUM EQUATION CONVERGED',L6,' IN ',I4,' ITER
     1ATIONS TO A RELATIVE ERROR BETWEEN THE LAST TWO SUCCESSIVE ITERATI
     2ONS',/,15X,'OF LESS THAN',E13.6,'.  THE ASSUMED BURNING RATE AT TH
     3E WALL USED IN THE MOMENTUM EQUATION WAS',E13.6,/,10X,'THE ELEMENT
     4AL CONSERVATION EQUATIONS CONVERGED',L6,' IN ',I4,' ITERATIONS TO
     5A RELATIVE ERROR BETWEEN THE LAST TWO SUCCESIVE ITERA-',/,15X,'TIO
     6NS OF LESS THAN',E13.6,'. THE ASSUMED ELEMENTAL COMPOSITION AT THE
     7 WALL USED IN THE ELEMENTAL CONSERVATION',/,15X,'EQUATIONS WAS  WE
     8(O,WALL)=',E13.6,/,30X,'WE(N,WALL)=',E13.6,/,30X,'WE(C,WALL)=',E13
     9.6)
      PRINT 9106,CVEQUI,TLCONC,CVCONW,TLCONC
 9106 FORMAT(10X,'THE FLOWFIELD EQUILIBRIUM EQUATIONS CONVERGED',L6,' TO
     1 A RELATIVE ERROR BETWEEN THE LAST TWO SUCCESSIVE ITERA-',/,15X,'T
     2IONS OF LESS THAN',E13.6,/,10X,'THE CHEMICAL EQUILIBRIUM EQUATIONS
     3 AT THE WALL CONVERGED',L6,' TO A RELATIVE ERROR BETWEEN THE LAST
     4TWO SUCCESSIVE ITE-',/,15X,'RATIONS OF LESS THAN',E13.6,/,5X,'IF A
     5LL THE ABOVE CONVERGED USING THE GIVEN EIGENVALUES AS BOUNDARY CON
     6DITIONS, THEN THE PROP AND BURNRT SUBROUTINES WERE',/,5X,'CALLED T
     7O UPDATE THE EIGENVALUES USED AS BOUNDARY CONDITIONS. THESE FOLLOW
     8.')
      PRINT 9108,VR5N,EVR5,VR6N,EVR6,VR7N,EVR7,VR40,VR4N,EVR4,TLMOML,
     1VR10,VR1N,EVR1,TLSPCL,VR20,VR2N,EVR2,TLSPCL,VR30,VR3N,EVR3,TLSPCL
 9108 FORMAT(/,30X,'OLD',22X,'NEW',16X,'RELATIVE ERROR',14X,'TOLERANCE',
     1/,5X,'FWO',41X,E13.6,12X,E13.6,
     2/,5X,'FWN',41X,E13.6,12X,E13.6,
     3/,5X,'FWC',41X,E13.6,12X,E13.6,
     4/,5X,'F(WALL)   ',9X,E13.6,12X,E13.6,12X,E13.6,12X,E13.6,
     5/,5X,'WE(O,WALL)',9X,E13.6,12X,E13.6,12X,E13.6,12X,E13.6,
     6/,5X,'WE(N,WALL)',9X,E13.6,12X,E13.6,12X,E13.6,12X,E13.6,
     7/,5X,'WE(C,WALL)',9X,E13.6,12X,E13.6,12X,E13.6,12X,E13.6)
      PRINT 9110,IMOMT,CVMOML
 9110 FORMAT(///,5X,'THE CURRENT PASS(',I4,') THRU THE INTERMEDIATE MOME
     1NTUM LOOP CONVERGED ---',L6)
      IF ((.NOT.CVMOML).AND.(IMOMT.LT.MXMOMT)) GO TO 900
 9270 CONTINUE
      RETURN
      END
```

NO DIAGNOSTICS.

```
      SUBROUTINE MOMT
C*****************************************************************
C**** ALL QUANTITIES HAVE UNITS CONSISTENT WITH THE  C.G.S SYSTEM
C**** DECLARATION STATEMENTS
C*****************************************************************
      LOGICAL CVENGL,CVMOML,CVSPCL,CVMOMT,CVELEM,CVEQUI,CVCONW,CVENER
      COMMON   SIG(6),EK(6),A(6,5),CP(6,101),HB(6),B(4,2),EQ(4,101),
     1 WT(6),FP(101,2),ETA(101),T(101,2),X(6,101,2),E(6,3),DE(3,101),
     2 WE(3,101,2),DS(6,101),WTM(101),RHOM(101),W(6,102,2),CPM(101),
     3 SIGP(6,6),EKP(6,6),WTP(6,6),VIS(6,101),THC(6,101),DB(6,6,101),
     4 PHI(6,6),VISM(101),THCM(101),DEN(6),SDEN(6),FO(6,6),FFO(6,6),
     5 FNO(5,5),FNT(5,5),JC(6),VV(2),DM(6,6,101),H(6,101),C(101),
     6 PR(101),F(101,2),ERRVEL(101),FPPW(2),ERRFPP(2),ERRELE(3,101),
     7 ER(6,101),XEDGE(6),GEN(6,101),WP(6,101),WPP(6,101),ERRT(101),
     8 P,NETA,DELTA,RU,BURNM,FBURN,RB,UE,FWBAR,IPROP,IENRG,IMOMT,
     9 ISPEC,NMOMT,NELEM,ITN(101),NENERG,MXTEMP,MXMOMT,MXSPEC,MNMOMT,
     0 MNELEM,MITN,MENERG,TLMOML,TLSPCL,TLMOMT,TLELEM,TLCONC,TLENER,
     1 CVENGL,CVMOML,CVSPCL,CVMOMT,CVELEM,CVEQUI,CVCONW,CVENER,FPP(101),
     2 IPC,FW1,FW2,FW3,CD(101),RR(101),XP(6,101),WEP(3,101),FJS(6,101),
     3 FJE(3,101),FHE(3,101),IKOUNT,HMIX(101),FNS(6,101),FNE(3,101)
      N=NETA-1
C*****************************************************************
C**** CALCULATE RR AND CD COEFFICIENTS
C*****************************************************************
      CD(1)=(C(2)-C(1))/DELTA
      CD(NETA)=(C(NETA)-C(NETA-1))/DELTA
      DO 2302 I=2,N
         RR(I)=RHOM(NETA)/RHOM(I)
         CD(I)=(C(I+1)-C(I-1))/(2.*DELTA)
 2302 CONTINUE
      RR(1)=RHOM(NETA)/RHOM(1)
      RR(NETA)=1.0
C*****************************************************************
 2370 NMOMT=NMOMT+1
      CVMOMT=.FALSE.
C*****************************************************************
C**** SET BOUNDARY CONDITIONS FOR THE MOMENTUM EQUATION
C         F(1,K) IS AN EIGENVALUE OF THE PROBLEM. COMES IN
C                FROM INIT IF IMOMT=1  OR
C                FROM BURNRT IF IMOMT.GT.1
C*****************************************************************
      DO 2305 K=1,2
         F(1,K)=FBURN
         FP(1,K)=0.0
         FP(NETA,K)=1.0
 2305 CONTINUE
C*****************************************************************
C**** SOLVE MOMENTUM EQUATION BY METHOD OF ACCELERATED SUCCESSIVE
C**** REPLACEMENTS.
C*****************************************************************
      K=2
         DO 2310 I=2,N
C*****************************************************************
C****       CALCULATE INTEGRAL OF FP (=F) BY NEWTON-COTES CLOSED END FOR
C*****************************************************************
            IF (I.GE.5) GO TO 2319
            L=I-1
            GO TO (2311,2312,2313),L
 2311       F(2,K)=F(1,K)+((FP(1,K)+FP(2,K-1))*(DELTA/2.0))
```

```
            GO TO 2317
 2312       F(3,K)=F(1,K)+((FP(1,K)+(4.*FP(2,K))+FP(3,K-1))*(DELTA/3.))
            GO TO 2317
 2313       F(4,K)=F(1,K)+((FP(1,K)+(3.*FP(2,K))+(3.*FP(3,K))+FP(4,K-1))
     1             *(3.*DELTA/8.))
            GO TO 2317
 2319       F(I,K)=F(I-4,K)+(((7.*FP(I-4,K))+(32.*FP(I-3,K))+(12.*FP(I-2
     1             ,K))+(32.*FP(I-1,K))+(7.*FP(I,K-1)))*(2.*DELTA/45.))
 2317       V1=(FP(I+1,K-1)-2.*FP(I,K-1)+FP(I-1,K))/(DELTA**2.0)
            V2=((CO(I)+F(I,K))*(FP(I+1,K-1)-FP(I-1,K)))/(2.*C(I)*DELTA)
            V3=(RR(I)-(FP(I,K-1)**2.))/C(I)
            V4=2./(DELTA**2.)
            TEMP=(FP(I+1,K-1)-FP(I-1,K))/(2.*C(I)*DELTA)
            IF (I.GE.5) GO TO 2419
            GO TO (2411,2412,2413),L
 2411       V5=-(DELTA/2.)*TEMP
            GO TO 2417
 2412       V5=-(DELTA/3.)*TEMP
            GO TO 2417
 2413       V5=-(3.*DELTA/8.)*TEMP
            GO TO 2417
 2419       V5=-(14.*DELTA/45.)*TEMP
 2417       V6=(2.*FP(I,K-1))/C(I)
            FP(I,K)=FP(I,K-1)+1.70*((V1+V2+V3)/(V4+V5+V6))
            ERRVEL(I)=ABS(FP(I,K)/FP(I,K-1)-1.)
 2310     CONTINUE
          F(NETA,K)=F(N,K)+(FP(N,K)+FP(NETA,K))*(DELTA/2.)
C*************************************************************************
C****     CALCULATE FPPW(K) FROM FOUR POINT FORWARD DIFFERENCE FORMULA
C*************************************************************************
          FPPW(K)=(1./(6.*DELTA))*(2.*FP(4,K)-9.*FP(3,K)+18.*FP(2,K)-11.*
     1    FP(1,K))
          ERRFPP(K)=ABS(FPPW(K)/FPPW(K-1)-1.)
          DO 2318 I=1,NETA
             F(I,1)=F(I,K)
             FP(I,1)=FP(I,K)
             FPPW(1)=FPPW(K)
 2318     CONTINUE
C*************************************************************************
C**** CALCULATE FPP(L) ACROSS FLOWFIELD
C*************************************************************************
          DO 2330 L=2,N
          FPP(L)=(FP(L+1,1)-FP(L-1,1))/(2.*DELTA)
 2330     CONTINUE
          FPP(1)=FPPW(1)
          FPP(NETA)=((3.*FP(NETA,1))-(4.*FP(NETA-1,1))+(FP(NETA-2,1)))/
     1              (2.*DELTA)
C*************************************************************************
C**** CHECK FOR CONVERGENCE OF VELOCITY PROFILE AND WALL SHEAR
C*************************************************************************
          DO 2315 I=1,NETA
             IF (ERRVEL(I).LE.TLMOMT) GO TO 2315
             GO TO 2380
 2315     CONTINUE
          IF (ERRFPP(2).LE.TLMOMT) GO TO 2316
          GO TO 2380
 2316     CVMOMT=.TRUE.
 2380 IF((NMOMT.LT.MNMOMT).AND.(.NOT.CVMOMT)) GO TO 2370
```

```
C*****************************************************************************
C**** PRINTOUT OF MOMENTUM EQUATION
C*****************************************************************************
      PRINT 2002
 2002 FORMAT(1H1,47X,'SOLUTION TO THE MOMENTUM EQUATION',///)
      PRINT 2003,IENRG,MXTEMP
 2003 FORMAT( 5X,'THIS IS THE ',I4,' PASS THRU THE OUTERMOST ENERGY LOOP
     1  --MAXIMUM NO OF PASSES IS ',I4)
      PRINT 2004,IMOMT,MXMOMT
 2004 FORMAT(5X,'THIS IS THE ',I4,' PASS THRU THE INTERMEDIATE MOMENTUM
     1LOOP  --MAXIMUM NO OF PASSES IS ',I4)
      PRINT 2005,IPROP
 2005 FORMAT(5X,'THE PHYSICAL PROPERTIES USED ARE FROM THE ',I4,' PASS I
     1HRU THE PROP SUBROUTINE',/,5X,'THE ASSUMED BURNING RATE AT THE WAL
     2L IS GIVEN BY F(1)')
      PRINT 2006,CVMOMT,NMOMT,MNMOMT,TLMOMT
 2006 FORMAT(///,5X,'THE MOMENTUM EQUATION CONVERGED ',L6,' IN ',I4,' IT
     1ERATIONS  --MAXIMUM NO OF ITERATIONS IS ',I4,' -- TO A',/,9X,'RELA
     2TIVE ERROR BETWEEN THE LAST TWO CONSECUTIVE ITERATIONS OF LESS THA
     3N ',E11.4)
      PRINT 2007,ERRFPP(2)
 2007 FORMAT(///,3X,'L',4X,'ETA(L)',13X,'F(L)',16X,'FP(L)',14X,'FPP(L)',
     114X,'ERRVEL(L)',10X,'ERRFPPW= ',F13.8)
      DO 2008 L=1,NETA
 2008 PRINT 2009,L,ETA(L),F(L,1),FP(L,1),FPP(L),ERRVEL(L)
 2009 FORMAT(2X,I3,2X,F6.2,4(7X,F13.8))
      CONTINUE
      RETURN
      END
```

NO DIAGNOSTICS.

```
      SUBROUTINE SPCLUP
C*****************************************************************
C**** ALL QUANTITIES HAVE UNITS CONSISTENT WITH THE  C.G.S SYSTEM
C**** DECLARATION STATEMENTS
C*****************************************************************
      LOGICAL CVENGL,CVMOML,CVSPCL,CVMOMT,CVELEM,CVEQUI,CVCONW,CVENER
      COMMON   SIG(6),EK(6),A(6,5),CP(6,101),HB(6),B(4,2),EQ(4,101),
     1 WT(6),FP(101,2),ETA(101),T(101,2),X(6,101,2),E(6,3),DE(3,101),
     2 WE(3,101,2),DS(6,101),WTM(101),RHOM(101),W(6,102,2),CPM(101),
     3 SIGP(6,6),EKP(6,6),WTP(6,6),VIS(6,101),THC(6,101),DB(6,6,101),
     4 PHI(6,6),VISM(101),THCM(101),DEN(6),SDEN(6),FO(6,6),FFO(6,6),
     5 FNO(5,5),FNT(5,5),JC(6),VV(2),DM(6,6,101),H(6,101),C(101),
     6 PR(101),F(101,2),ERRVEL(101),FPPW(2),ERRFPP(2),ERRELE(3,101),
     7 ER(6,101),XEDGE(6),GEN(6,101),WP(6,101),WPP(6,101),ERRT(101),
     8 P,NETA,DELTA,RU,BURNM,FBURN,RB,UE,FWBAR,IPROP,IENRG,IMOMT,
     9 ISPEC,NMOMT,NELEM,ITN(101),NENERG,MXTEMP,MXMOMT,MXSPEC,MNMOMT,
     0 MNELEM,MITN,MENERG,TLMOML,TLSPCL,TLMOMT,TLELEM,TLCONC,TLENER,
     1 CVENGL,CVMOML,CVSPCL,CVMOMT,CVELEM,CVEQUI,CVCONW,CVENER,FPP(101),
     2 IPC,FW1,FW2,FW3,CD(101),RR(101),XP(6,101),WEP(3,101),FJS(6,101),
     3 FJE(3,101),FHE(3,101),IKOUNT,HMIX(101),FNS(6,101),FNE(3,101)
      COMMON/BLK1/EMFO,EMFN,EMFC,ELEMRT(101),FLUXRT(101)
      COMMON/BLK2/OEMFO,OEMFN,OEMFC
      DIMENSION WEST(2,101,2)
      OEMFO=WE(1,1,1)
      OEMFN=WE(2,1,1)
      OEMFC=WE(3,1,1)
  504 CVSPCL=.FALSE.
      ISPEC=ISPEC+1
C*****************************************************************
C**** INITIALIZE AND STORE ELEMENTAL MASS FRACTION PROFILES
C*****************************************************************
      DO 507 L=1,NETA
  507 ITN(L)=0
      DO 5075 L=1,NETA
      DO 5075 J=1,2
 5075 WEST(J,L,1)=WE(J,L,1)
      VROO=FJE(1,1)/WE(1,1,1)
      VRNO=FJE(2,1)/WE(2,1,1)
      VRCO=FJE(3,1)/(WE(3,1,1)-1.)
C*****************************************************************
C**** SOLVE ELEMENTAL CONSERVATION EQUATIONS
C*****************************************************************
      NELEM=0
      CALL ELEMT
      IF (CVELEM) GO TO 506
      GO TO 5270
C*****************************************************************
C**** SOLVE CHEMICAL EQUILIBRIUM EQUATIONS IN THE FLOWFIELD
C*****************************************************************
  506 CALL EQUIL
      IF (CVEQUI) GO TO 508
      GO TO 5270
  508 ITN(1)=0
      IKOUNT=3
C*****************************************************************
C**** SOLVE CHEMICAL EQUILIBRIUM EQUATIONS AT THE WALL WITHOUT UPDATING
```

```
C**** THE ELEMENTAL MASS FRACTIONS PSEUDO-BOUNDARY CONDITIONS
C**** DO THIS ONLY IN THE FIRST PASS THRU SPCLUP
C*************************************************************************
      IF (ISPEC.GT.1) GO TO 509
      CALL CONWAL
      IF (CVCONW) GO TO 509
      GO TO 5270
  509 CALL PROP
C*************************************************************************
C**** TEST FOR CONVERGENCE OF ELEMENTAL FLUX TO ELEMENTAL MASS FRACTION
C**** RATIO OF CARBON AT THE WALL
C*************************************************************************
      LTEST=0
      DO 5085 L=1,NETA
      DO 5085 J=1,2
 5085 WEST(J,L,2)=WE(J,L,1)
      VRON=FJE(1,1)/WE(1,1,1)
      VRNN=FJE(2,1)/WE(2,1,1)
      VRCN=FJE(3,1)/(WE(3,1,1)-1.)
      DO 5095 L=1,NETA
      DO 5095 J=1,2
      ERROR=ABS(WEST(J,L,2)/WEST(J,L,1)-1.)
      IF (ERROR.LE.TLSPCL) LTEST=LTEST+1
 5095 CONTINUE
      ERROR=ABS(VRON/VRO0-1.)
      IF (ERROR.LE.TLSPCL) LTEST=LTEST+1
      ERROR=ABS(VRNN/VRN0-1.)
      IF (ERROR.LE.TLSPCL) LTEST=LTEST+1
      ERROR=ABS(VRCN/VRC0-1.)
      IF (ERROR.LE.TLSPCL) LTEST=LTEST+1
      CONTINUE
      LTSTMX=2*NETA+3
      IF (LTEST.EQ.LTSTMX) CVSPCL=.TRUE.
      PRINT 5092,CVSPCL,LTEST
 5092 FORMAT(1H1,/////,40X,'CVSPCL=',L6,20X,'LTEST=',I5)
      IF ( (.NOT.CVSPCL).AND.(ISPEC.LT.MXSPEC) ) GO TO 504
 5270 CONTINUE
      RETURN
      END
```

NO DIAGNOSTICS.

```
      SUBROUTINE ELEMT
C*****************************************************************
C**** ALL QUANTITIES HAVE UNITS CONSISTENT WITH THE  C.G.S SYSTEM.
C**** DECLARATION STATEMENTS
C*****************************************************************
      LOGICAL CVENGL,CVMOML,CVSPCL,CVMOMT,CVELEM,CVEGUI,CVCONW,CVENER
      COMMON   SIG(6),EP(6),A(6,5),CP(6,101),HP(6),B(4,2),EQ(4,101),
     1 WT(6),FO(101,2),ETA(101),T(101,2),Y(6,101,2),E(6,3),DE(3,101),
     2 WE(3,101,2),DS(6,101),VTM(101),RHOM(101),W(6,102,2),CPM(101),
     3 SIGP(6,6),EKP(6,6),WTP(6,6),VIS(6,101),THC(6,101),DP(6,6,101),
     4 PHI(6,6),VISM(101),THCM(101),GEN(6),SDEN(6),FO(6,6),FFO(6,6),
     5 FNO(5,5),FNT(5,5),JC(6),VV(2),DM(6,6,101),H(6,101),C(101),
     6 PR(101),F(101,2),ERRVEL(101),FPPW(2),ERRFPP(2),ERRELE(3,101),
     7 ER(6,101),XEDGE(6),GEN(6,101),WP(6,101),WPP(6,101),ERRT(101),
     8 P,NETA,DELTA,RU,BURNM,FBURN,RB,UE,FWBAR,IPROP,IENRG,IMOMT,
     9 ISPEC,NMOMT,NELEM,ITN(101),NENERG,MXTEMP,MXMOMT,MXSPEC,MNMOMT,
     0 MNELEM,MITN,MENERG,TLMOML,TLSPCL,TLMOMT,TLELEM,TLCONC,TLENER,
     1 CVENGL,CVMOML,CVSPCL,CVMOMT,CVELEM,CVEGUI,CVCONW,CVENER,FPP(101),
     2 IPC,FW1,FW2,FW3,CD(101),KR(101),XP(6,101),WEP(3,101),FJS(6,101),
     3 FJE(3,101),FHE(3,101),IKOUNT,HMIX(101),FNS(6,101),FNE(3,101)
      DIMENSION COEFF(3,101)
      CVELEM=.FALSE.
      N=NETA-1
C*****************************************************************
C**** INITIALIZE AND SET BOUNDARY CONDITIONS
C*****************************************************************
      DO 3305 J=1,3
         WE(J,1,2)=WE(J,1,1)
         WE(J,NETA,2)=WE(J,NETA,1)
         DO 3305 L=1,NETA
            ERRELE(J,L)=0.0
 3305 CONTINUE
C*****************************************************************
C**** CALCULATE COEFFICIENTS FOR ELEMENTAL CONSERVATION EQUATIONS
C*****************************************************************
 3401 DO 3330 J=1,3
         DO 3328 L=2,N
            COEFF(J,L)=0.
            IF (ABS( DE(J,L)).LT.1.0E-30) GO TO 3328
            COEFF(J,L)=( RHOM(L+1)*RHOM(L+1)*DE(J,L+1) -
     1                   RHOM(L-1)*RHOM(L-1)*DE(J,L-1) +
     2                   2.*DELTA*RHOM(NETA)*VISM(NETA)*F(L,1) )  /
     3                 (4.*RHOM(L)*RHOM(L)*DE(J,L))
            IF (COEFF(J,L).GE.1.0) COEFF(J,L)=0.0
            IF (COEFF(J,L).LE.-1.0) COEFF(J,L)=-0.0
 3328    CONTINUE
 3330 CONTINUE
C*****************************************************************
C**** PRINTOUT COEFFICIENTS FOR ELEMENTAL CONSERVATION EQUATIONS
C*****************************************************************
      PRINT 3011
 3011 FORMAT(1H1,///,41X,'COEFFICIENTS FOR ELEMENTAL CONSERVATION EQUAT
     1ONS',//,3X,'L',4X,'ETA(L)',10X,'COEFF(0,L)',10X,'COEFF(N,L)',10X,'
     2COEFF(C,L)')
      DO 3012 L=2,N
         PRINT 3013,L,ETA(L),COEFF(1,L),COEFF(2,L),COEFF(3,L)
 3012 CONTINUE
 3013 FORMAT(2X,I3,2X,F6.2,3(4X,E13.6))
C*****************************************************************
C**** SOLVE ELEMENTAL CONSERVATION EQUATIONS BY METHOD OF
```

```
C**** ACCELERATED SUCCESSIVE REPLACEMENTS.
C*************************************************************************
 3325 NELEM=NELEM+1
           K=2
      DO 3308 L=2,N
         DO 3310 J=1,3
            CORR=(1.0/2.0)*(WE(J,L+1,K-1)-(2.*WE(J,L,K-1))+
     1           WE(J,L-1,K))+(COEFF(J,L)*(WE(J,L+1,K-1)-WE(J,L-1,K-1)))
            WE(J,L,K)=WE(J,L,K-1)-1.7*CORR
 3310    CONTINUE
         WE(1,L,K)=1.0 - WE(2,L,K) - WE(3,L,K)
         DO 3311 J=1,3
            IF (WE(J,L,K-1).GT.1.0E-06) GO TO 3512
            GO TO 3310
 3512       ERRELE(J,L)=ABS(WE(J,L,K)/WE(J,L,K-1)-1.)
            GO TO 3311
 3510       ERRELE(J,L)=ABS(WE(J,L,K)-WE(J,L,K-1))
 3311 CONTINUE
 3308 CONTINUE
      DO 3315 J=1,3
         DO 3313 L=1,NETA
            WE(J,L,1)=WE(J,L,2)
 3313    CONTINUE
 3315 CONTINUE
C*************************************************************************
C**** TEST FOR CONVERGENCE OF SOLUTION
C*************************************************************************
      DO 3320 J=1,2
         DO 3318 L=2,N
            IF (ERRELE(J,L).LE.TLELEM) GO TO 3318
            GO TO 3322
 3318    CONTINUE
 3320 CONTINUE
      CVELEM=.TRUE.
 3322 CONTINUE
 3382 CONTINUE
      IF ((NELEM.LT.MAXELEM).AND.(.NOT.CVELEM)) GO TO 3325
C*************************************************************************
C**** PRINTOUT OF ELEMENTAL CONSERVATION EQUATIONS RESULTS
C*************************************************************************
      PRINT 3002
 3002 FORMAT(1H1,30X,'SOLUTION TO THE THREE ELEMENTAL CONSERVATION EQUAT
     1IONS')
      PRINT 3003,TEMP,IPASS
 3003 FORMAT(//,5X,'TEMP =',F8.2,' DEG K AND THE',I4,' PASS THRU THE ELECTROST ENERGY L
     1OOP  --MAXIMUM NO. OF PASSES IS ',I4)
      PRINT 3004,IPASS1,MAXIT
 3004 FORMAT(5X,'THIS IS THE ',I4,' PASS THRU THE INTERMEDIATE MOMENTUM
     1LOOP  --MAXIMUM NO OF PASSES IS ',I4)
      PRINT 3005,ISPEC,MAXSPEC
 3005 FORMAT(5X,'ELEMENTAL SPECIES ',I2,' OF ',I2,' SPECIES THRU THE ELECTRON SPECIES LOOP
     1  --MAXIMUM NO OF PASSES IS ',I4)
      PRINT 3006,IPASS
 3006 FORMAT(5X,'THE THERMODYNAMICAL PROPERTIES USED ARE FROM THE ',I4,' PASS I
     1THRU THE PROPERTIES LOOP',//,5X,'THE ASSUMED ELEMENTAL COMPOSITIONS
     2AT THE WALL ARE GIVEN BY THE ',3(J,1)')
      PRINT 3007,CVELEM,MAXELEM,TLELEM
```

```
3007 FORMAT(///,5X,'THE THREE ELEMENTAL CONSERVATION EQUATIONS CONVERGE
    1D',L6,' IN ',I4,'ITERATIONS  -=MAXIMUM NO OF ITERATIONS IS ',I4,'
    2-- TO A',/,9X,'RELATIVE ERROR BETWEEN THE LAST TWO SUCCESIVE ITERA
    3TIONS OF LESS THAN ',E11.4)
     PRINT 3008
3008 FORMAT(///,3X,'L',4X,'ETA(L)',8X,'WE(O,L)',12X,'WE(N,L)',12X,'WE(C
    1,L)',10X,'ERRELE(O,L)',8X,'ERRELE(N,L)',8X,'ERRELE(C,L)')
     DO 3009 L=1,NETA
3009 PRINT 3010,L,ETA(L),(WE(J,L,1),J=1,3),(ERRELE(J,L),J=1,3)
3010 FORMAT(2X,I3,2X,F6.2,6(6X,E13.6))
     CONTINUE
     DO 9999 L=1,NETA
     IF (WE(3,L,1).LT.0.0) WE(3,L,1)=0.0
9999 CONTINUE
     RETURN
     END
```

NO DIAGNOSTICS.

```
      SUBROUTINE EQUIL
C*************************************************************************
C**** ALL QUANTITIES HAVE UNITS CONSISTENT WITH THE  C.G.S SYSTEM
C**** DECLARATION STATEMENTS
C*************************************************************************
      LOGICAL CVENGL,CVMOML,CVSPCL,CVMOMT,CVELEM,CVEQUI,CVCONW,CVENER
      COMMON   SIG(6),EK(6),A(6,5),CP(6,101),HB(6),B(4,2),EQ(4,101),
     1 WT(6),FP(101,2),ETA(101),T(101,2),X(6,101,2),E(6,3),UE(3,101),
     2 WE(3,101,2),DS(6,101),VTM(101),RHOM(101),W(6,102,2),CPM(101),
     3 SIGP(6,6),EKP(6,6),WTP(6,6),VIS(6,101),THC(6,101),DB(6,6,101),
     4 PHI(6,6),VISM(101),THCM(101),DEN(6),SDEN(6),FQ(6,6),FFQ(6,6),
     5 FNO(5,5),FNT(5,5),JC(6),VV(2),DM(6,6,101),H(6,101),C(101),
     6 PR(101),F(101,2),ERRVEL(101),FPPW(2),ERRFPP(2),ERRELE(3,101),
     7 ER(6,101),XEDGE(6),GEN(6,101),WP(6,101),WPP(6,101),ERRT(101),
     8 P,NETA,DELTA,RU,BURNM,FBURN,RR,UE,FWBAR,IPROP,IENRG,IMOMT,
     9 ISPEC,NMOMT,NELEM,ITN(101),NENERG,MXTEMP,MXMOMT,MXSPEC,MNMOMT,
     0 MNELEM,MITN,MENERG,TLMOML,TLSPCL,TLMOMT,TLELEM,TLCONC,TLENER,
     1 CVENGL,CVMOML,CVSPCL,CVMOMT,CVELEM,CVEQUI,CVCONW,CVENER,FPP(101),
     2 IPC,FW1,FW2,FW3,CD(101),RR(101),XP(6,101),WEP(3,101),FJS(6,101),
     3 FJE(3,101),FHE(3,101),TKOUNT,HMIX(101),FNS(6,101),FNE(3,101)
C*************************************************************************
C**** SWEEP FLOWFIELD EXCLUDING SOLID BOUNDARY AND BOUNDARY LAYER EDGE
C*************************************************************************
      CVEQUI=.FALSE.
      L= NETA
      LCHECK=0
 4310 L=L-1
      DO 4360 I=1,6
 4360 X(I,L,1)=X(I,L+1,1)
C*************************************************************************
C**** SOLVE SYSTEM OF NON-LINEAR EQUATIONS BY  NEWTON-RAPHSON SYSTEM
C*************************************************************************
 4306 ITN(L)=ITN(L)+1
      T1=(2.*X(1,L,1))+  (EQ(2,L)*SQRT(X(1,L,1)/P)) -
     1   ((EQ(1,L)*(WE(3,L,1)*WTM(L)/12.0111))/(SQRT(P*X(1,L,1))+EQ(1,L)
     2   )) + (2.*WE(3,L,1)*WTM(L)/12.0111) - (WE(1,L,1)*WTM(L)/WT(3))
      B1= 2. + (EQ(2,L)/(2.*SQRT(P*X(1,L,1)))) +
     1   ((EQ(1,L)*(WE(3,L,1)*WTM(L)/12.0111))/(2.*((SQRT(P*X(1,L,1))+E
     2   Q(1,L))**2.)))*(SQRT(P/X(1,L,1))))
 4365 X(1,L,2)=X(1,L,1)-(T1/B1)
      IF (X(1,L,2).LE.0.) GO TO 4363
      GO TO 4364
 4363 B1=1.1*B1
      GO TO 4365
 4364 T2=(2.*X(2,L,1))+ (EQ(3,L)*SQRT(X(2,L,1)/P)) - (WE(2,L,1)*WTM(L)/W
     1   T(4))
      B2=2. + (EQ(3,L)/(2.*SQRT(P*X(2,L,1))))
      X(2,L,2)=X(2,L,1)-(T2/B2)
      X(3,L,2)=EQ(2,L)*SQRT(X(1,L,2)/P)
      X(4,L,2)=EQ(3,L)*SQRT(X(2,L,2)/P)
      X(5,L,2)=((WE(3,L,1)*WTM(L)/12.0111)*(1.-(EQ(1,L)/(SQRT(P*X(1,L,2)
     1          )+EQ(1,L)))))
      X(6,L,2)=(((WE(3,L,1)*WTM(L)/12.0111)*EQ(1,L))/(SQRT(P*X(1,L,2))+
     1          EQ(1,L)))
      WTM(L)=WTM(L)/(X(1,L,2)+X(2,L,2)+X(3,L,2)+X(4,L,2)+X(5,L,2)+X(6,
     1     L,2))
C*************************************************************************
C**** CHECK FOR CONVERGENCE AT LOCATION I
C*************************************************************************
```

```
      IF (X(1,L,2).GE.X(5,L,2)) ER(1,L)=ABS(X(1,L,2)/X(1,L,1)-1.)
      IF (X(1,L,2).LT.X(5,L,2)) ER(1,L)=ABS(X(5,L,2)/X(5,L,1)-1.)
      ER(2,L)=ABS(X(2,L,2)/X(2,L,1)-1.)
      TEMP=AMAX1(ER(1,L),ER(2,L))
      IF (TEMP.LE.TLCONC) GO TO 4302
      GO TO 4309
 4302 DO 4332 I=1,6
         X(I,L,1)=X(I,L,2)
 4332 CONTINUE
      LCHECK=LCHECK+1
      IF (L.GT.2) GO TO 4309
      IF (LCHECK.EQ.(NPTA-2)) CVEQUI=.TRUE.
      GO TO 4312
 4304 DO 4334 I=1,6
         X(I,L,1)=X(I,L,2)
 4334 CONTINUE
      IF(ITN(L).LT.MITN) GO TO 4306
      GO TO 4312
 4312 CONTINUE
      RETURN
      END
```

NO DIAGNOSTICS.

```
      SUBROUTINE CONWAL
C*****************************************************************
C**** ALL QUANTITIES HAVE UNITS CONSISTENT WITH THE  C.G.S SYSTEM
C**** DECLARATION STATEMENTS
C*****************************************************************
      LOGICAL CVENGL,CVMOML,CVSPCL,CVMOMT,CVELEM,CVEQUI,CVCONW,CVENER
      COMMON   SIG(6),EK(6),A(6,5),CP(6,101),HB(6),B(4,2),EQ(4,101),
     1 WT(6),EP(101,2),ETA(101),T(101,2),X(6,101,2),E(6,3),UE(3,101),
     2 WE(3,101,2),DS(6,101),WTM(101),RHOM(101),W(6,102,2),CPM(101),
     3 SIGP(6,6),EKP(6,6),WTP(6,6),VIS(6,101),THC(6,101),DB(6,6,101),
     4 PHI(6,6),VISM(101),THCM(101),DEN(6),SDEN(6),FQ(6,6),FFQ(6,6),
     5 FNO(5,5),FNT(5,5),JC(6),VV(2),DP(6,6,101),H(6,101),C(101),
     6 PR(101),F(101,2),ERRVEL(101),FPPW(2),ERRFPP(2),ERRELE(3,101),
     7 ER(6,101),XEDGE(6),GEN(6,101),WP(6,101),WPP(6,101),ERRT(101),
     8 P,NETA,DELTA,RU,BURNM,FBURN,RB,UE,FWBAR,IPROP,IENRG,IMOMT,
     9 ISPEC,NMOMT,NELEM,ITN(101),NENERG,MXTEMP,MXMOMT,MXSPEC,MNMOMT,
     0 MNELEM,MITN,MENERG,TLMOML,TLSPCL,TLMOMT,TLELEM,TLCONC,TLENER,
     1 CVENGL,CVMOML,CVSPCL,CVMOMT,CVELEM,CVEQUI,CVCONW,CVENER,FPP(101),
     2 IPC,FW1,FW2,FW3,CD(101),RR(101),XP(6,101),WEP(3,101),FJS(6,101),
     3 FJE(3,101),FHE(3,101),IKOUNT,RMIX(101),FNS(6,101),FNE(3,101)
      COMMON/BLK1/EMFO,EMFN,EMFC,ELEMRT(101),FLUXRT(101)
      COMMON/BLK2/OEMFO,OEMFN,OEMFC
      CVCONW=.FALSE.
      ITN(1)=0
C*****************************************************************
C**** EVALUATE GOX AND GC AT THE SURFACE
C**** UPDATE PSEUDO- BOUNDARY CONDITION AT THE WALL, IF IKOUNT=1
C*****************************************************************
      TP6=0.0
      FACT=0.80
      IF ( (IKOUNT.EQ.3).AND.(IPROP.EQ.0) ) TP6=WE(1,1,1)/WE(2,1,1)
      IF ( (IKOUNT.EQ.3).AND.(IPROP.GT.0) ) TP6=OEMFO/OEMFN
      IF (IPROP.EQ.0) GO TO 6999
      IF ( (IKOUNT.EQ.1).AND.(FJE(1,1)/FJE(2,1).LE.0.0) )
     1   TP6=FACT*WE(1,1,1)/WE(2,1,1)
      IF ( (IKOUNT.EQ.1).AND.(FJE(1,1)/FJE(2,1).GT.0.0).AND.(IMOMT.LE.2)
     1   ) TP6=FACT*WE(1,1,1)/WE(2,1,1) + (1.-FACT)*FJE(1,1)/FJE(2,1)
      IF ( (IKOUNT.EQ.1).AND.(FJE(1,1)/FJE(2,1).GT.0.0).AND.(IMOMT.GT.2)
     1   ) GO TO 6998
      GO TO 6999
 6998 FRT= (ELEMRT(IMOMT-1)-ELEMRT(IMOMT-2))/(FLUXRT(IMOMT-1)-FLUXRT(IMO
     1      MT-2))
      TP6=(ELEMRT(IMOMT-2)-FRT*FLUXRT(IMOMT-2))/(1.0-FRT)
 6999 GOX=TP6
      GC=-1.0-GOX
      IF (GOX.LE.0.0) RETURN
C*****************************************************************
C**** SOLVE SYSTEM OF NONLINEAR EQUATIONS BY NEWTON RAPHSON ALGORITHM
C*****************************************************************
      DO 6332 I=1,6
 6332 X(I,1,1)=X(I,2,1)
 6306 ITN(1)=ITN(1)+1
      T1=(WT(3)*(((2.+(2.*EQ(4,1)/EQ(1,1)))*X(1,1,1)) + ((EQ(2,1)+EQ(4,1
     1   ))*SQRT(X(1,1,1)/P))) -  ((GOX*WT(4))* ((2.*X(2,1,1)) +(EQ(3,1
     2   )*SQRT(X(2,1,1)/P))))
      B1=( 2. + (2.*EQ(4,1)/EQ(1,1)) + ((EQ(2,1)+EQ(4,1))/(2.*SQRT(P*X(1
     1   ,1,1))))* WT(3)
 6365 X(1,1,2)=X(1,1,1) - (T1/B1)
      IF (X(1,1,2).LT.0.) GO TO 6363
```

```
      GO TO 6364
 6363 B1=1.1*B1
      GO TO 6365
 6364 T2=(12.0111*(((EQ(4,1)/EQ(1,1))*X(1,1,2))+(EQ(4,1)*SQRT(X(1,1,2)/
     1   P)))) -  ((GC*WT(4))*((2.*X(2,1,1))+(EQ(3,1)*SQRT(X(2,1,1)/P))
     2   )) - WTM(1)
      B2=(-GC*WT(4))*( 2. + (EQ(3,1)/(2.*SQRT(X(2,1,1)*P))))
 6366 X(2,1,2)=X(2,1,1) - (T2/B2)
      IF (X(2,1,2).LT.0.) GO TO 6367
      GO TO 6338
 6367 B2=1.1*B2
      GO TO 6366
 6338 X(3,1,2)=EQ(2,1)*SQRT(X(1,1,2)/P)
      X(4,1,2)=EQ(3,1)*SQRT(X(2,1,2)/P)
      X(5,1,2)=EQ(4,1)/EQ(1,1)*X(1,1,2)
      X(6,1,2)=EQ(4,1)*SQRT(X(1,1,2)/P)
      L=1
      WTM(L)=WTM(L)/(X(1,L,2)+X(2,L,2)+X(3,L,2)+X(4,L,2)+X(5,L,2)+X(6,
     1     L,2))
C*************************************************************************
C**** CHECK FOR CONVERGENCE AT THE WALL
C*************************************************************************
      ER(2,1)=ABS(X(2,1,2)/X(2,1,1)-1.)
      ER(6,1)=ABS(X(6,1,2)/X(6,1,1)-1.)
      TEMP=AMAX1(ER(2,1),ER(6,1))
      IF (TEMP.LE.TLCONC) GO TO 6302
      GO TO 6304
 6302 DO 6380 I=1,6
         X(I,1,1)=X(I,1,2)
 6380 CONTINUE
      CVCONW=.TRUE.
      GO TO 6312
 6304 DO 6334 I=1,6
         X(I,1,1)=X(I,1,2)
 6334 CONTINUE
      IF (ITN(1).LT.MITN) GO TO 6306
 6312 CONTINUE
C*************************************************************************
C**** CALCULATE ELEMENTAL MASS FRACTIONS AND RATIOS AT THE WALL
C*************************************************************************
      DO 6315 I=1,6
 6315 W(I,1,1)=WT(I)*X(I,1,1)/WTM(1)
      EMFO=E(1,1)*W(1,1,1) + E(2,1)*W(2,1,1) + E(3,1)*W(3,1,1) +
     1     E(4,1)*W(4,1,1) + E(5,1)*W(5,1,1) + E(6,1)*W(6,1,1)
      EMFN=E(1,2)*W(1,1,1) + E(2,2)*W(2,1,1) + E(3,2)*W(3,1,1) +
     1     E(4,2)*W(4,1,1) + E(5,2)*W(5,1,1) + E(6,2)*W(6,1,1)
      EMFC=E(1,3)*W(1,1,1) + E(2,3)*W(2,1,1) + E(3,3)*W(3,1,1) +
     1     E(4,3)*W(4,1,1) + E(5,3)*W(5,1,1) + E(6,3)*W(6,1,1)
      EMFON= EMFO/EMFN
      EMFCN= (EMFC-1.)/EMFN
C*************************************************************************
C**** PRINT OUT WALL SPECIES COMPOSITIONS
C*************************************************************************
      PRINT 6002
 6002 FORMAT(1H1,25X,'SOLUTION TO THE CHEMICAL EQUILIBRIUM EQUATIONS FOR
     1 THE SPECIES COMPOSITIONS --AT THE WALL')
      PRINT 6003,IENRG,MXTEMP
 6003 FORMAT(///,5X,'THIS IS THE ',I4,' PASS THRU THE OUTERMOST ENERGY L
     1OOP  --MAXIMUM NO OF PASSES IS ',I4)
```

```
      PRINT 6004,IMOMT,MXMOMT
 6004 FORMAT(5X,'THIS IS THE ',I4,' PASS THRU THE INTERMEDIATE MOMENTUM
     1LOOP  --MAXIMUM NO OF PASSES IS ',I4)
      PRINT 6005,ISPEC,MXSPEC
 6005 FORMAT(5X,'THIS IS THE ',I4,' PASS THRU THE INNERMOST SPECIES LOOP
     1  --MAXIMUM NO OF PASSES IS ',I4)
      PRINT 6006,IPROP,MITN
 6006 FORMAT(5X,'THE PHYSICAL PROPERTIES USED ARE FROM THE ',I4,' PASS T
     1HRU THE PROP SUBROUTINE',/,5X,'THE WALL ELEMENTAL COMPOSITIONS USE
     2D ARE FROM THE PREVIOUS SOLUTION TO THE ELEMENTAL EQUATIONS',/,5X,
     3'THE MAXIMUM NUMBER OF ITERATIONS AT THE WALL IS ',I4,'. THE NO OF
     4 ITERATIONS REQUIRED AT THE WALL IS GIVEN BELOW')
      PRINT 6007,CVCONW,TLCONC
 6007 FORMAT(///,5X,'THE WALL SPECIES COMPOSITIONS CONVERGED ',L6,' TO A
     1 RELATIVE ERROR BETWEEN THE LAST TWO',//,9X,'SUCCESIVE ITERATIONS I
     2O LESS THAN ',E11.4)
      PRINT 6008
 6008 FORMAT(///,3X,'L',3X,'ETA(L)',2X,'ITN(L)',5X,'X(O2,L)',10X,'X(N2,L
     1)',11X,'X(O,L)',11X,'X(N,L)',10X,'X(CO2,L)',9X,'X(CO,L)')
      L=1
      PRINT 6009,L,ETA(L),ITN(L),(X(I,L,1),I=1,6)
 6009 FORMAT(2X,I3,2X,F6.2,2X,I4,6(4X,E13.6))
      PRINT 6010,EMFO,EMFN,EMFC,EMFON,EMFCN
 6010 FORMAT(///,50X,'WE(O,W)=',E13.6,
     1          /,50X,'WE(N,W)=',E13.6,
     2          /,50X,'WE(C,W)=',E13.6,
     3        ///,46X,'WE(O,W)/WE(N,W)=',E13.6,
     4          /,41X,'(WE(C,W)-1))/WE(N,W)=',E13.6)
      PRINT 6011,IKOUNT
 6011 FORMAT(///,55X,'IKOUNT=',I3)
      CONTINUE
      RETURN
      END
```

NO DIAGNOSTICS.

```
      SUBROUTINE GENER
C*****************************************************************
C**** ALL QUANTITIES HAVE UNITS CONSISTENT WITH THE  C.G.S SYSTEM
C**** DECLARATION STATEMENTS
C*****************************************************************
      LOGICAL CVENGL,CVMOML,CVSPCL,CVMOMT,CVELEM,CVEQUI,CVCONW,CVENER
      COMMON   SIG(6),EK(6),A(6,5),CP(6,101),HR(6),B(4,2),EQ(4,101),
     1 WT(6),FP(101,2),ETA(101),T(101,2),X(6,101,2),E(6,3),UE(3,101),
     2 WE(3,101,2),DS(6,101),WTM(101),RHOM(101),W(6,102,2),CPM(101),
     3 SIGP(6,6),EKP(6,6),WTP(6,6),VIS(6,101),THC(6,101),DB(6,6,101),
     4 PHI(6,6),VISM(101),THCM(101),DEN(6),SDEN(6),FQ(6,6),FFQ(6,6),
     5 FNO(5,5),FNT(5,5),JC(6),VV(2),DM(6,6,101),H(6,101),C(101),
     6 PR(101),F(101,2),ERRVEL(101),FPPW(2),ERRFPP(2),ERRELE(3,101),
     7 ER(6,101),XEDGE(6),GEN(6,101),WP(6,101),WPP(6,101),ERRT(101),
     8 P,NETA,DELTA,RU,BURNM,FBURN,RG,UE,FWBAR,IPROP,IENRG,IMOMT,
     9 ISPEC,NMOMT,NELEM,ITN(101),NENERG,MXTEMP,MXMOMT,MXSPEC,MNMOMT,
     0 MNELEM,MITN,MENERG,TLMOML,TLSPCL,TLMOMT,TLELEM,TLCONC,TLENER,
     1 CVENGL,CVMOML,CVSPCL,CVMOMT,CVELEM,CVEQUI,CVCONW,CVENER,FPP(101),
     2 IPC,FW1,FW2,FW3,CD(101),RR(101),XP(6,101),WEP(3,101),FJS(6,101),
     3 FJE(3,101),FHE(3,101),IKOUNT,HMIX(101),FHS(6,101),FNE(3,101)
C*****************************************************************
C**** CALCULATE SPECIES GENERATION TERMS BY SOLVING THE SPECIES
C**** CONSERVATION EQUATIONS. ADD UP GENERATION TERMS TO OBTAIN THE
C**** NET RATE OF TOTAL MASS AND ELEMENTAL MASS GENERATION
C*****************************************************************
      CONST=SQRT(RB/(2.*RHOM(NETA)*VISM(NETA)*UE))
      DO 8301 L=1,NETA
         PRE=2.*RHOM(L)*UE/RB
         DS(1,L)=0.0
         DS(2,L)=0.0
         DS(3,L)=0.0
         DS(4,L)=0.0
         DS(5,L)=0.0
         DS(6,L)=0.0
         DO 8303 I=1,6
            IF (L.EQ.1) GO TO 8305
            IF (L.EQ.NETA) GO TO 8307
            DELJI=(FJS(I,L+1)-FJS(I,L-1))/(2.*DELTA)
            DELWI=(W(I,L+1,1)-W(I,L-1,1))/(2.*DELTA)
            GO TO 8309
 8305       DELJI=(FJS(I,2)-FJS(I,1))/DELTA
            DELWI=(W(I,2,1)-W(I,1,1))/DELTA
            GO TO 8309
 8307       DELJI=(FJS(I,NETA)-FJS(I,NETA-1))/DELTA
            DELWI=(W(I,NETA,1)-W(I,NETA-1,1))/DELTA
 8309       GEN(I,L)=((CONST*DELJI)-(F(L,1)*DELWI))*PRE
            DS(1,L)=DS(1,L)+DELWI
            DS(2,L)=DS(2,L)+DELJI
            DS(3,L)=DS(3,L)+GEN(I,L)
 8303    CONTINUE
         DS(4,L)=E(1,1)*GEN(1,L) + E(2,1)*GEN(2,L) + E(3,1)*GEN(3,L) +
     1           E(4,1)*GEN(4,L) + E(5,1)*GEN(5,L) + E(6,1)*GEN(6,L)
         DS(5,L)=E(1,2)*GEN(1,L) + E(2,2)*GEN(2,L) + E(3,2)*GEN(3,L) +
     1           E(4,2)*GEN(4,L) + E(5,2)*GEN(5,L) + E(6,2)*GEN(6,L)
         DS(6,L)=E(1,3)*GEN(1,L) + E(2,3)*GEN(2,L) + E(3,3)*GEN(3,L) +
     1           E(4,3)*GEN(4,L) + E(5,3)*GEN(5,L) + E(6,3)*GEN(6,L)
 8301 CONTINUE
```

```
C*****************************************************************
C**** PRINT OUT SPECIES GENERATION TERMS
C*****************************************************************
      PRINT 8002
 8002 FORMAT(1H1,45X,'SPECIES GENERATION IN THE BOUNDARY LAYER')
      PRINT 8003,IENRG,MXTEMP,IPROP
 8003 FORMAT(///,5X,'THIS IS THE ',I4,' PASS THRU THE OUTERMOST ENERGY L
     1OOP  --MAXIMUM NO OF PASSES IS ',I4,/,5X,'THE PHYSICAL PROPERTIES
     2USED ARE FROM THE ',I6,' PASS THRU THE PROP SUBROUTINE',/,5X,'THE
     3SPECIES GENERATION TERMS ARE OBTAINED BY SOLVING THE SPECIES CONSE
     4RVATION EQUATIONS WITH THE',/,9X,'COMPOSITION PROFILES OBTAINED FR
     5OM THE LAST PASS THRU THE SPECIES LOOP.  THIS IS NOT AN',/,9X,'ITE
     6RATIVE SOLUTION')
      PRINT 8004
 8004 FORMAT(///,3X,'L',3X,'ETA(L)',7X,'GEN(O2,L)',9X,'GEN(N2,L)',10X,'G
     1EN(O,L)',11X,'GEN(N,L)',9X,'GEN(CO2,L)',8X,'GEN(CO,L)')
      DO 8005 L=1,NETA
 8005 PRINT 8006,L,ETA(L),(GEN(I,L),I=1,6)
 8006 FORMAT(2X,I3,2X,F6.2,6(5X,E13.6))
      PRINT 8007
 8007 FORMAT(///,3X,'L',3X,'ETA(L)',8X,'SUMDELWI',10X,'SUMDELJI',9X,'NET
     1 MASS GEN',6X,'GEN ELEMT O',7X,'GEN ELEMT N',7X,'GEN ELEMT C')
      DO 8008 L=1,NETA
 8008 PRINT 8006,L,ETA(L),(DS(I,L),I=1,6)
      RETURN
      END
```

NO DIAGNOSTICS.

```
      SUBROUTINE ENERGY
C*****************************************************************
C**** ALL QUANTITIES HAVE UNITS CONSISTENT WITH THE  C.G.S SYSTEM
C**** DECLARATION STATEMENTS
C*****************************************************************
      LOGICAL CVENGL,CVMOML,CVSPCL,CVMOMT,CVELEM,CVEQUI,CVCONW,CVENER
      COMMON   SIG(6),EK(6),A(6,5),CP(6,101),P9(6),B(4,2),EQ(4,101),
     1 WT(6),FP(101,2),ETA(101),T(101,2),X(6,101,2),E(6,3),DE(3,101),
     2 WE(3,101,2),DS(6,101),WTM(101),RHOM(101),W(6,102,2),CPM(101),
     3 SIGP(6,6),EKP(6,6),WTP(6,6),VIS(6,101),THC(6,101),DB(6,6,101),
     4 PHI(6,6),VISM(101),THCM(101),DEN(6),SDEN(6),FO(6,6),FFO(6,6),
     5 FNO(5,5),FNT(5,5),JC(6),VV(2),DM(6,6,101),H(6,101),C(101),
     6 PR(101),F(101,2),ERRVEL(101),FPPW(2),ERRFPP(2),ERRELE(3,101),
     7 ER(6,101),XEDGE(6),GEN(6,101),WP(6,101),WPP(6,101),ERRT(101),
     8 P,NETA,DELTA,RU,BURNM,FBURN,RB,UE,FWBAR,IPROP,IENRG,IMOMT,
     9 ISPEC,NMOMT,NELEM,ITN(101),NENERG,MXTEMP,MXMOMT,MXSPEC,MNMOMT,
     0 MNELEM,MITN,MENERG,TLMOML,TLSPCL,TLMOMT,TLELEM,TLCONC,TLENER,
     1 CVENGL,CVMOML,CVSPCL,CVMOMT,CVELEM,CVEQUI,CVCONW,CVENER,FPP(101),
     2 IPC,FW1,FW2,FW3,CD(101),RR(101),XP(6,101),WEP(3,101),FJS(6,101),
     3 FJE(3,101),FHE(3,101),IKOUNT,HMIX(101),FNS(6,101),FNE(3,101)
      DIMENSION RT(101)
 9309 CVENER=.FALSE.
      NENERG=NENERG+1
C*****************************************************************
C**** SET BOUNDARY CONDITIONS FOR ENERGY EQUATION
C*****************************************************************
      T(1,2)=T(1,1)
      T(NETA,2)=T(NETA,1)
      N=NETA-1
C*****************************************************************
C**** SOLVE ENERGY EQUATION BY SUCCESSIVE ACCELERATED REPLACEMENTS
C*****************************************************************
      C4=SQRT(RB/(2.*RHOM(NETA)*VISM(NETA)*UE))
      C6=UE*UE*2.38662419E-08
C*****************************************************************
C**** EVALUATE COEFFICIENTS AT LOCATION L
C*****************************************************************
      DO 9303 L=2,N
         C1=C(L)*CPM(L)/PR(L)
         C2=((C(L+1)*CPM(L+1)/PR(L+1))-(C(L-1)*CPM(L-1)/PR(L-1)))/(2.*
     1      DELTA)
         C3=CPM(L)*F(L,1)
         C5=CP(1,L)*FJS(1,L) + CP(2,L)*FJS(2,L) + CP(3,L)*FJS(3,L) +
     1      CP(4,L)*FJS(4,L) + CP(5,L)*FJS(5,L) + CP(6,L)*FJS(6,L)
         C7=(FP(L,1)*CPM(L))/(CPM(NETA)*T(NETA,1))
         C8=C(L)*FPP(L)*FPP(L)
         C9=FP(L,1)*RHOM(NETA)/RHOM(L)
         C10=RB/(2.*RHOM(L)*UE)
         C11= H(1,L)*GEN(1,L) + H(2,L)*GEN(2,L) + H(3,L)*GEN(3,L) +
     1        H(4,L)*GEN(4,L) + H(5,L)*GEN(5,L) + H(6,L)*GEN(6,L)
         CF1=C1
         CF2=C2+C3-(C4*C5)
         CF3=C6*C7
         CF4=C6*(C8-C9)-(C10*C11)
         TPP=T(L+1,1)-2.*T(L,1)+T(L-1,2)
         TP=T(L+1,1)-T(L-1,2)
         DEL2=DELTA*DELTA
         TOP=CF1*TPP/DEL2 + CF2*TP/DELTA + CF3*T(L,1) + CF4
         BOT=-2.*CF1/DEL2 + CF3
         CORR=TOP/BOT
```

```
C*************************************************************************
C**** CALCULATE NEW APPROXIMATION OF T(L) AND RELATIVE ERROR
C*************************************************************************
         T(L,2)=T(L,1)-1.70*CORR
         ERRT(L)=ABS((T(L,2)-T(L,1))/T(L,1))
 9303 CONTINUE
C*************************************************************************
C**** UPDATE TEMPERATURE DISTRIBUTION
C*************************************************************************
      RT(1)=1.0
      RT(NETA)=0.0
      DO 9305 L=2,N
         T(L,1)=T(L,2)
         RT(L)=(T(L,1)-T(NETA,1))/(T(1,1)-T(NETA,1))
 9305 CONTINUE
C*************************************************************************
C**** TEST FOR CONVERGENCE OF TEMPERATURE PROFILE
C*************************************************************************
      DO 9307 L=2,N
         IF (ERRT(L).LE.TLENEP) GO TO 9307
         IF (NENERG.LE.MENERG) GO TO 9309
         GO TO 9311
 9307 CONTINUE
      CVENER=.TRUE.
 9311 CONTINUE
C*************************************************************************
C**** PRINT RESULTS OF THE ENERGY EQUATION
C*************************************************************************
      PRINT 9002
 9002 FORMAT(1H1,49X,'SOLUTION TO THE ENERGY EQUATION')
      PRINT 9003,IENRG,MXTEMP,IPROP
 9003 FORMAT(///,5X,'THIS IS THE ',I4,' PASS THRU THE OUTERMOST ENERGY L
     1OOP  --MAXIMUM NO OF PASSES IS ',I4,/,5X,'THE PHYSICAL PROPERTIES
     2USED ARE FROM THE ',I6,' PASS THRU THE PROP SUBROUTINE')
      PRINT 9004,CVENER,NENERG,MENERG,TLENER
 9004 FORMAT(///,5X,'THE ENERGY EQUATION CONVERGED ',L6,'IN ',I4,' ITERA
     1TIONS  --MAXIMUM NO OF ITERATIONS IS ',I4,'  --TO A',/,9X,'RELATIV
     2E ERROR BETWEEN THE LAST TWO SUCCESIVE ITERATIONS OF LESS THAN ',
     3E11.4)
      PRINT 9005
 9005 FORMAT(///,3X,'L',5X,'ETA(L)',20X,'T(L)',23X,'ERRT(L)',24X,'RT(L)'
     1)
      DO 9006 L=1,NETA
 9006 PRINT 9007,L,ETA(L),T(L,1),ERRT(L),RT(L)
 9007 FORMAT(2X,I3,4X,F6.2,15X,E13.6,15X,E13.6,15X,E13.6)
      CONTINUE
      RETURN
      END
```

NO DIAGNOSTICS.

```
      SUBROUTINE OUTPUT
C*************************************************************************
C**** ALL QUANTITIES HAVE UNITS CONSISTENT WITH THE  C.G.S SYSTEM
C**** DECLARATION STATEMENTS
C*************************************************************************
      LOGICAL CVENGL,CVMOML,CVSPCL,CVMOMT,CVELEM,CVEQUI,CVCONW,CVENER
      COMMON   SIG(6),EK(6),A(6,5),CP(6,101),HB(6),B(4,2),EQ(4,101),
     1 WT(6),FP(101,2),ETA(101),T(101,2),X(6,101,2),E(6,3),UE(3,101),
     2 WE(3,101,2),DS(6,101),WTM(101),RHOM(101),W(6,102,2),CPM(101),
     3 SIGP(6,6),EKP(6,6),WTP(6,6),VIS(6,101),THC(6,101),DB(6,6,101),
     4 PHI(6,6),VISM(101),THCM(101),DEN(6),SDEN(6),FO(6,6),FFO(6,6),
     5 FNO(5,5),FNT(5,5),JC(6),VV(2),DM(6,6,101),H(6,101),C(101),
     6 PR(101),F(101,2),ERRVEL(101),FPPW(2),ERRFPP(2),ERRELE(3,101),
     7 ER(6,101),XEDGE(6),GEN(6,101),WP(6,101),WPP(6,101),ERRT(101),
     8 P,NETA,DELTA,RU,BURNM,FBURN,RB,UE,FWBAR,IPROP,IENRG,IMOMT,
     9 ISPEC,NMOMT,NELEM,ITN(101),NENERG,MXTEMP,MXMOMT,MXSPEC,MNMOMT,
     0 MNELEM,MITN,MENERG,TLMOML,TLSPCL,TLMOMT,TLELEM,TLCONC,TLENER,
     1 CVENGL,CVMOML,CVSPCL,CVMOMT,CVELEM,CVEQUI,CVCONW,CVENER,FPP(101),
     2 IPC,FW1,FW2,FW3,CD(101),RR(101),XP(6,101),WEP(3,101),FJS(6,101),
     3 FJE(3,101),FNE(3,101),IKOUNT,HMIX(101),FNS(6,101),FNE(3,101)
      DIMENSION HRAT(101),Y(101)
      CALL PROP
      TEMP=(HMIX(1)-HMIX(NETA))
      DO 7305 L=1,NETA
 7305 HRAT(L)=(HMIX(L)-HMIX(NETA))/TEMP
      BURNM1= -FJE(1,1)/WE(1,1,1)
      BURNM2= -FJE(2,1)/WE(2,1,1)
      BURNM3= -FJE(3,1)/(WE(3,1,1)-1.)
      PRE=SQRT(RHOM(NETA)*VISM(NETA)*RB/(2.*UE))
      DO 7501 L=1,NETA
 7501 RHOM(L)=1./RHOM(L)
      Y(1)=0.0
      DO 7510 L=2,NETA
      IF (L.EQ.2) Y(2)=PRE*(RHOM(1)+RHOM(2))*DELTA/2.0
      IF (L.EQ.3) Y(3)=PRE*(RHOM(1)+4.*RHOM(2)+RHOM(3))*DELTA/3.0
      IF (L.EQ.4) Y(4)=PRE*(RHOM(1)+3.*RHOM(2)+3.*RHOM(3)+RHOM(4))*3.*
     1                  DELTA/8.
      IF (L.GE.5) Y(L)=PRE*(7.*RHOM(L-4)+32.*RHOM(L-3)+12.*RHOM(L-2)+
     1                  32.*RHOM(L-1)+7.*RHOM(L))*2.*DELTA/45. + Y(L-4)
 7510 CONTINUE
      DO 7511 L=1,NETA
 7511 RHOM(L)=1.0/RHOM(L)
 7100 FORMAT(6(E13.6))
      DO 7101 L=1,NETA
 7101 PUNCH 7100,(WE(J,L,1),J=1,3),FP(L,1),T(L,1),F(L,1)
      DO 7102 L=1,NETA
      PUNCH 7100,WTM(L),RHOM(L),VISM(L),C(L),THCM(L),CPM(L)
      PUNCH 7100,PR(L),FPP(L),(EQ(K,L),K=1,4)
      PUNCH 7100,(X(I,L,1),I=1,6)
      PUNCH 7100,(W(I,L,1),I=1,6)
      PUNCH 7100,(CP(I,L),I=1,6)
      PUNCH 7100,(VIS(I,L),I=1,6)
      PUNCH 7100,(THC(I,L),I=1,6)
      PUNCH 7100,(H(I,L),I=1,6)
      PUNCH 7100,(FJS(I,L),I=1,6)
      PUNCH 7100,(FNS(I,L),I=1,6)
      PUNCH 7100,(FJE(J,L),J=1,3),(FNE(J,L),J=1,3)
      PUNCH 7100,(DE(J,L),J=1,3),RR(L),HMIX(L),HRAT(L)
 7102 PUNCH 7100,(GEN(I,L),I=1,6)
```

```
      PUNCH 7103,BURNM1,BURNM2,BURNM3
 7103 FORMAT(3(E13.6))
      DO 7109 L=1,NETA
 7109 PUNCH 7104,L,ETA(L),Y(L),UB(1,1,L)
 7104 FORMAT(I6,3(E13.6))
      PRINT 9
    9 FORMAT(1H1,30X,'THESIS *** BOUNDARY LAYER MULTICOMPONENT COMBUSTIO
     1N *** APRIL 1973')
      PRINT 11,XEDGE(1),P,TLMOML,MXMOMT,XEDGE(2),T(1,1),TLSPCL,MXSPEC,
     1          XEDGE(3),T(NETA,1),TLMOMT,MNMOMT,XEDGE(4),UE,TLELEM,
     2          MNELEM,XEDGE(5),RB,TLCONC,MITN,XEDGE(6),BURNM,TLENER,
     3          MENERG,MXTEMP,DELTA,NETA
   11 FORMAT(///,
     1   6X,'XEDGE(O2)  =',E13.6,5X,'PRESSURE   =',E13.6,5X,'TLMOML =',
     2   E13.6,9X,'MXMOMT =',I6,/,
     3   6X,'XEDGE(N2)  =',E13.6,5X,'TEMP(WALL) =',E13.6,5X,'TLSPCL =',
     4   E13.6,9X,'MXSPEC =',I6,/,
     5   6X,'XEDGE(O)   =',E13.6,5X,'TEMP(EDGE) =',E13.6,5X,'TLMOMT =',
     6   E13.6,9X,'MNMOMT =',I6,/,
     7   6X,'XEDGE(N)   =',E13.6,5X,'VELOC EDGE =',E13.6,5X,'TLELEM =',
     8   E13.6,9X,'MNELEM =',I6,/,
     9   6X,'XEDGE(CO2) =',E13.6,5X,'RADIUS     =',E13.6,5X,'TLCONC =',
     0   E13.6,9X,'MITN   =',I6,/,
     1   6X,'XEDGE(CO)  =',E13.6,5X,'ASSUMED RT =',E13.6,5X,'TLENER =',
     2   E13.6,9X,'MENERG =',I6,/,96X,'MXTEMP =',I6,//,
     3   50X,'GRID SIZE =',F6.3,/,46X,'NO. OF POINTS =',I6)
 7099 FORMAT(///)
 7000 FORMAT(5X,I4,F6.2,6(5X,E13.6))
      PRINT 7099
      PRINT 7051
 7051 FORMAT(8X,'L',6X,'ETA(L)',7X,'WE(O,L)',11X,'WE(N,L)',11X,'WE(C,L)'
     1,11X,'FP(L)',13X,'T(L)',14X,'F(L)',/)
      DO 7001 L=1,NETA
 7001 PRINT 7000,L,ETA(L),(WE(J,L,1),J=1,3),FP(L,1),T(L,1),F(L,1)
      PRINT 7099
      PRINT 7052
 7052 FORMAT(8X,'L',6X,'ETA(L)',7X,'WTM(L)',12X,'RHOM(L)',11X,'VISM(L)',
     111X,'C(L)',14X,'THCM(L)',11X,'CPM(L)',/)
      DO 7002 L=1,NETA
 7002 PRINT 7000,L,ETA(L),WTM(L),RHOM(L),VISM(L),C(L),THCM(L),CPM(L)
      PRINT 7099
      PRINT 7053
 7053 FORMAT(8X,'L',6X,'ETA(L)',7X,'PR(L)',13X,'FPP(L)',12X,'EQ(CO,L)',
     110X,'EQ(O,L)',11X,'EQ(N,L)',11X,'EQ(S,L)',/)
      DO 7003 L=1,NETA
 7003 PRINT 7000,L,ETA(L),PR(L),FPP(L),(EQ(K,L),K=1,4)
      PRINT 7099
      PRINT 7054
 7054 FORMAT(8X,'L',6X,'ETA(L)',7X,'X(O2,L)',11X,'X(N2,L)',11X,'X(O,L)',
     112X,'X(N,L)',12X,'X(CO2,L)',10X,'X(CO,L)',/)
      DO 7004 L=1,NETA
 7004 PRINT 7000,L,ETA(L),(X(I,L,1),I=1,6)
      PRINT 7099
      PRINT 7055
 7055 FORMAT(8X,'L',6X,'ETA(L)',7X,'W(O2,L)',11X,'W(N2,L)',11X,'W(O,L)',
     112X,'W(N,L)',12X,'W(CO2,L)',10X,'W(CO,L)',/)
      DO 7005 L=1,NETA
 7005 PRINT 7000,L,ETA(L),(W(I,L,1),I=1,6)
```

```
      PRINT 7099
      PRINT 7056
 7056 FORMAT(8X,'L',6X,'ETA(L)',7X,'CP(O2,L)',10X,'CP(N2,L)',10X,'CP(O,L
     1)',11X,'CP(N,L)',11X,'CP(CO2,L)',9X,'CP(CO,L)',/)
      DO 7006 L=1,NETA
 7006 PRINT 7000,L,ETA(L),(CP(I,L),I=1,6)
      PRINT 7099
      PRINT 7057
 7057 FORMAT(8X,'L',6X,'ETA(L)',7X,'VIS(O2,L)',9X,'VIS(N2,L)',9X,'VIS(O,
     1L)',10X,'VIS(N,L)',10X,'VIS(CO2,L)',8X,'VIS(CO,L)',/)
      DO 7007 L=1,NETA
 7007 PRINT 7000,L,ETA(L),(VIS(I,L),I=1,6)
      PRINT 7099
      PRINT 7058
 7058 FORMAT(8X,'L',6X,'ETA(L)',7X,'THC(O2,L)',9X,'THC(N2,L)',9X,'THC(O,
     1L)',10X,'THC(N,L)',10X,'THC(CO2,L)',8X,'THC(CO,L)',/)
      DO 7008 L=1,NETA
 7008 PRINT 7000,L,ETA(L),(THC(I,L),I=1,6)
      PRINT 7099
      PRINT 7059
 7059 FORMAT(8X,'L',6X,'ETA(L)',7X,'H(O2,L)',11X,'H(N2,6)',11X,'H(O,L)',
     112X,'H(N,L)',12X,'H(CO2,L)',10X,'H(CO,L)',/)
      DO 7009 L=1,NETA
 7009 PRINT 7000,L,ETA(L),(H(I,L),I=1,6)
      PRINT 7099
      PRINT 7060
 7060 FORMAT(8X,'L',6X,'ETA(L)',7X,'FJS(O2,L)',9X,'FJS(N2,L)',9X,'FJS(O,
     1L)',10X,'FJS(N,L)',10X,'FJS(CO2,L)',8X,'FJS(CO,L)',/)
      DO 7010 L=1,NETA
 7010 PRINT 7000,L,ETA(L),(FJS(I,L),I=1,6)
      PRINT 7099
      PRINT 7061
 7061 FORMAT(8X,'L',6X,'ETA(L)',7X,'FNS(O2,L)',9X,'FNS(N2,L)',9X,'FNS(O,
     1L)',10X,'FNS(N,L)',10X,'FNS(CO2,L)',8X,'FNS(CO,L)',/)
      DO 7011 L=1,NETA
 7011 PRINT 7000,L,ETA(L),(FNS(I,L),I=1,6)
      PRINT 7099
      PRINT 7062
 7062 FORMAT(8X,'L',6X,'ETA(L)',7X,'FJE(O,L)',10X,'FJE(N,L)',10X,'FJE(C,
     1L)',10X,'FNE(O,L)',10X,'FNE(N,L)',10X,'FNE(C,L)',/)
      DO 7012 L=1,NETA
 7012 PRINT 7000,L,ETA(L),(FJE(J,L),J=1,3),(FNE(J,L),J=1,3)
      PRINT 7099
      PRINT 7063
 7063 FORMAT(8X,'L',6X,'ETA(L)',7X,'DE(O,L)',11X,'DE(N,L)',11X,'DE(C,L)'
     1,11X,'RR(L)',13X,'HMIX(L)',11X,'HRAT(L)',/)
      DO 7013 L=1,NETA
 7013 PRINT 7000,L,ETA(L),(DE(J,L),J=1,3),RR(L),HMIX(L),HRAT(L)
      PRINT 7099
      PRINT 7064
 7064 FORMAT(8X,'L',6X,'ETA(L)',7X,'GEN(O2,L)',9X,'GEN(N2,L)',9X,'GEN(O,
     1L)',10X,'GEN(N,L)',10X,'GEN(CO2,L)',8X,'GEN(CO,L)',/)
      DO 7014 L=1,NETA
 7014 PRINT 7000,L,ETA(L),(GEN(I,L),I=1,6)
      PRINT 7099
      PRINT 7015,BURNM1,BURNM2,BURNM3
 7015 FORMAT(///,20X,'WALL MASS TRANSFER ** BASED ON ELEMENT OXYGEN =',E
     115.6,/,20X,'WALL MASS TRANSFER ** BASED ON ELEMENT NITROGEN =',E15
     2.6,/,20X,'WALL MASS TRANSFER ** BASED ON ELEMENT CARBON =',E15.6)
```

```
      PRINT 7099
      PRINT 7016
 7016 FORMAT(20X,'L',5X,'ETA(L)',5X,'YCOORD.(L)',/)
      DO 7017 L=1,NETA
 7017 PRINT 7018,L,ETA(L),Y(L),UB(1,1,L)
 7018 FORMAT(23X,I4,5X,F6.2,5X,E13.6,5X,E13.6)
      PRINT 7105
 7105 FORMAT(1H1,///,5('END OF RUN * NORMAL EXIT * '))
      CONTINUE
      RETURN
      END
```

NO DIAGNOSTICS.

BIBLIOGRAPHY

1. Scala, S. M., The Ablation of Graphite in Dissociated Air Part I: Theory, General Electric Co., Report R62SD72 (Sept. 1962).

2. Scala, S. M., and L. M. Gilbert, "Sublimation of Graphite at Hypersonic Speeds," AIAA Journal, 3, p. 1635 (Sept. 1965).

3. Coffin, K. P., and R. S. Brokaw, A General System for Calculating Burning Rates of Particles and Drops, and Comparison of Calculated Rates for Carbon, Boron, Magnesium, and Iso-octane, NACA Tech. Note 3929 (Feb. 1957).

4. Dorrance, W. H., Viscous Hypersonic Flow, McGraw-Hill Book Co., New York (1962).

*5. Crocco, L. "Sullo Strato Limite Laminare nei Gas Lungo una Lamina Plana," Rend. Mat. Univ. Roma, 2, p. 138 (1941).

6. Probstein, R. F., and W. D. Hayes, Hypersonic Flow Theory, Academic Press, New York (1959).

7. Scala, S. M., and G. L. Vidale, "Vaporization Processes in the Hypersonic Laminar Boundary Layer," Int. J. Heat and Mass Transfer, 1, p. 4 (1960).

8. Lees, L., "Convective Heat Transfer with Mass Addition and Chemical Reactions," in Combustion and Propulsion Third AGARD Collogium, Pergamon Press, New York (1958).

9. Elzy, E. and R. M. Sisson, Tables of Similar Solutions to the Equations of Momentum, Heat and Mass Transfer in Laminar Boundary Layer Flow, Oregon State University, Engineering Experiment Station, Bulletin No. 40 (Feb. 1967).

10. Prober, R., Transport Phenomena in the Laminar Boundary Layer Flow of a Multicomponent Fluid, Ph.D. Thesis, University of Wisconsin (1961).

11. Blasius, H., The Boundary Layer in Fluids with Little Friction, NACA Tech. Memo. 1256 (1950).

12. Howarth, L., On the Calculation of the Steady Flow in the Boundary Layer Near the Surface of a Cylinder in a Stream, (British) Aeronautical Research Council, Report 1632 (1935).

*13. Pohlhausen, E., "Der Warmeaustausch zwischen festen Korpern und Flussigkeiten mit kleiner Reibung und kleiner Warmeleitung," Z. Angew. Math. Mech., 1, p. 115 (1921).

14. Emmons, H. W., and D. Leigh, Tabulation of the Blasius Function with Blowing and Suction, Interim Technical Report No. 9, Combustion Aeronautical Laboratory, Harvard University (1953).

15. Falkner, V. M., Simplified Calculation of the Laminar Boundary Layer, (British) Aeronautical Research Council, Report 1884 (1941).

16. Falkner, V. M. and S. W. Skan, "Some Approximate Solutions of the Boundary Layer Equations," Phil. Mag., 12, p. 863 (1931).

17. Hartree, D. R., "On an Equation Occurring in Falkner and Skan's Approximate Treatment of the Equations of the Boundary Layer," Proc. Cambr. Phil. Soc., 33, Part II, p. 223 (1937).

*18. Mangler, W., Deutsche Luftfahrtforschung UM 3087 (1944).

19. Goldstein, S., Modern Developments in Fluid Dynamics, Vol. II, Oxford University Press, London (1938).

20. Eckert, E. R. G., Heat Transfer and Temperature Profiles in Laminar Boundary Layers on a Sweat Cooled Wall, Air Materiel Command, Tech. Report 5646 (1947).

21. Fay, J. A., and F. R. Riddell, "Theory of Stagnation Point Heat Transfer in Dissociated Air," J. Aeronautical Sci., 25, p. 73 (1958).

22. Bird, R. B., W. E. Stewart, and E. N. Lightfoot, Transport Phenomena, John Wiley & Sons, New York (1960).

23. Williams, F. A., Combustion Theory, Addison-Wesley Publishing Co., Reading, Mass. (1965).

24. Onsager, L., Phys. Rev., 38, p. 2265 (1931).

25. Hirschfelder, J. O., C. F. Curtiss and R. B. Bird, Molecular Theory of Gases and Liquids, John Wiley & Sons, New York (1954).

*26. Tollmien, W., referenced in Schlichting (27)

27. Schlichting, H., Boundary Layer Theory, 4th Ed., McGraw-Hill Book Co., New York (1960).

28. Prandtl, L., Motion of Fluids with Very Little Viscosity, NACA Tech. Memo. 452 (1928).

29. Tirskii, G. A., "Analysis of the Chemical Composition of the Laminar Multicomponent Boundary Layer on the Surface of Hot Plastics," trans. from Komischeskie Issledovaniya, 2, p. 570 (1964).

30. Esch, D. D., R. W. Pike, C. D. Engel, R. C. Farmer and J. F. Balhoff, Stagnation Region Heating of a Phenolic-Nylon Ablator during Return from Planetary Missions, Louisiana State University, Reacting Fluids Labs., Final Report on NASA Grant NGR 19-001-059 (Sept. 1971).

31. Li, T. Y., and H. T. Nagamatsu, "Similar Solutions for the Compressible Boundary Layer Equations," J. Aeronautical Sci., 20, p. 653 (1953).

32. Lees, L., "Laminar Heat Transfer Over Blunt-nosed Bodies at Hypersonic Flight Speeds," Jet Propulsion, 26, p. 259 (1956).

33. Blasius, H., Z. Math. Physik, 56, p. 1 (1908).

34. Illingworth, C. R., Proc. Roy. Soc. London, p. 199 (1949).

35. Levy, S., J. Aeronautical Sci., 21, p. 459 (1949).

36. Hischfelder, J. O., R. B. Bird and E. L. Spotz, Chem. Revs., 44, p. 205 (1949).

37. Luft, N. W. and O. P. Kharbanda, Rsch. Corresp., 1, p. 536 (1954).

38. _____., Joint Army-Navy-Air Force (JANAF) Thermochemical Tables, CFSTI, Springfield, Va. (1965).

39 Kobe, K. A., "Thermochemistry for the Petrochemical Industry," Petrolium Refiner, (Jan. 1949 through Nov. 1954).

40. Gill, S., "A Process for the Step-by-Step Integration of Differential Equations in an Automatic Digital Computing Machine," Proc. Cambridge Phil. Soc., 47, p. 96 (1951).

41. Lapidus, L., Digital Computation for Chemical Engineers, McGraw-Hill Book Co., New York (1962).

42. Lew, H. G., The Use of the Method of Accelerated Successive Replacements for the Solution of Boundary Layer Equations, General Electric Co., Report R68SD8 (Jan. 1968).

43. Conte, S. D., Elementary Numerical Analysis, McGraw-Hill Book Co., New York (1956).

44. Cohen, C. B. and Eli Reshotko, Similar Solutions for the Compressible Laminar Boundary Layer with Heat Transfer and Pressure Gradient, NACA Report 1293 (1956).

*Secondary Source

VITA

Tomas Felipe Camacho was born September 7, 1943 in Havana, Cuba, and graduated from high school there in 1960. He attended Armstrong State University and Georgia Institute of Technology, from which he received a Bachelor in Chemical Engineering in 1965.

The author was employed by E. I. duPont in Wilmington, Delaware, and Union Camp Corporation in Savannah, Georgia, before entering graduate school at Georgia Tech in 1968. He received an M.S. in Chemical Engineering in 1969 and an M.S. in Industrial Management in 1971. During 1968 and 1969 he served as a Graduate Teaching Assistant in the School of Chemical Engineering. He is a member of the American Institute of Chemical Engineers and of Sigma Xi, and is a Registered Professional Engineer in the State of Georgia.

Mr. Camacho married Patricia Leith Pengue of Savannah, Georgia, and they have a daughter, Kellie Michelle.